Rack and Stack: Design of Payload Racks to Support Future Habitation Platforms and Exploration Missions

Recommendations for Payload Rack Adaptations for Functionality on a Lunar Surface Habitat

Moon to Mars eXploration Systems and Habitation (M2M X-Hab) 2025 Academic Innovation Challenge

Authors:
Lowen Walter, Isha Venkatesh, Tobi Farbstein, Jakob Swilley, Esme Lowry, Thomas Callen, Preston Withun, Vanya Krishna, Katherine Snowdon, Albert Chen, Colin Stenger, Huan Shuo Chang, Jacob Lee, Joshua Walker, Lizzie Kooistra, Lukas Zahuranic, Vanessa Cano, Yeon Woo Kim, Ava Cardenas, Daniela Bardi Silva, Hannah Yohannes, Megan Piper, Noah Negron, Suhani Thakur, Hamza Qureshi, Vamsi Gollapalli

Principle Investigator:
Nilton Rennó

Project Sponsor (NASA Marshall Space Flight Center):
Tracie Prater

Table of Contents

List of Figures

List of Tables

1 Introduction

1.1 Project Overview

Long-term human space exploration and habitation require payload racks to store, maintain, and track experiments for long periods of time. Without them, extraterrestrial experimentation, vital to advances here on Earth, would be virtually impossible to carry out at the necessary level. Current designs focus on storage and experimentation on the International Space Station (ISS), a microgravity environment. More resilient payload rack designs are necessary for space experimentation to become increasingly independent of crew and Earth support. Thus, the Bioastronautics and Life Support Systems (BLiSS) team has worked to characterize a payload rack that has been adapted to work in a lunar gravity environment.

The Moon to Mars eXploration Systems and Habitation (M2M X-Hab) 2025 Academic Innovation Challenge features a project titled "Rack and Stack: Design of Payload Racks to Support Future Habitation Platforms and Exploration Missions" [1]. The project calls for the development of payload racks which "can better enable science and utilization activities for a lunar surface mission" [1]. The deliverables for the project are full CAD models of the proposed system, as well as a full-scale structural prototype and bench-top payload prototype that uses a lunar regolith phytoremediation experiment as a test article.

1.2 Team Breakdown

The project team is organized into five subteams: structures, electrical, habitation, human factors, and experimental payload. Habitation, human factors, and experimental payload began grouped together and then separated as the project scope grew larger to accommodate the large volume of general members.

The Rack and Stack team is composed of over forty active members from eleven different science, engineering, and architectural disciplines and ranging from first-year undergraduate students to Ph.D. candidates.

2 Problem Definition

2.1 NASA EXPRESS Racks

The EXpedite the PRocessing of Experiments to Space Station (EXPRESS) Racks, developed by NASA Marshall Space Flight Center, are used to "simplify and expedite analytical and physical integration" of ISS subrack payloads [2]. They provide accommodations for 8 Orbital Middeck (OM) lockers and 2 International Subrack Interface Standard (ISIS) lockers, which can store customer experiments or equipment needed by crew members aboard the ISS. The rack concept was derived from "researchers' desire to have a simple hardware interface and a streamlined process to get their experiments to orbit quickly" [3]. The racks can host single-, double-, or quad-sized lockers for a wider variety of payload sizes. The rack also provides each individual payload locker with resources such as heating, cooling, waste gas venting, power, and water, which are needed to maintain the experiment within.

Since the EXPRESS racks are outfitted for use on the ISS, they were designed to function solely in a microgravity environment. On the lunar surface, which has a gravity of 1.62 m/s^2, there are various ergonomic, structural, and resource considerations to take into account. Payload handling becomes more difficult due to their increased weight, the loads which the rack and lockers must withstand increases as well, and liquid flow rates used to service the lockers are impacted.

2.2 Customer Needs

The stakeholder objectives are broadly encapsulated by the fourteen top-level requirements listed in Table 1.

R1	The system shall be contained within the dimensions of the heritage EXPRESS racks.
R2	The system shall be fully functional within the lunar surface environment.
R3	The system shall align to the human systems integration design standards of the Human Integration Design Handbook (Revision 1), STD-3001, and OCHMO-HB-004 Anthropometry, Biomechanics, and Strength.
R4	The system shall be two fault tolerant to failures with FMEA rankings equal to and greater than 9.
R5	The system shall align to the safety standards of the ISS Pressurized Payloads Interface Requirements Document, NASA STD-3001 and the Human Integration Design Handbook (Revision 1).
R6	The system design and functionality shall be verifiable in 1G of gravity.
R7	The system shall be compatible with standard ISIS payload and Orbiter middeck payload housing sizes and standards.
R8	The system shall require no more than 2 astronauts for standard operations (e.g. assembly, maintenance, repair).
R9	The system shall host and maintain the designated, standardized payload environments.
R10	The system shall track, monitor, and transmit payload environmental telemetry.
R11	The placement of the system shall be rearrangeable within the planetary habitat.
R12	The system shall allow for the control of payload resources.
R13	The system shall be one-fault tolerant to failures with FMEA rankings equal to and greater than 5.
R14	The payload locker placements shall be modular within the rack.

Table 1: Top-level System Requirements

Further system requirements are outlined in Appendix C.

2.3 Scoping the Project

In order to create a project that could be completed during the 2024-25 academic school year with the resources available, certain key aspects of the system and its handling were deemed out of scope. Since implementing full system autonomy was beyond the skills of the members of our project, we ruled dormancy, defined as system functionality when there are no crew members on the base, and start up following quiescent periods out of scope. Furthermore, due to limited knowledge of lunar habitat resourcing, we opted to treat intake and outtake sources for our resources as a "black box". Fire suppression and atmospheric regulation were both considered out of scope for this project due to their complicated nature of control. Finally, any payload locker interfacing beyond

the capabilities outlined in this report, system transportation, and launch and landing forces were deemed out of scope in an attempt to limit the technical complexity of the project.

3 System Design

3.1 Concept of Operations

A high-level Concept of Operations can be seen in Figure 1. Crew and ground interaction with our proposed Payload Experimentation Rack for Research and Investigation (PERRI) is very similar to that with the current EXPRESS racks. The rack would be kept within the lunar habitat, with sensors continuously monitoring each payload environment. Environmental controls would allow for autonomous maintenance of this environment, as well as manual override both from the crew and from the ground. Payload resourcing would be carried out in accordance to these control loops to ensure each payload receives the air, water, or light it needs.

When a user desires to interact with one or more of the payloads, they would be able to use our graphical user interface (GUI) to select their desired payload locker and make necessary manual changes to the environment inside. If needed, they can also remove the payload locker from the rack and set it down on the pull-out desk attached to the rack. From there, they can open the top or front of the locker to work directly with the payload inside. The locker can then be resealed and reloaded into the rack and the user can enter in the GUI any notes they have on the payload by logging changes under their user profile.

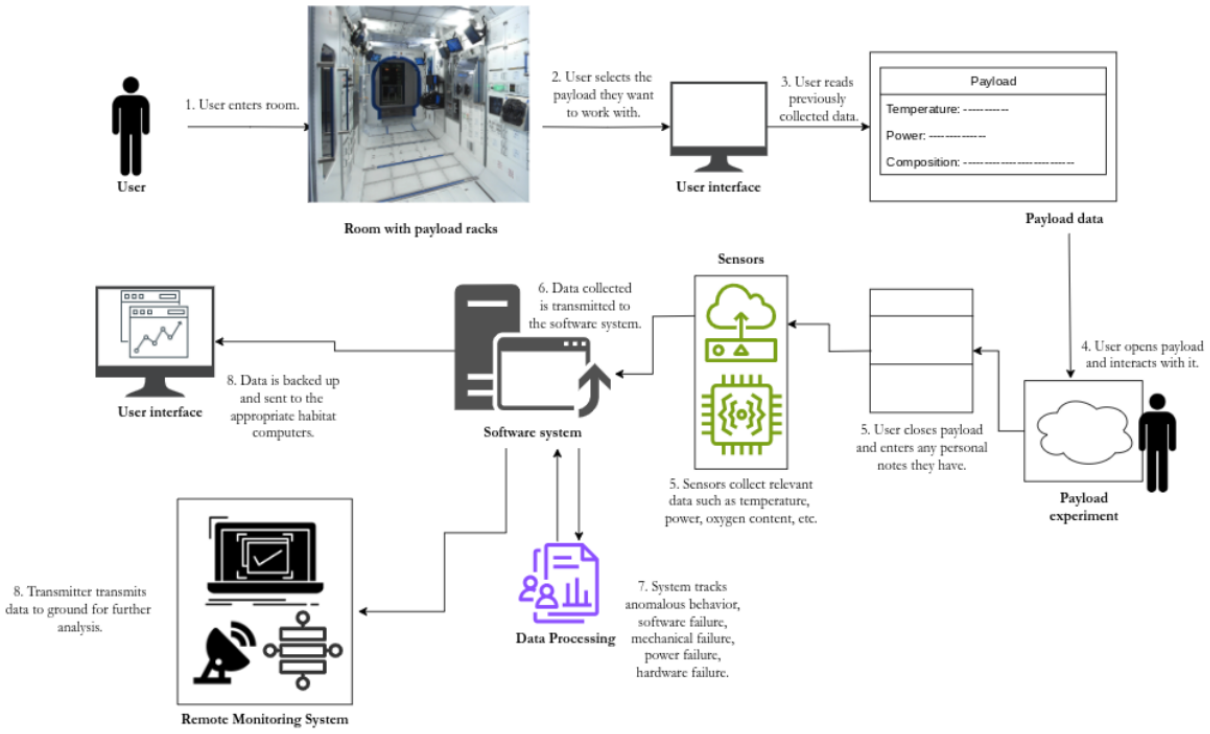

Figure 1: System Concept of Operations

3.2 Proposed Systems Architecture

3.2.1 Structural Design

The structural design of the full rack system will be separated into the following sections: frame, shell, rack handle, mobility, sliding rails, desk, roller rails, latch, payload locker. This section will describe how the system would be introduced in-flight, as the idealized design. Figure 2 shows the full rack with labels showing its main components.

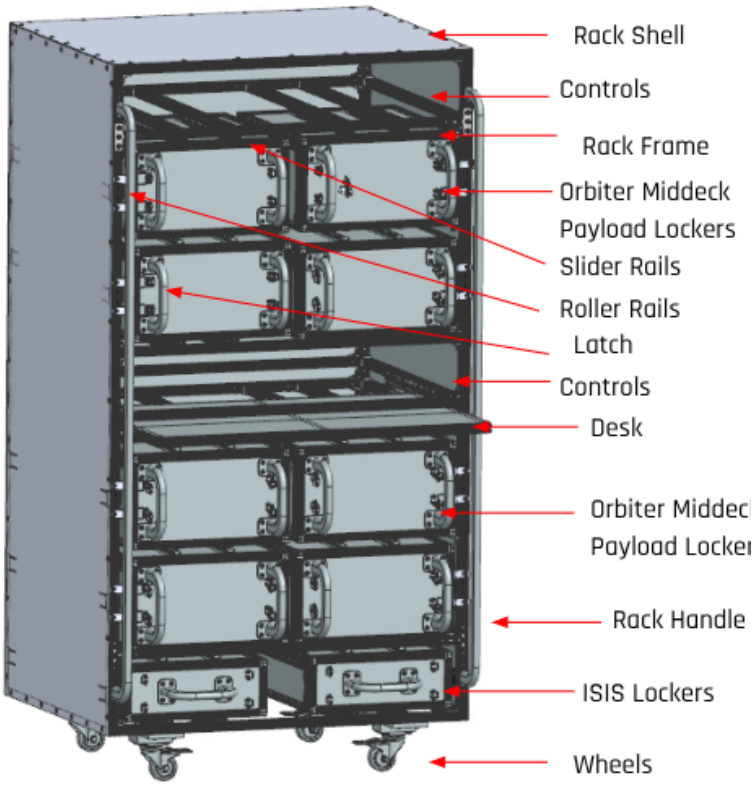

Figure 2: Full Rack CAD Model with Component Labels

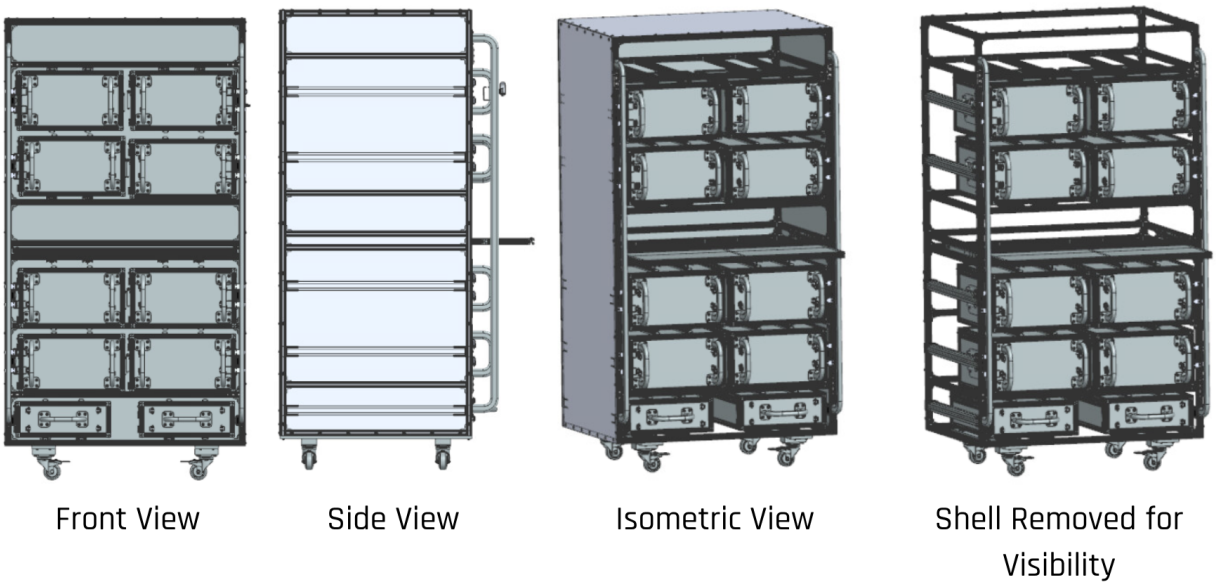

Figure 3: Full Rack CAD Model from Different Views

As a part of our design, different payload sizes are necessary to comply with SSI-1.08: The system shall accommodate at least two payload geometries. These payloads still interface with the rails, but with 4 attachment points instead of 2. Figure 4 shows the different payload locker configurations designed. The red locker is a double horizontal payload locker, and fills the space of two side by side large payloads. The blue locker is a double vertical payload locker, and fills the space of two large payloads. The yellow locker is a quad payload locker, and fills the space of four large payloads. The green boxes show the slider rail attachment points to each locker.

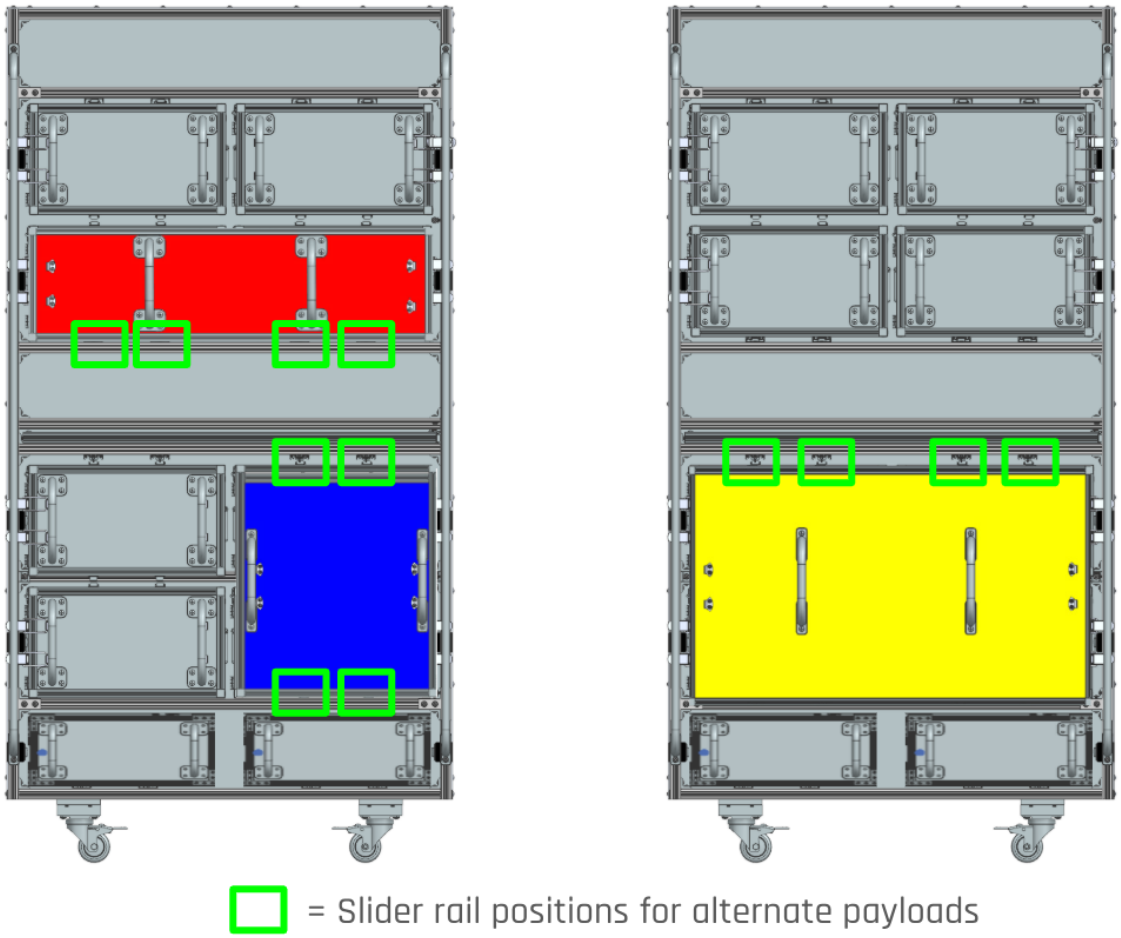

Figure 4: Different Payload Locker Configurations

3.2.2 Frame

The rack frame forms the main structural component of the rack. All of the payloads, control units, desk, and other components are attached and supported within the frame. All of the components ultimately depend upon the frame for load bearing and protection. This section will outline the design of the rack frame subsystem. The idealized design will describe how the system would be introduced in-flight. The prototype design will talk about an adapted version of the idealized system that was used for testing.

Key Design Decisions T-slotted profiles from the 80/20 company were chosen for the rack frame material. These profiles were chosen because they are incredibly easy to assemble and customize. The t-slots make it simple to attach different profiles, fasteners, and components to the frame. This greatly reduces the amount of effort required to custom design each aspect of the frame. Additionally, 80/20 has a large inventory of parts available to mount to the slots that would further simplify the design process. The t-slotted profiles used are made of a lightweight aluminum. The specific size chosen was 1010, meaning the square face is 1” by 1” wide.

Idealized Design In an idealized system, the rack frame would be made out of aluminum 80/20 T-slotted material. The frame uses T-nuts, screws, and L-brackets in order to hold the frame pieces together.

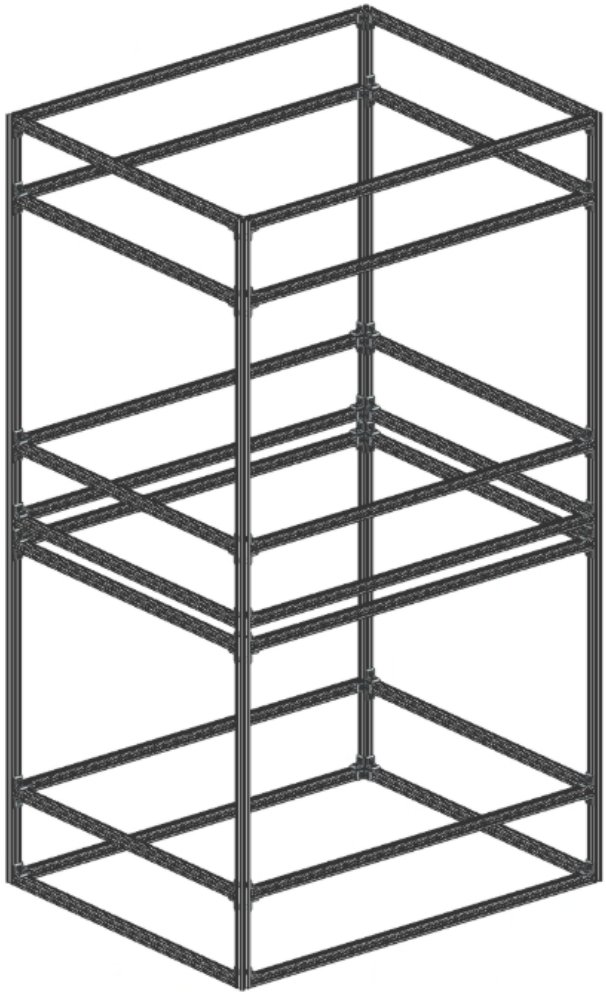

Figure 5: Rack Frame CAD

The mobility section does not have a frame surrounding it. Each payload bay, control bay, and the desk each have sections of frame surrounding it for structural support.

3.2.3 Shell

The goal of the shell component of the structural subsystem is to encase the entire rack around the frame to protect inner components from any unwanted exterior objects, forces, energy such as static buildup, and most importantly, lunar dust while adding structural stability to the entire frame. The shell covers four faces of the rack, leaving the forward face open for payload interaction and the bottom face open for wheel attachments.

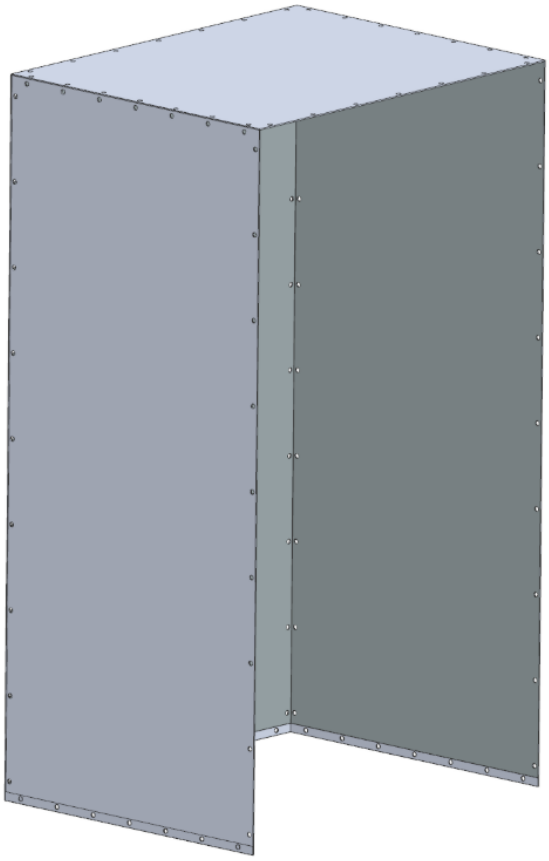

Figure 6: Rack Shell CAD

Key Design Decisions Key design decisions include using acrylic material that is either black/opaque, electric insulating, and at 1/8" thickness to be permissible with mass budget (estimated 44 lbs).

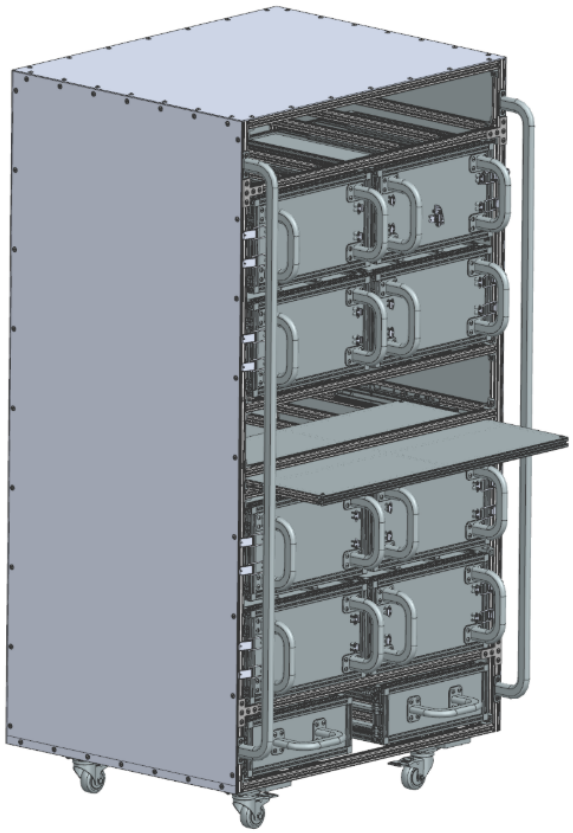

Figure 7: Shell CAD in Full Rack Assembly

Idealized Design The shell encapsulates top, side, and back faces of the rack with fasteners applied along respective 80/20 sections outside of the shell to ensure stability. The idealized design has the material implemented as $\frac{1}{8}$" thick black/opaque acrylic with electric insulation properties as stated above. Figure 6 shows the shell CAD alone. In the full rack assembly in Figure 7, the shell can be seen with fasteners along the outside border attaching it to the 80/20 frame.

3.2.4 Rack Handle

The purpose of the rack handles in the idealized rack is to provide a stable, efficient, and user-friendly structure for transportation of equipment and materials. The design of the rack handles focuses on optimizing strength and durability while maintaining ease of mobility. By using lightweight yet strong materials such as aluminum and incorporating ergonomic features, the system aims to reduce physical strain during handling and ensure smooth operation on the lunar surface.

Key Design Decisions In designing the Rack Handles, we evaluated our choices based on the functionality, safety, and compatibility they would provide according to heritage systems. The idealized design consists of aluminum handles with dimensions of 65" length, 0.75" width, and 1.5" depth. The handles feature rounded edges for safety, adhering to NASA standards for ergonomic gripping and human factors. This design assumes a high-strength, lightweight material that can withstand the operational forces expected in space environments, while also being comfortable and intuitive.
Trade decisions included material selection, handle geometry, mounting hardware (using four $\frac{1}{4}$"-20

cap screws), and overall integration with the rack structure. These decisions were informed by a review of past NASA hardware, hand calculations for deciding the number of screws necessary to withstand the forces, which we were able to calculate, and human-factors considerations to ensure both safety and usability in the lunar environment. Figure 8 shows the hand calculations performed to determine that four screws are capable of withstanding the total push/pull force from a crew member on the rack handle.

4 bolts- 70000 psi
Using all of the pushing/pulling force according to our requirements: 596 N
Type of metal used for the screw= 18-8 Stainless Steel Button Head Hex Drive Screws

Surface area of screws: $\pi(0.125)^2$
Psi * Area = Force_{max} (lbs)
70000 * $\pi(0.125)^2$ = 3436.117 lb
lb to N = 15284.61 N
Total support from all 4 screws (4 per attachment) = 4 * 15284.61 N = 61138.44 N

Figure 8: Hand Calculations for Rack Handle

Idealized Design For each rack handle there are two attachments, with two screws each. This will allow for the expected amount of forces this rack will have to withstand in mobility. It also has a 3" gap between handle and surface to accommodate a gloved hand. The idealized design of the rack handles is shown in Figure 9.

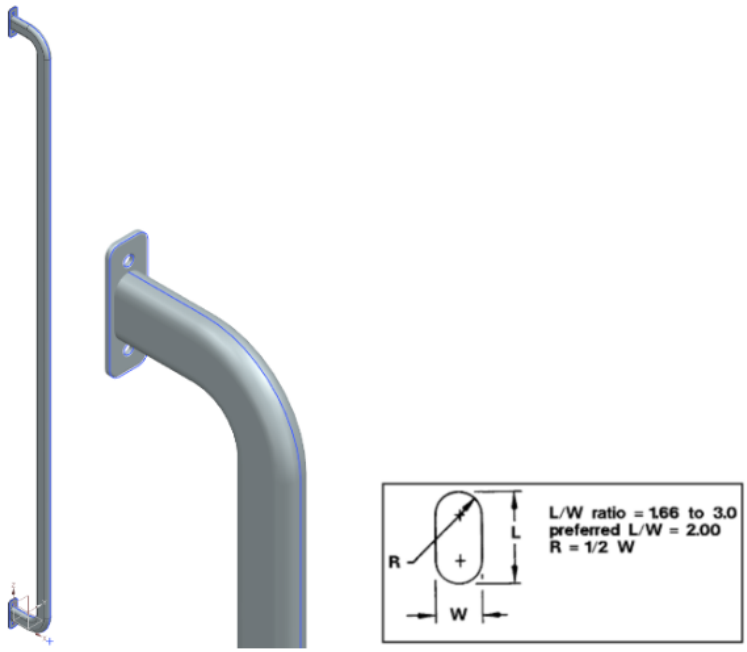

Figure 9: Ideal Rack Handle CAD

3.2.5 Mobility

The mobility subsystem provides PERRI with the ability to be smoothly and reliably moved within its operating environment. This will allow astronauts to configure the testing setup so that the rack can be in an optimized position within a habitation module. After moving the rack, astronauts will be able to lock its position to prevent any movement from external loads. Additionally, this subsystem is designed to structurally support the entire frame.

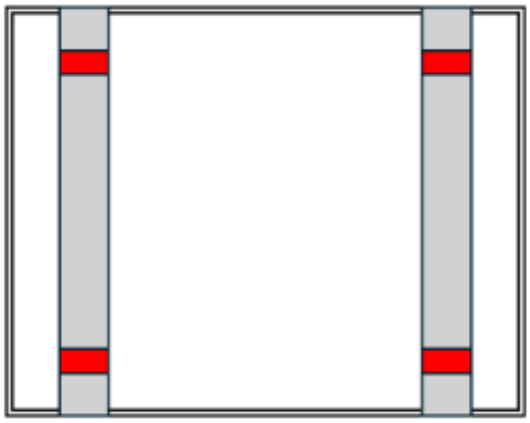

Figure 10: Rack Mobility Subsystem Footprint

Key Design Decisions The mobility method for the subsystem was chosen to be rubber wheels with brakes. In order to mount the wheels to the bottom of the 80/20 frame, the team designed a custom aluminum mounting plate where the wheels were kept below the floor of the rack. The bottom view of the footprint can be seen in Figure 10, where the red sections are the wheels. This mounting plate was necessary since all researched commercial castor mounting plates allowed the wheels to rotate far outside the footprint of the rack since it would be mounted to the center of the 80/20 bars. The mounting plate was decided to be two metal aluminum planks to provide support for the load and to minimize the mass of the plates. The hand calculations for the design can be found in Figure 11. This found that the design could support the full weight of the rack at Earth gravity with negligible bending.

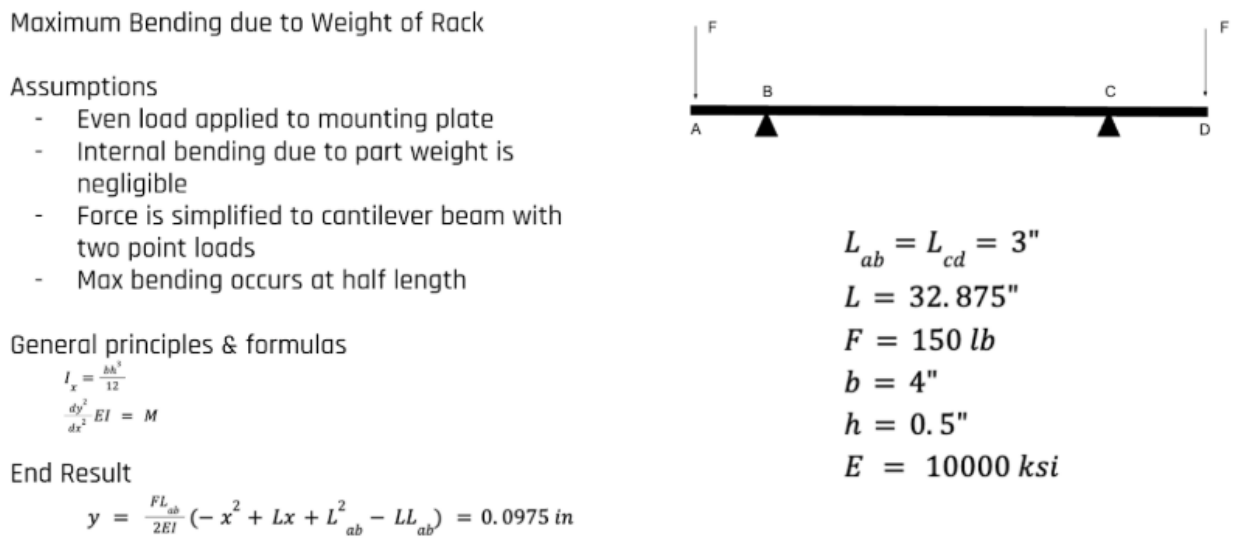

Figure 11: Rack Mobility Subsystem Hand Calculations

An additional spacer plate was added to the top of each wheel's mounting plate to increase the distance between the floor of the rack and the locking mechanism. This allowed for easy access to the locking mechanism. Prior to adding these spacers, the team found that users would have a hard time accessing the locking mechanism. This was caused by the fact that users needed to push down on the brake with the tight clearance.

Idealized Design Figure 12 shows one of the two mounting plates that will be mounted to the bottom of the rack. The mobility subsystem uses rubber wheels with brakes, and is mounted beneath the 80/20 frame using a custom aluminum mounting plate. This plate ensures that the wheels stay primarily within the footprint of the rack, preventing excessive rotation beyond the frame's boundaries. When the rack is locked in place, the wheels are rotated towards the front of the rack and can be locked by either stepping on them or by hand. The brakes extrude past the edge of the rack and are easily accessible in the standard configuration. The four castors allow omnidirectional movement while unlocked, while also providing support for the rack.

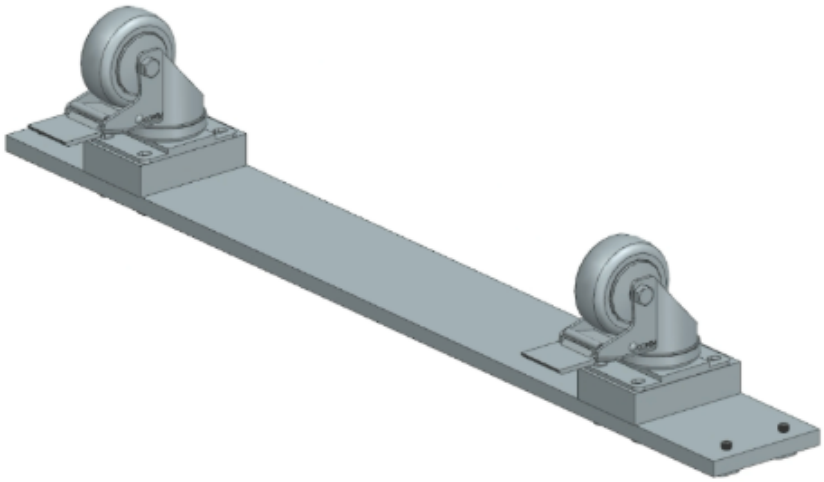

Figure 12: Idealized Mobility Subsystem Design

3.2.6 Sliding Rails

The sliding rails are intended to support the weight of the payload and allow it to slide in and extend out of the rack. We wanted the payloads to be easily removable, and after trade studies and research, we were able to choose a rail design that was detachable, to the function of payload removal from the rack as well.

Key Design Decisions After our trade study identified 80/20-compatible rails as the preferred method, we consulted with the experimental payload, human factors, and electrical subteams to address additional system criteria relevant to their needs. We asked about desired travel lengths, preferred payload orientations, and setup constraints to avoid interference with control interfaces, which were allocated to a specific rack area.

From these discussions, we determined the rails should extend far enough to make approximately $\frac{3}{4}$ of the payload depth accessible, requiring a travel length of at least $\frac{3}{4}$ the payload's length. We also decided to orient the rails to support the payload from either above or below using two rails, keeping the space between adjacent payloads clear to accommodate various payload geometries.

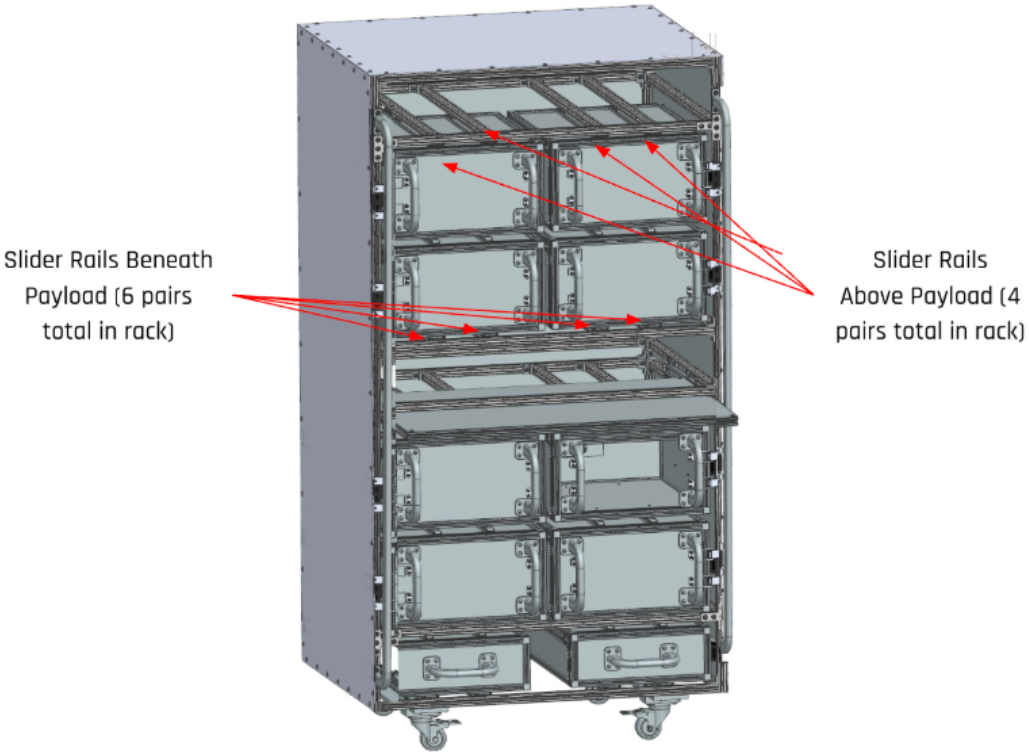

Figure 13: Sliding Rail Positions

The change in rail orientation raised concerns about the system's ability to support the payload, as this configuration differed from the rails' intended use. To address this, we contacted the manufacturer, who stated they could not guarantee the rails would support the load in our orientation. However, since similar rails had successfully supported comparable loads, we conducted hand calculations on a rail model rated to carry 100 pounds in a horizontal orientation, which we treated as the maximum allowable stress.

Using the stress formula σ=MyIσ=IMy, we adjusted yy (distance from the neutral axis) and II (area moment of inertia) to reflect the new load-bearing orientation. To simplify, we approximated the rail's cross-section as a rectangle, though it is actually crescent-shaped, and used the manufacturer's given dimensions.
Key dimensions from the 80/20 specification were:

- K (rail thickness, side view): 0.5" (12.7 mm)
- L (rail width): 1.798" (45.64 mm)
- B (travel length): 14.763" (375 mm)

For a conservative estimate, we used the thinnest section of the crescent-shaped rail for K, which measured 3.175 mm, to represent the worst-case scenario in our stress analysis.

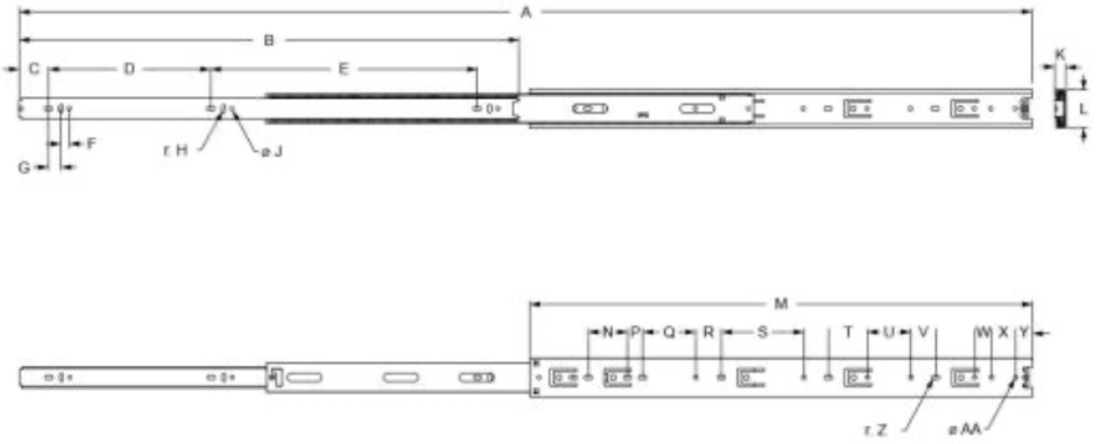

Figure 14: Sliding Rail From 8020.net

Our hand calculations showed the rails could support approximately 28.8 pounds—an underestimate, as we used the smallest thickness and ignored the rest of the crescent shape, which would improve structural stability. This 28.8-pound capacity included a safety factor of about 1.44, based on the requirement to support a 20-pound load (scaled from 133 pounds on Earth to lunar gravity). However, the calculated maximum deflection was about 6 cm, which was concerning. We trusted that the galvanized steel and rail geometry would perform better than the simplified calculations suggested, but decided that load testing would provide more accurate results.

As a contingency, we planned to add a third load-bearing rail on one side to replace the non-load-bearing roller rail, introducing a third attachment point and better distributing the load.

A key benefit of the selected rails is their compatibility with the 80/20 frame, thanks to attachment points designed to slot directly into the 80/20 structure. We mounted the rails to the frame and then to the payload locker. A side-view image in Figure 15 from shows this attachment method.

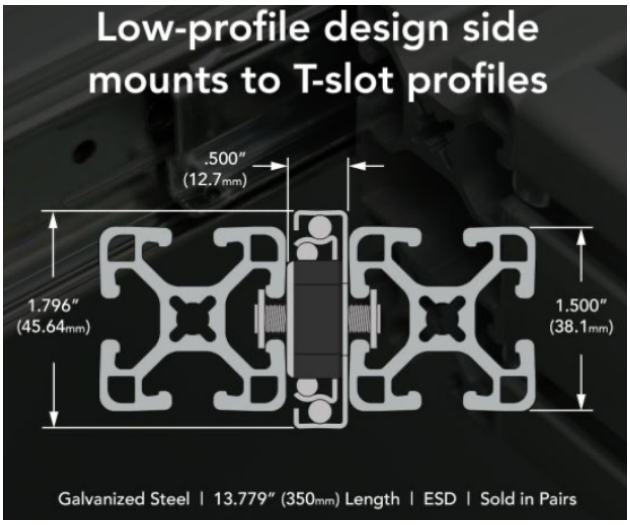

Figure 15: Sliding Rail Interface From 8020.net

The subsystem includes a feature that allows the most extended part of the rails to detach using a quick-release pin, accessible when the rail is fully extended. Flicking the pin disengages the section, and sliding it back onto the rail re-engages the latch, allowing normal extension again. This is essential, as it lets us attach the detachable section directly to the payload locker and remove it without disassembling the entire rail system.

We also implemented a redundant latching system to prevent payloads from falling out. The rails include a closing bumper that requires extra force to move once fully closed, helping to prevent unintentional extension due to accidental crew contact or vibrations during operation. These mechanisms are illustrated in images from the 80/20 website.

Figure 16: Sliding Rail Quick Release Mechanism and Closing Bumper From 8020.net

Idealized Design In the idealized system, the sliding rails would look very similar to the way it was described in the subsystem design portion of this report. Ideally though, as it is in the CAD, the rails would have a travel length of 17.5" rather than the rails for the prototype which have a travel length of 14.763." This extra length is particularly important for the smaller payloads that have a depth of 23.75" to allow for more of the payload locker to be accessed easily since the Human Factors subteam desired the travel length to be at least $\frac{3}{4}$ of the length of the payload. Figure 17 shows the idealized design in CAD.

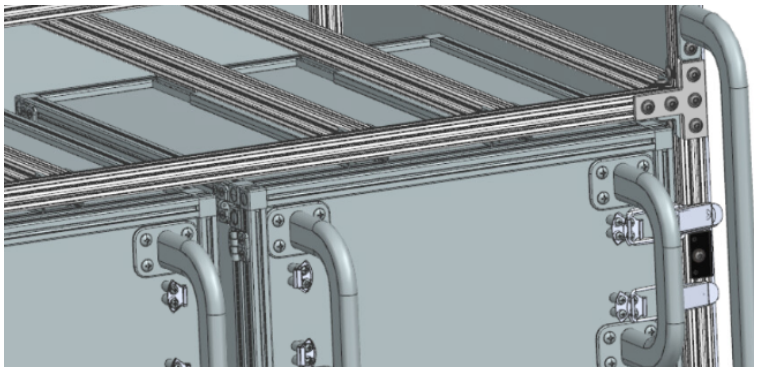

Figure 17: Sliding Rails in CAD Assembly

3.2.7 Desk

The purpose of the desk and rail system in the idealized rack is to support payloads or technical devices for astronauts to use during rack operations. It provides a stable, functional workspace within the constraints of the spacecraft environment.

Key Design Decisions The design of the desk and rail system was driven by structural performance requirements and mass constraints, supported by hand calculations and trade studies. The final decision was to select a desk thickness of 0.4 inches. This thickness strikes a balance between weight and deflection criteria. It meets the performance requirement with a deflection of 0.094 inches, just below the 0.1-inch acceptable limit, while also reducing the structure's weight compared to the initial design. This choice confirms that the desk remains within acceptable performance limits without unnecessarily increasing weight beyond operational needs. These decisions came about through the following hand calculations to determine the minimum thickness.

Deflection of a 0.5-inch Thick Aluminum Desk
Given:

- Desk dimensions: $L = 24$ in, $W = 39$ in, $h = 0.5$ in
- Desk weight: 45.65 lbs
- Payload weight: 20 lbs
- Elastic modulus of aluminum: $E = 10 \times 10^6$ psi
- Moment of Inertia:

$$I = \frac{bh^3}{12} = \frac{39 \times (0.5)^3}{12} = 0.40625 \text{ in}^4 \tag{1}$$

Deflection formula:

$$\delta_{\max} = \frac{WL^3}{3EI} \tag{2}$$

Substituting values:

$$\delta_{\max} = \frac{(65.65)(24)^3}{3(10 \times 10^6)(0.40625)} = 0.0745 \text{ in} \tag{3}$$

Since $\delta_{\max} < 0.1$ in, the desk will not bend noticeably.

Deflection of a 0.25-inch Thick Aluminum Desk
For $h = 0.25$ in:

$$I = \frac{bh^3}{12} = \frac{39 \times (0.25)^3}{12} = 0.0508 \text{ in}^4 \tag{4}$$

Substituting into the deflection equation:

$$\delta_{\max} = \frac{(42.825)(24)^3}{3(10 \times 10^6)(0.0508)} = 0.3885 \text{ in} \tag{5}$$

Since $\delta_{\max} > 0.1$ in, this desk will bend too much.

Minimum Thickness Calculation
Solving for h when $\delta_{\max} \leq 0.1$ in:

$$I = \frac{WL^3}{3E\delta_{\max}} \tag{6}$$

$$\frac{bh^3}{12} = \frac{(42.825)(24)^3}{3(10 \times 10^6)(0.1)} \tag{7}$$

$$39h^3 = 2,3681 \tag{8}$$

$$h^3 = \frac{2.3681}{39} = 0.0607 \tag{9}$$

$$h = \sqrt[3]{0.0607} = 0.393 \text{ in} \tag{10}$$

Thus, the minimum thickness required is $h \geq 0.40$ inches.

Because this thickness still contributed too much weight, the team chose to reduce the sheet to $\frac{1}{16}$ inch and compensate by adding 80/20 support rails underneath. This approach reduced overall mass while maintaining the required stiffness and functionality. The desk dimensions (24" × 39") and 2-$\frac{3}{8}$" overhang were selected to optimize workspace, while the 21-$\frac{5}{8}$" rail length allowed smooth extension and retraction. Mounting fasteners compatible with the 80/20 system were selected to support modular integration and mechanical stability.

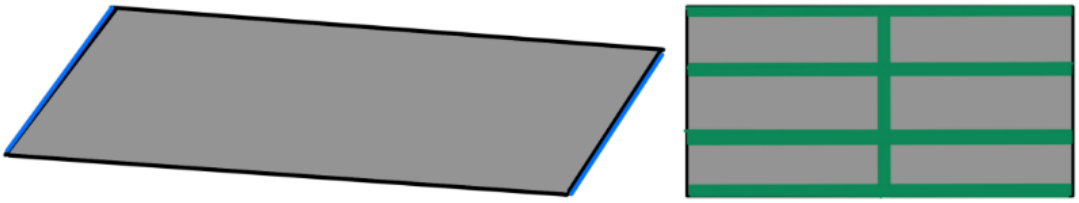

Figure 18: Desk Support Structure Layout

Idealized Design In an idealized lunar habitat, the desk and rail system would serve as a lightweight, modular workstation mounted inside a pressurized module. The system would be optimized for low-gravity operation, user stability, and flexible integration with other habitat infrastructure.

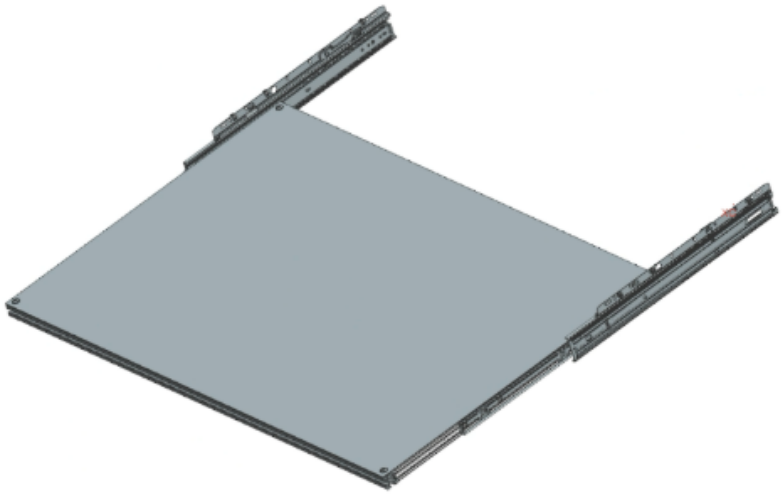

Figure 19: Top View of Desk CAD Model

The physical configuration of the desk subsystem consists of a thin 6061 aluminum work surface ($\frac{1}{16}$"), supported by a grid of 80/20 aluminum framing—as shown in the previous figures. The horizontal 80/20 rails run the full width of the desk and are mounted directly beneath the aluminum sheet to limit bending. Vertical 80/20 rails intersect the horizontal ones, forming rigid cells that distribute the load and reduce deflection in multiple directions. Additionally, the desk is mounted to the rack structure using mounting fasteners compatible with 80/20, allowing easy assembly or repositioning.

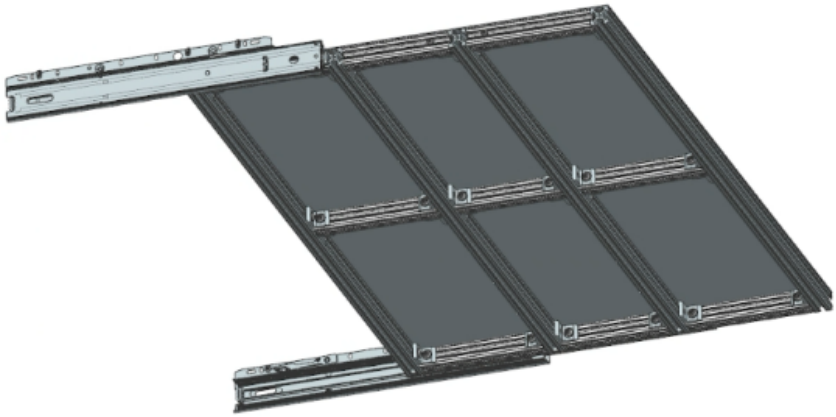

Figure 20: Bottom View of Desk CAD Model

For user interaction, the desk extends via a 21-$\frac{5}{8}$" rail to allow astronauts seated or standing to adjust position and reach without excessive movement—important in a low-gravity environment. Additionally, the 2-$\frac{3}{8}$" overhang when extended allows equipment or notebooks to be placed comfortably while maintaining support.

3.2.8 Roller Rails

The purpose of the roller rails is to ensure clear and efficient movement of the payload lockers to glide in and out of the rack as needed. The roller rail wheels line up with the sides of the payload lockers to align the single axis movement needed. The roller rail lengths match up with the inner dimensions of the frame (inside the 80/20 slotted bars), meaning they are 30.5" each.

Key Design Decisions 80/20 steel roller rails were chosen for their stability with ease of integration into the frame with compatible end caps for attachment. The capacity of 20 lbs per wheel (160 lbs per 30" section) solicits an operating mass range to ensure the payload locker does not exceed capacity. Between the compatibility of the roller rails with other 80/20 products used in the frame and stable mass operating range for the payload lockers, the roller rails were chosen for implementation.

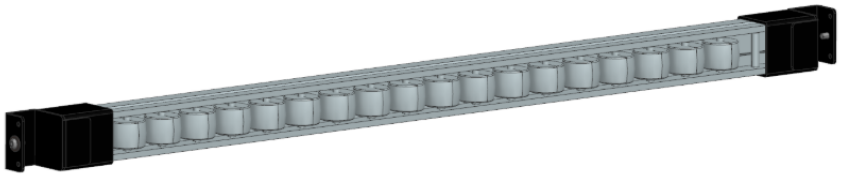

Figure 21: Roller Rail CAD

Idealized Design The roller rails attach to the exterior of the frame at the midsection of each payload locker. The design includes two rails and two payload lockers within the width of the entire frame, so it is imperative to ensure that there is enough clearance between the payload lockers when they are put against the roller rails. Figure 21 shows the roller rail assembly including the rail, endcap, and fasteners. Figure 22 shows two roller rails in the full rack environment with one adjacent to a payload locker and the other free to observe frame attachment. Figure **??** shows the wheels of the roller rail aligning with the side of a payload locker.

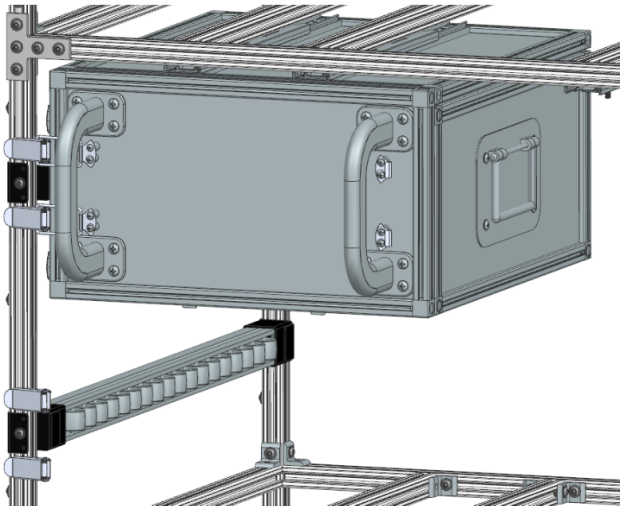

Figure 22: Roller Rails in Full Rack Assembly

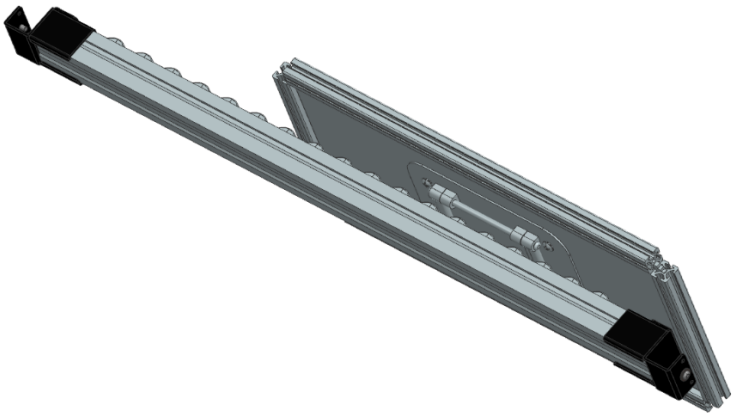

Figure 23: Roller Rail Alignment with Side of Payload Locker

3.2.9 Latch

The purpose of the latch system in the rack is to ensure that the payloads are secured, and will stay secured even when the rack is in movement or disturbed. The latch is also supposed to only allow access to the payload through a specific and intended action.

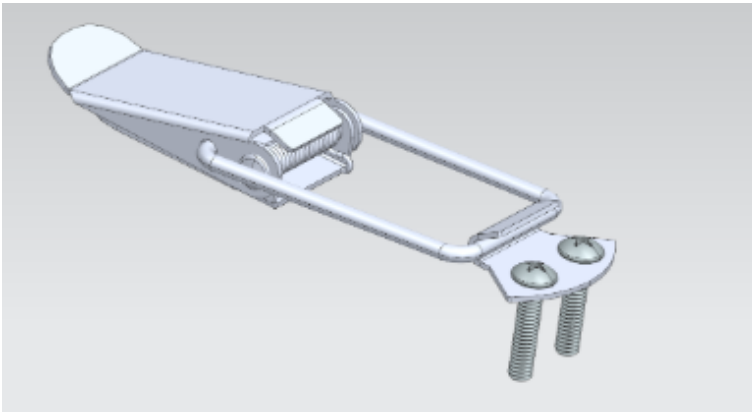

Figure 24: Latch CAD

Key Design Decisions We wanted a latch that was easy to use, sits on the external side of the payload, unlikely to get stuck, and of low complexity. Therefore, we decided to choose the toggle latch lock. The toggle latch utilizes a torsion spring with a hoop, and a hook for securing. This latch was chosen because it was easy to secure, and easy to assemble on the external side of the payload. For this specific latch design, the hoop is caught onto a hook. The two are positioned such that the only way for the hoop to move from the hook would be for the rear lever to be lifted to push the hoop forwards out of the hook's clasp. The lever is constrained down with a torsion spring, and lifting the back lever requires constant force in one direction. This means that in order to unlatch, the user needs to put constant nontrivial force in a specific direction towards a distance.

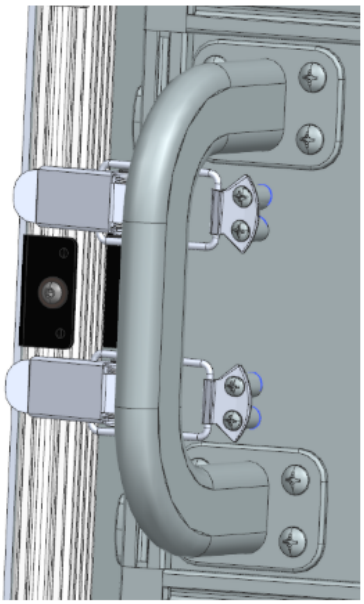

Figure 25: Latch in Rack Assembly

3.2.10 Payload Locker

The purpose of the payload locker is to support an experiment and provide storage space, while also enabling the conduct of additional research or experiments. It is designed to record and store sensor inputs on a common storage device, ensuring organized data collection and multifunctional use within a compact structure.

The payload handles are designed to provide a reliable and ergonomic interface for transporting and maneuvering the lockers in a lunar environment. Their purpose is to ensure safe handling, minimize operator fatigue, and maintain structural stability during movement. By following NASA heritage guidelines and using lightweight, high-strength materials like aluminum, the design balances durability with ease of use, enabling effective operation in both Earth-based testing and Lunar missions.

Key Design Decisions The design of the payload locker uses 20 mm 80/20 aluminum extrusions, which were selected for the locker frame to maintain compatibility with the main rack while reducing size for inner payload accommodation. Three-way and two-way corner connectors were implemented at the locker's edges, offering an additional 8 mm margin that facilitates smoother insertion and alignment along the slider rails. Slotted framing hinges were used as the opening mechanism for the front and top doors. For airtightness and structural integrity, 5 mm acrylic and aluminum panels were inserted into the 80/20 frame gaps to create a gas-tight seal. All components, including hinges, latches, and fasteners, were sourced from McMaster-Carr to ensure consistency, compatibility, and ease of procurement. The locker also includes front and top handles, in line with the 2D preliminary design, to support ergonomic operation.

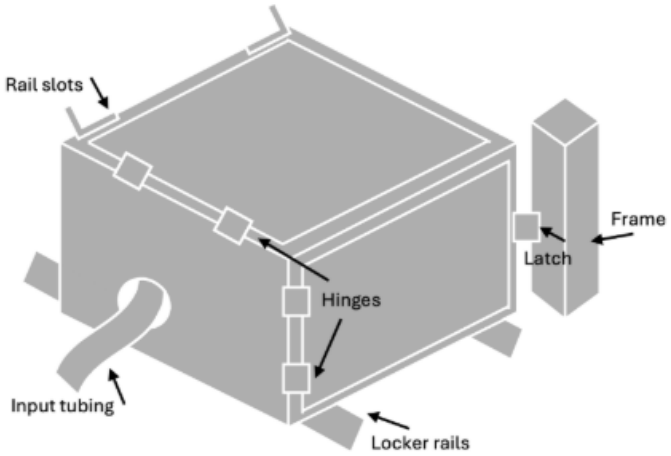

Figure 26: Preliminary Payload Locker Design

In designing the payload handles, we evaluated our choices based on the functionality, safety, and compatibility they would provide according to heritage systems. The idealized design consists of aluminum handles with dimensions of 8" in length, 0.75" in width, and 1.5" in depth. The handles feature rounded edges for safety, adhering to NASA standards for ergonomic gripping and human factors. This design assumes a high-strength, lightweight material that can withstand the operational forces expected in space environments, while also being comfortable and intuitive.

Trade decisions included material selection, handle geometry, mounting hardware (using $\frac{1}{4}$"-20 cap screws), and overall integration with the rack structure. These decisions were informed by a review of past NASA hardware, hand calculations, and human-factors considerations to ensure both safety and usability in the lunar environment.

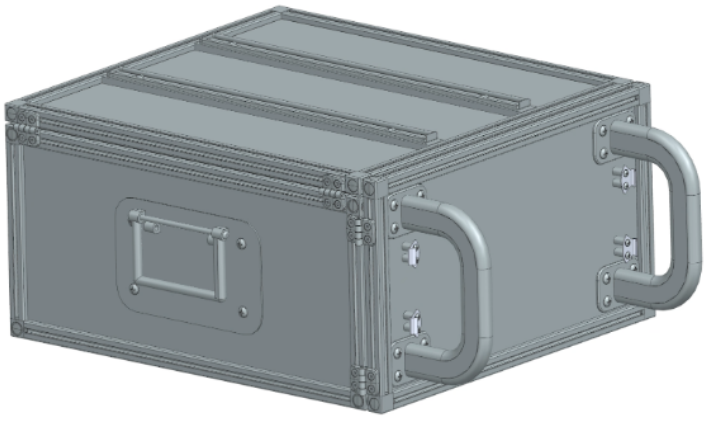

Figure 27: Payload Locker CAD (Orbiter Middeck Dimension)

Idealized Design Figure 27 shows the CAD of the idealized payload locker. There are two handles on the front to pull the locker out, and two side handles for moving it. As seen in Figure 28, doors can be opened from the front and the top, providing flexible access to the experiment in the payload. Furthermore, a custom gasket would be made for a gas-tight fit, which will contain

all gases involved in the experiment, keeping the interior environment secure and closed, and the outside environment safe from unwanted gases and dust.

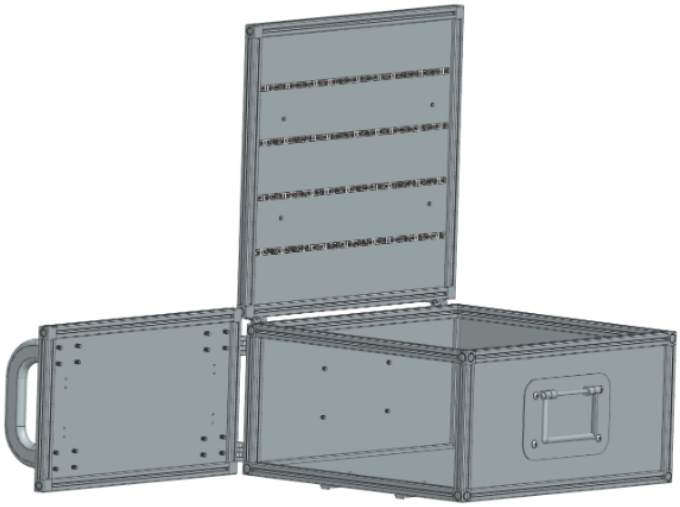

Figure 28: Open Payload Locker

In Figure 29, the side acrylic was hidden to reveal the interior of the idealized Orbiter Middeck Dimension payload locker. LED lights are installed at the top door for lighting the experiment, CO_2 sensors, and the Raspberry Pi camera for monitoring the experiment.

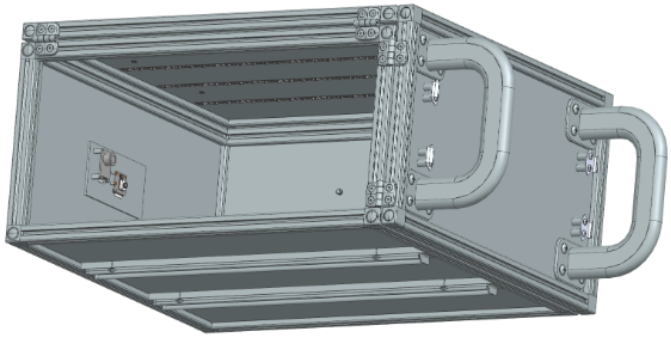

Figure 29: Inner View with 4 LED strips, CO_2 Sensor, and Camera

Figure 30 shows the key features include foldable side and ergonomic front handles, acrylic side panels for visibility, a top and front door for access, 80/20 aluminum framing for structural integrity, an integrated CO_2 sensor and camera, and LED lighting for internal illumination.

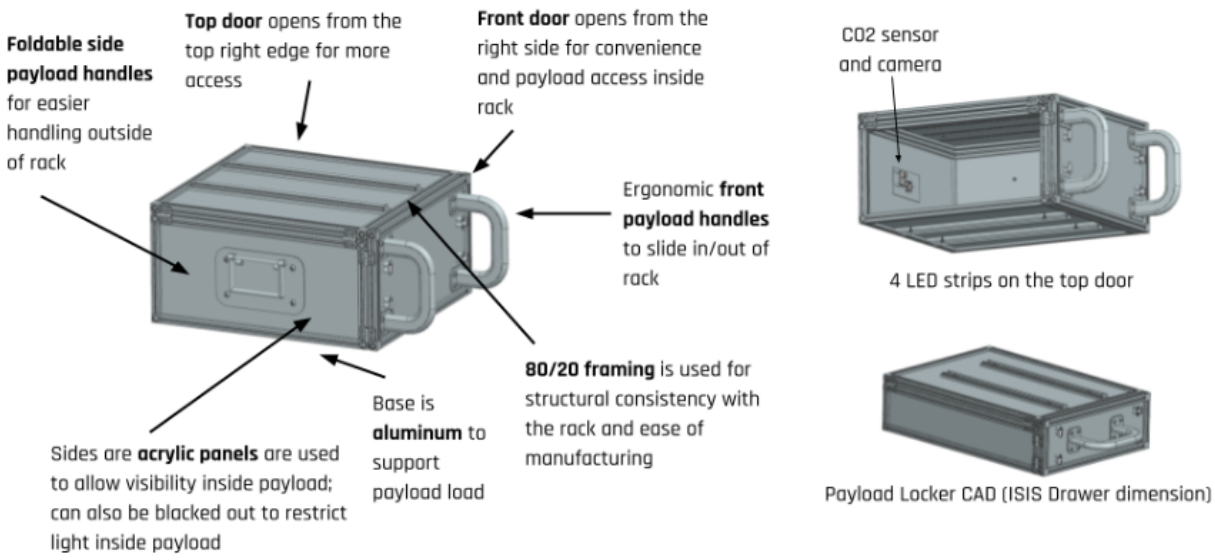

Figure 30: Payload Locker Specifications

Overall, the idealized design for the payload locker was designed through cooperation with the experimental design group, the human factors group, and our structural group, to create a payload locker that fulfills the system requirements between experimental and human factors, to create a design that's versatile, structurally sound and capable, accessible, and provides as much experimental productivity and human compatibility as possible.

The payload locker uses 20 mm 80/20 aluminum bars with dimensions of 18.125"(W) $\times$ 10.50"(H) $\times$ 20.50"(D), and features acrylic and aluminum wall panels. It includes top and bottom slide rails for flexible rack mounting, two front door handles, and foldable side handles for easy handling. A CO_2 sensor, a Raspberry Pi camera, and 4 strips of LED lighting are installed inside for environmental monitoring.

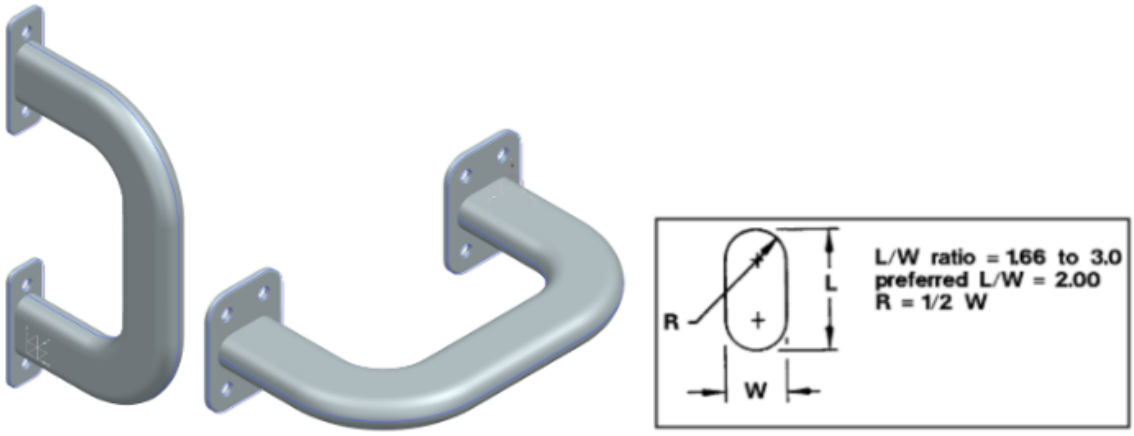

Figure 31: Payload Locker Handles

3.2.11 User Interface

We created a graphical user interface in Next.js, linked to the back-end through an http connection, to monitor and control the environmental settings within each payload.

Digital vs. Manual Controls Our first major digital design decision was to replace traditional manual controls with a digital user interface. This approach allows both the ground team and the lunar crew to access and modify the same interface and control system, which is especially important given the limited availability of the crew and potential periods of system dormancy or isolation. Digital controls also offer greater precision, as reflected in user feedback from our usability study (see Appendix B). To protect against accidental changes, digital interfaces confer an advantage through built-in safety features such as confirmation prompts and deliberate navigation pathways to editing settings.

Figma Design Before coding our design, we prototyped possible UI designs and interactions on the design on Figma, an online design tool. Our final design is shown below.

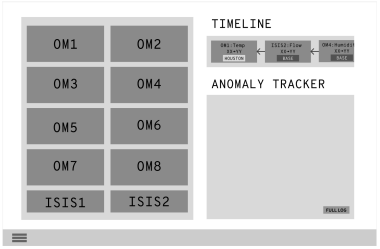

(a) Landing Page

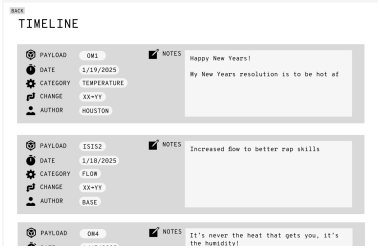

(b) Timeline Page

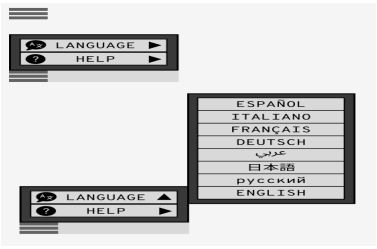

(c) Idealized Language Support

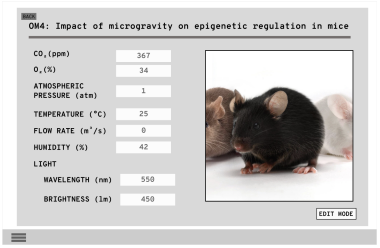

(d) View Payload Page

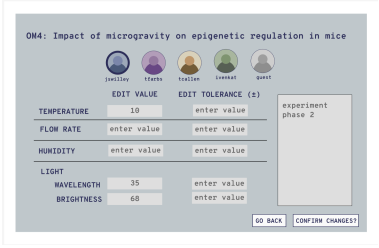

(e) Edit Payload Page

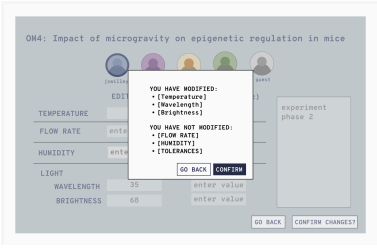

(f) Edit Payload Confirmation

Figure 32: Figma Final Design

Usability Study and Iteration To characterize and iteratively improve our front-end design, we conducted an IRB-approved usability study on 24 participants, expanded in section 6.4. The data collected included task completion time, task accuracy, NASA Modified System Usability Scale (NMSUS) scores, and qualitative feedback. We collected videos of user screens as they navigated through their task, and audio recordings of users answering qualitative feedback questions.

Landing Page The main page of our user interface prioritizes simplicity and reducing the cognitive load on the user through the principle of gray-out. It features a graphical mimicry of the rack and its two payload drawer types–Orbital Middeck (OM) lockers and International Standard Sub-rack Interface (ISIS) drawers. The timeline on the upper right allows one to view the most

recent changes pushed to the payload in chronological order. The font was changed from the Figma to keep in line with copyright. The caption below was an addition based on usability testing, which had shown great confusion in the way people thought the progression of time was displayed (see Appendix B for more detailed testing results). An idealized version would include additional language support using internalization to fully support all astronaut backgrounds.

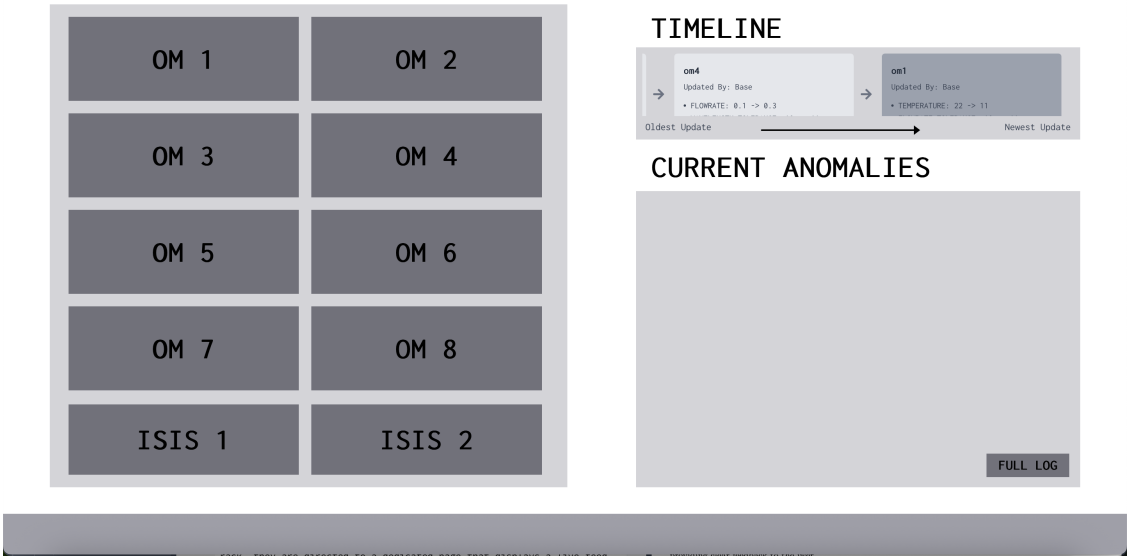

Figure 33: UI Landing Page

Full Timeline Page If a user clicks on one of the payload chips in the interface, they are redirected via a hyperlink to a dedicated timeline page that is specific to the selected payload. This page displays a full history of changes related to that payload, allowing users to scroll through all modifications made. Changes from the Figma design include the removal of icons to increase simplicity and reduce crowding.

Figure 34: UI Timeline Page

View Payload If a user clicks on one of the payloads in the graphical mimicry of the rack, they are directed to a dedicated page that displays a live feed of the payload's environmental data, streamed via an HTTP connection to the backend. This page also includes a live camera view of the payload, allowing astronauts to monitor experiment status without physically opening the locker. In an ideal system, the lunar crew would select which data and video streams to downlink to the ground team in advance, as continuous streaming to Earth would be impractical.

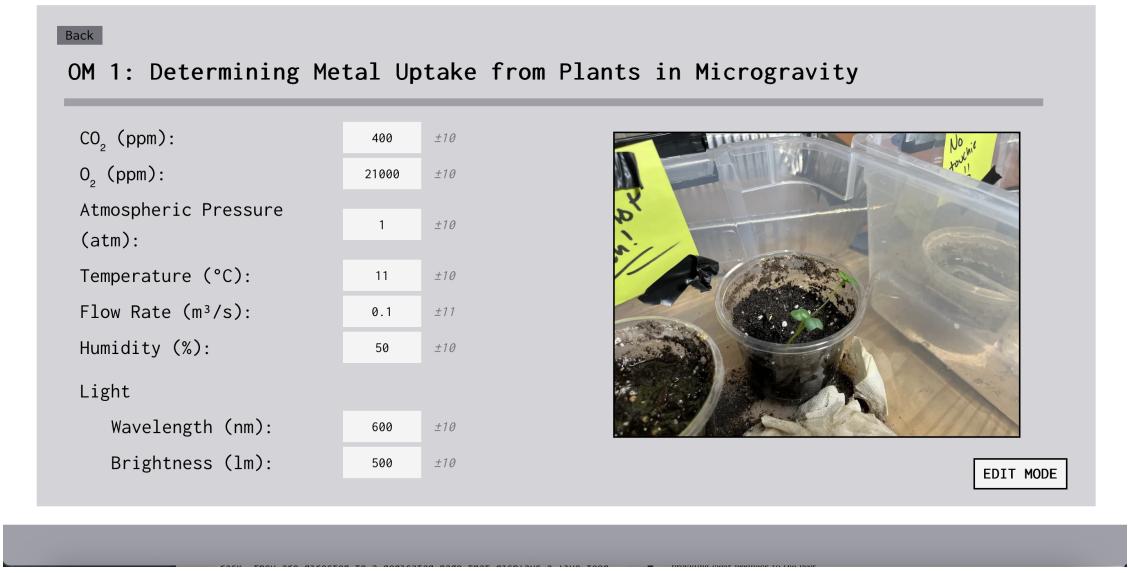

Figure 35: UI View Page

Edit Payload Users can enter Edit Mode to modify the environmental settings of a payload, assign their profile, and leave notes about their changes. The Edit Mode button is deliberately placed in a corner and styled with a contrasting color and font to stand out visually - ensuring

users engage with it intentionally and reducing the risk of accidental edits. Upon entering Edit Mode, a popup message confirms which settings have been changed and which remain unchanged, providing clear feedback to the user. After usability testing, the selection of user profiles was made mandatory, units were included, and whether notes were made was included in the confirmation popup.

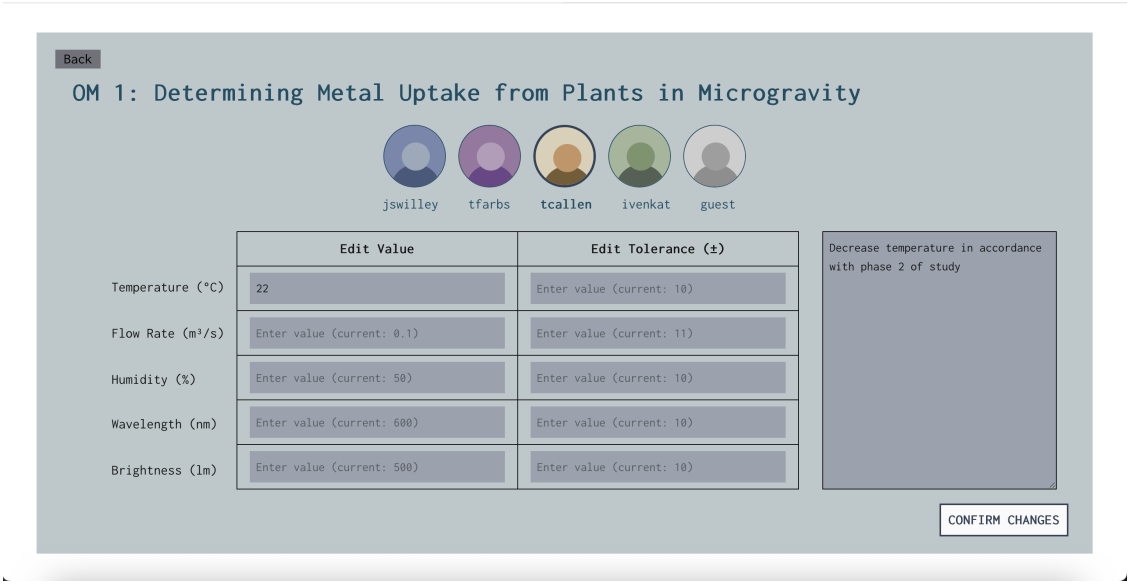

Figure 36: UI Edit Page

Anomaly Mode If an anomaly is detected in the back-end, the entire user interface dynamically changes in both color and layout to attract attention, shifting from its usual grayed-out state to a more alerting design. The updated page prominently displays the time of detection, the specific error identified, and a suggested course of action for the user to take. Usability testing showed confusion surrounding the meaning of the color gray, which was supposed to refer to a past error. Therefore, we changed the title from "Anomaly Tracker" to "Current Anomalies", and moved all gray errors to the full log. Additionally, an idealized anomaly mode would communicate with backup manual controls to include audio warnings as well.

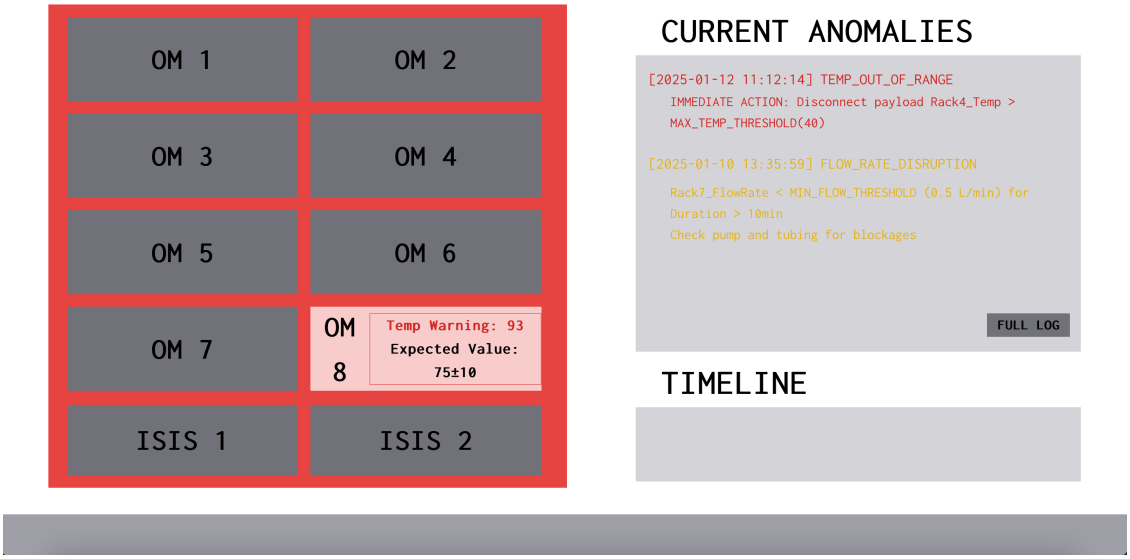

Figure 37: UI Anomaly Page

3.2.12 Habitation System

The habitation system provides essential environmental support for a wide range of scientific experiments, particularly those involving botanical life. As shown in Figure 38, the habitation system maintains controlled conditions by manipulating temperature, humidity, air flow, and light levels. The habitation system also contains the capabilities for fire detection, manual removal of liquid waste, and exhaust of gaseous waste. By replicating Earth-like conditions, the habitation system can enable long-duration studies. supporting a range of biological research on the lunar surface.

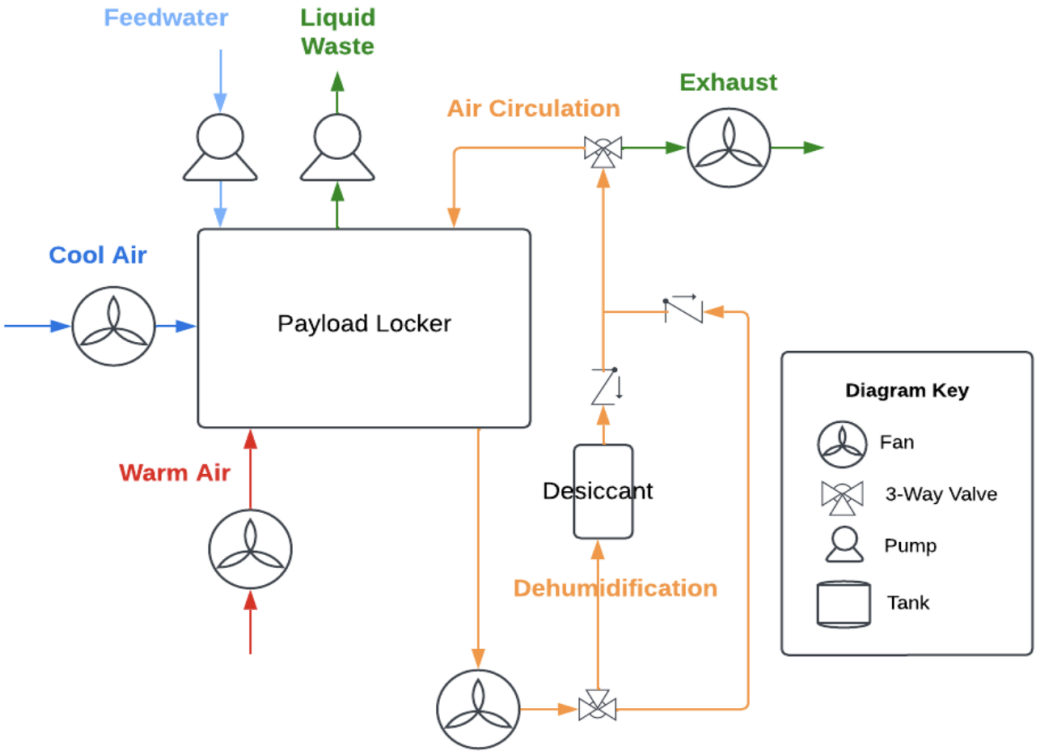

Figure 38: Habitation Piping and Instrumentation of a Single Payload Locker

Temperature Regulation In an idealized system, the rack would pull cool air and warm air from the lunar habitat. The warm or cool air would be funneled into the payload lockers with the help of fans aft of the payload locker. Within the lunar habitat, the rack's integrated thermal control system would distribute heat where needed and remove excess heat from areas that become too warm. If sized correctly, this design could eliminate the need for separate, localized heating or cooling units within the lunar habitat. By centralizing temperature regulation, the system can operate more efficiently, reduce energy consumption, and simplify maintenance and system architecture.

Manual Waste Removal The manual waste removal system would consist of a peristaltic pump that is easily accessible to the crew. The selected pump could operate with many settings. As such, this would allow the pump to process spills of all volumes, as well as a wide array of ratios of sediment to liquid.

Feedwater The feedwater system consists of a self-sealing pump and a spray interface that is integrated into the payload locker wall. The feedwater system would be automated and manual, working to automatically provide humidity or feedwater to the payload housed inside the locker. The user can input a frequency at which feedwater could be distributed, or could manually dispense water if desired.

Air Circulation and Dehumidification An idealized system for air circulation and dehumidification would consist of an inline fan, a desiccant fitting with backflow prevention in the form of check valves, and an integrated exhaust line with a fan. In addition, a pressure relief valve will be installed upstream of the inline fan, as air exits the payload, to prevent high-pressure airflow from entering the fan or for gaseous waste to be vented. The desiccant fitting would be filled with silica gel that would require replacement at pre-determined times depending on how often humidity would need to be scrubbed. Through the use of sensors, humidity scrubbing could be bypassed through the use of a three-way solenoid valve that would direct flow to bypass the desiccant fitting.

3.2.13 Electrical System

The electrical system of the proposed model is designed to allow easy monitoring, control, and configuration of each payload through its user interface (see Section 3.2.11), while also supporting autonomous regulation of each locker's internal environment via the habitation components (see Section 3.2.12). To accomplish this, the design follows that of a distributed system, relaying commands from the user interface, through a managing controller, and to their respective payload lockers (Figure 39).

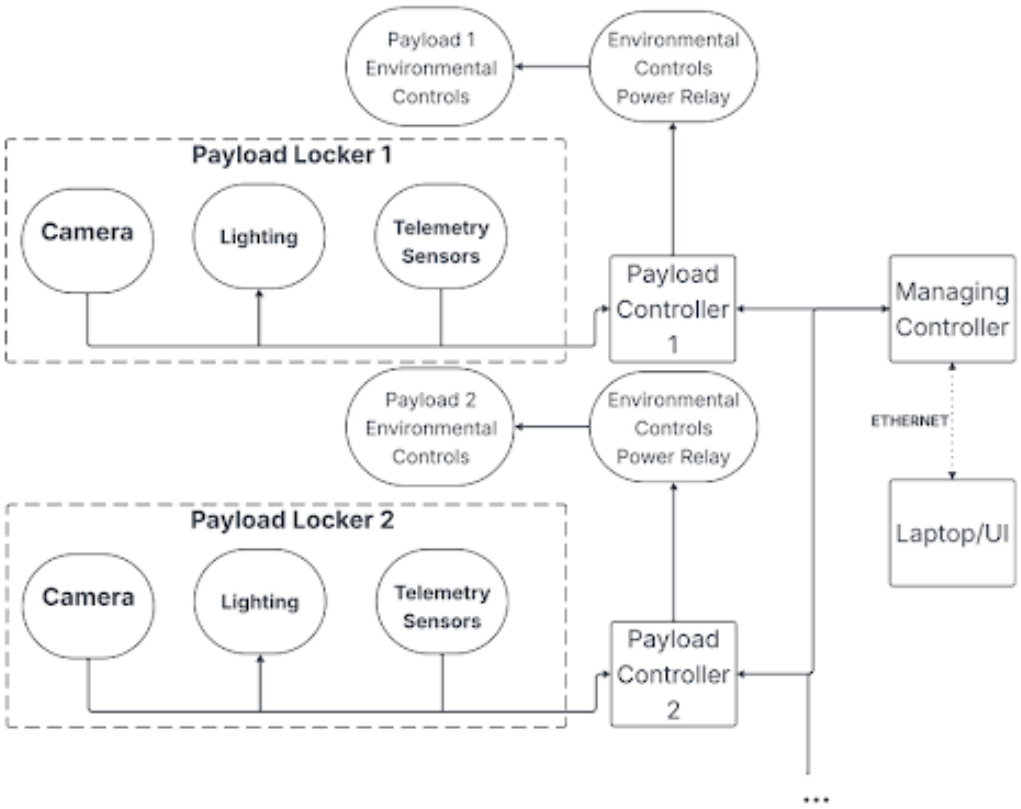

Figure 39: Communication and power flow between the user interface, central controller, and individual payload subsystems.

Laptop and User Interface Beginning with the client-facing component of the electrical system, a laptop hosts the user interface. Through an Ethernet connection with the system's managing controller, the laptop receives data on the status of each locker and its environment. Furthermore, it sends user-inputted configuration commands back to the managing controller for relay to the appropriate locker.

Managing Controller The managing controller functions as a communication switch between the laptop and the payload (worker) controllers. In addition to handling data exchange with the laptop, it provides the same function for each payload controller, because it is connected in parallel to all worker controllers, each of which corresponds to a dedicated payload locker. The architecture allows the laptop to require only a single point of connection to communicate with all payloads, reducing the laptop's overhead and necessary bandwidth.

Payload/Worker Controller Each payload locker is equipped with a dedicated payload controller. Each payload controller interfaces with the payload's sensors, camera, lighting, environmental controls, and the managing controller. Given the data received from sensors within the payload and the specified environmental configuration (e.g. desired temperature and humidity), each payload controller has the ability to independently and autonomously compare sensor readings to the environment configuration and adjust the environment accordingly by activating the appropriate environmental control mechanisms. In addition to regulating the locker environment, each payload controller forwards sensor data and a video stream to the managing controller to be retrieved by the laptop and displayed on the user interface.

Sensors and Lighting To allow for a comprehensive description of the internal environment of the locker, the following data is recorded with sensors within the locker: temperature, humidity, pressure, and air composition (oxygen, carbon dioxide, and carbon monoxide). Each locker is also equipped with a camera for visual monitoring and internal lighting to ensure consistent image quality.

4 System Prototyping

4.1 Structural Prototype

The prototype design section will talk about an adapted version of the idealized system that was used for testing. This prototype was used to test design decisions, characterize the system, and conduct load and functionality testing. Table 2 below shows the key differences between the idealized design and the structural prototype. Following sections below go into more detail by subsystem.

Part	Prototype Change	Reason for Change
Latches	None	—
Slider Rails	None	—
Frame	Crossbars to replace shell	Reduce prototype cost
Shell	Removed	Reduce prototype cost
Rack Handle	Wood handles	Ease of manufacturability
Roller Rails	None	—
Desk and Rail	None	—
Payload Locker	Frame only	Only needed for human factors testing

Table 2: Idealized vs. Prototype Similarities and Differences

4.1.1 Frame Prototype Design

The prototype design as seen in Figure 40 was nearly an exact replica of the CAD design, using 80/20 T-slotted profile. While some slight error in the dimensions may have been made, key dimensions and profiles as seen in the CAD model were included in the prototype rack frame. Additionally, cross members on the sides of the frame were added for structural support as there is no shell over the frame like designed for the idealized version.

Figure 40: Prototype Rack

4.1.2 Shell Prototype Design

Instead of constructing the shell onto our prototype, testing was conducted through finite element analysis.

4.1.3 Rack Handle Prototype Design

For our prototype, we chose to use pine wood shaped in a circular form to simulate the motion and handling of the final rack design. While this material and geometry did not exactly match the aluminum structure intended for the final version, it served as an effective stand-in for initial testing. The pine wood prototype was lightweight, easy to assemble, and allowed us to focus on evaluating horizontal forces encountered when moving the rack. This approach gave us valuable insights and helped identify potential adjustments needed for the final design. The differences between the prototype and the idealized design were necessary for efficient testing in developing and modifying our final design. These are summarized in Table 3.

Feature	**Prototype**	**Idealized**
Material	Pine wood	Aluminum
Shape	Circular	Rounded out rectangle
Strength and Durability	Low strength and flexible with force	High strength, suitable for pulling a lot of weight
Ease of Assembly	Easy and quick to assemble when bought as a pole	Requires precision fabrication and tools
Weight	Lightweight	Heavier
Functionality	Simulates movement and basic handling	Supports full load and end-use conditions
Cost	Low-cost, ideal for rapid prototyping	Higher cost due to material cost and manufacturing details
Testing Focus	Horizontal force and movement simulation	Full structural and functional testing
Mounting	Use brackets to slot into the 80/20	Use mounting with 2 screws per bracket

Table 3: Idealized vs. Prototype Rack Handle Similarities and Differences

Pine wood was selected as a substitute for aluminum due to its lower cost, ease of assembly, and suitability for rapid prototyping. While it did not replicate the structural strength of the final material, it allowed the team to focus on evaluating the motion and ergonomics of the rack, particularly how horizontal forces would be applied during movement. The circular shape of the prototype served to approximate the intended functionality without requiring full-scale fabrication. Additionally, the lighter and more manageable material ensured safe handling and quick modifications, enabling timely adjustments based on test results. These differences provided accommodated project constraints related to time, cost, and resources.

4.1.4 Mobility Prototype Design

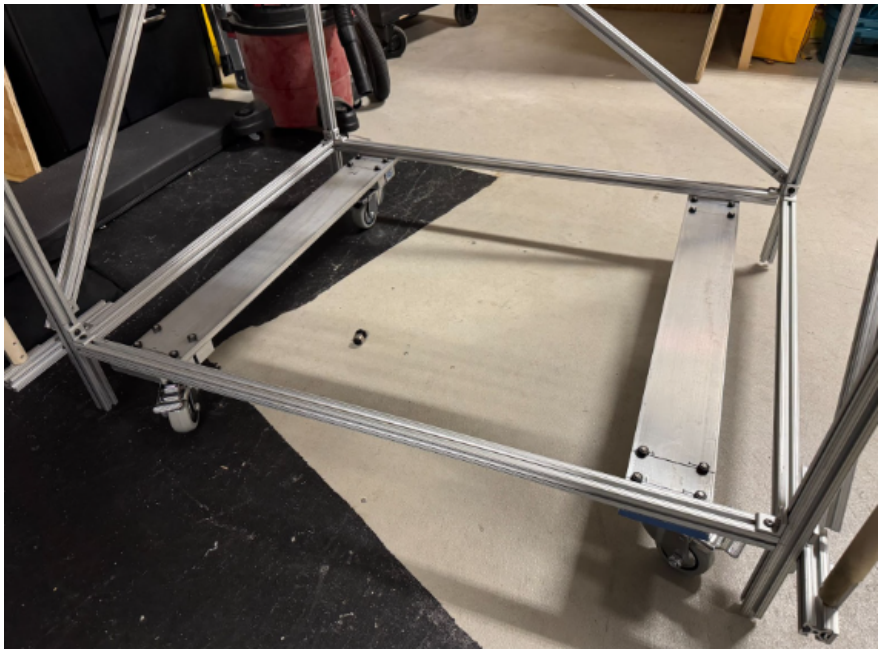

Figure 41: Prototype Mobility

The design for the prototype is currently extremely similar to the idealized design. While there are changes that will be suggested in the path to flight section, the idealized design contained no complications that made it impossible for the team to build. However, there were minor changes to the spacers due to the available materials at the time of building them. Since the spacers were added later in the design process, the team did not have the correct sized aluminum bars to use as the spacers. However, the team did have access to smaller blocks of material that could be combined to form the same shape as the idealized spacers with the same dimensions. The prototype spacers ended up consisting of four separate spacers for each screw. Additionally, the spacing between these spacers was small, leading to the combined load profile on the spacers themselves to be extremely similar.

4.1.5 Sliding Rail Prototype Design

Figure 42: Prototype Sliding Rail

The prototype has the same rails as described in the subsystem design section since this is the exact model we bought. The only difference between this rail and the CAD, which is representative of the idealized version, is that the CAD has the longer rails, as mentioned in the Idealized Design section. Consequently, the idealized rails would also have more bolts, and attachment components like T-slots and nuts than were used on the prototype. As long as the rails are properly scaled

in strength rating to provide extra support towards the moment experienced at the end of fully extended rails, then the behavior should be similar to that of the behavior that can be observed from the testing that occurred on our prototype.

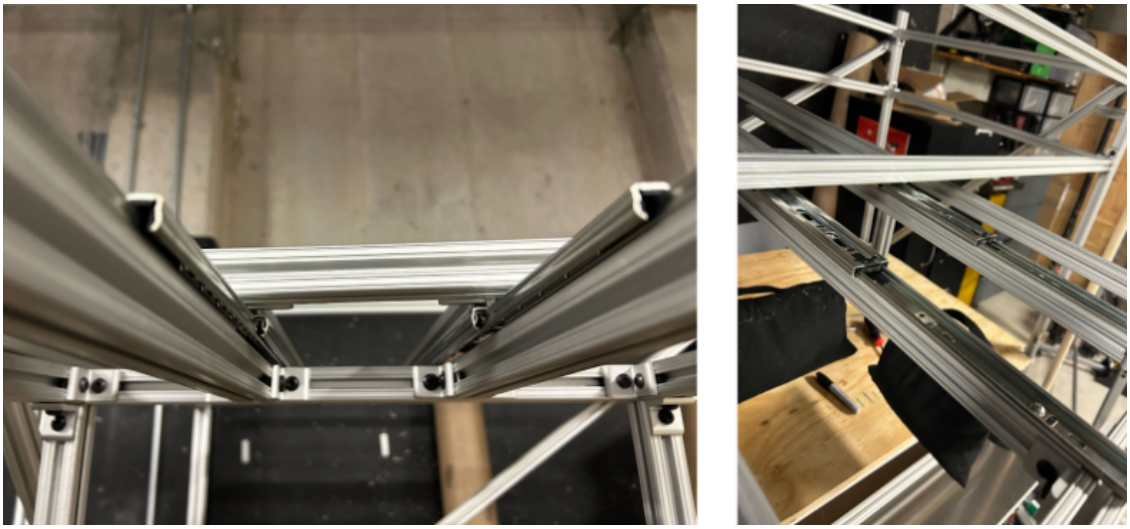

Figure 43: Left: Front View of Rails Extended, Right: Isometric View of Rails Extended

4.1.6 Desk Prototype Design

The prototype design retained the same $\frac{1}{16}$" thick 6061 aluminum sheet and rail mounting system as the idealized configuration but removed several internal 80/20 support beams from the center of the desk. This change reduced the total weight of the structure, which was necessary because the sliding rails used during Earth-based testing could not support the full load of the original configuration under gravity. While the idealized design includes three horizontal 80/20 beams across the underside of the desk to maintain structural stiffness in a microgravity environment, the prototype omitted these to avoid exceeding the load-bearing capacity of the rail system. As a result, the prototype had a lower load capacity and was not intended to replicate the full astronaut interaction forces expected in the lunar habitat. Instead, the focus was on demonstrating basic functionality, such as sliding, extension, and structural integration within the frame. These differences were crucial for accommodating Earth testing conditions, where gravity significantly affects the forces acting on the desk and rails.

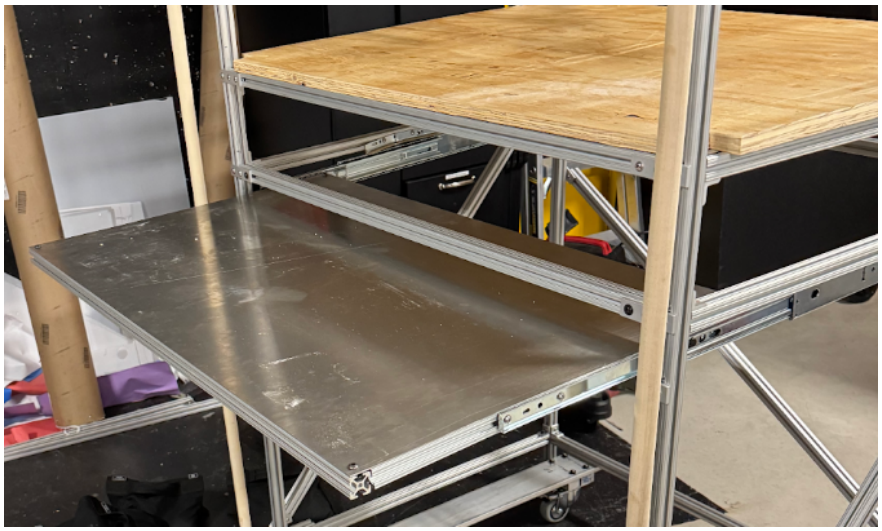

Figure 44: Prototype Desk

4.1.7 Roller Rail Prototype Design

The roller rail attachment endcap did not exactly match the model that was used in the CAD, but the measurements matched up in terms of placement of the rail. The prototype frame dimensions were slightly larger, so the length of the roller rail was increased from 30.5" to 31.4". Figure **??** shows the prototype roller rail implemented onto the rack with the exterior payload locker shell adjacent to the guiding wheels.

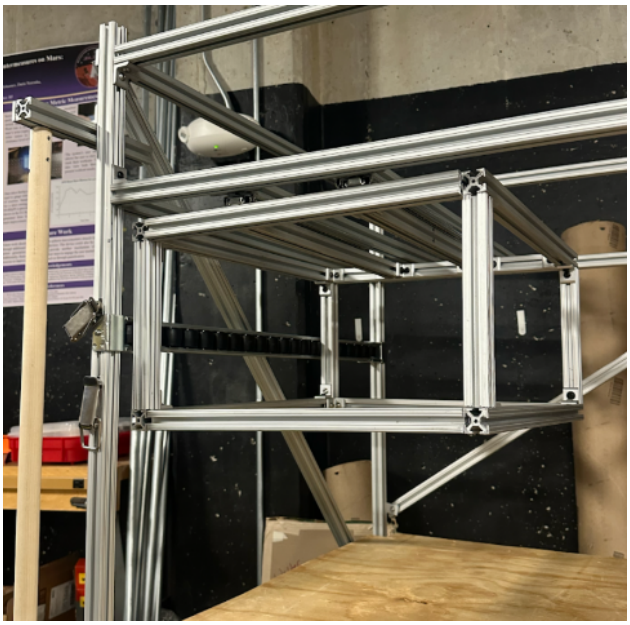

Figure 45: Prototype Roller Rail in Assembly

4.1.8 Latch Prototype Design

For the prototype design, toggle latches were purchased. These latches were similar enough to the ideal design, although the stationary part of the latch crosses into the locker's path of motion. This led to the latch being placed on an angular position to ensure free movement of the payload locker as seen in Figure 46.

Figure 46: Prototype Latch in Assembly

4.1.9 Payload Locker Prototype Design

The payload locker was built using 80/20 aluminum, having dimensions of 18.125" width, 10.50" height, and 20.50" depth. It was made to be a model of the largest payload locker that the rack was designed to handle. Only the cubic frame was put together for the sake of time, resources, and manufacturability.

Figure 47: Prototype Payload Locker

The prototype differs from the idealized payload locker in several key ways, as it was built solely for testing purposes. It does not include the acrylic and aluminum wall panels or the front and side handles, since these features were unnecessary for the planned tests and would have added significant fabrication time. Instead of the 20 mm 80/20 aluminum used in the idealized design, the prototype frame was constructed with 1-inch 80/20 bars. Additionally, the three-way and two-way corner pieces were omitted, as the prototype was only intended to validate payload handling and sliding into the rack frame. Unlike the idealized version, which would be manufactured with precision tools like a mill or CNC machine to meet tight tolerances, the prototype was assembled with basic cutting methods and lacks high manufacturing accuracy.

4.2 Bench-Top Prototype

The purpose of the bench-top prototype is to test the electrical and habitation capabilities of the rack. By removing the plumbing and electrical subsystems from the rack structure, this can allow for rapid prototyping and better visualization of the system for testing.

4.2.1 Deviations From Ideal

The bench-top prototype will use components analogous to that of the rack on the lunar habitat. Since we do not have access to the spaceflight qualified components, it is important to note that the components used on the bench-top prototype will be used for characteristic testing and preliminary verification of the habitation system. The bench-top prototype will feature input and output consumables different from those of the idealized rack as outlined below in Table 4.

Consumable	**Idealized**	**Bench-Top Prototype**
Feedwater	Lunar habitat potable water source	Bucketed water supply
Cool Air Input	Lunar habitat AC line(s)	Beverage cooler with ice
Hot Air Input	Heat sources throughout lunar habitat	Patch heated hot air tank
Power	Designated power supply	Separate power for each component
Liquid Waste Output	Lunar habitat waste management system	Routed to liquid waste bucket

Table 4: Bench-Top Prototype Deviations From the Idealized Design

The payload locker used for bench-top prototype testing was a lower-fidelity model that aimed to maintain the idealized dimensions and materials without including features that did not have functionality in the payload capability tests. These differences are outlined below in Table 5.

Idealized Design	Prototype Design
Airtight seal using gaskets or epoxy	Resign / hot glue, not verifiably air tight
Payload access doors on the top and front of locker	One access point on top of locker via removable acrylic panel
All plumbing located aft of the payload locker	Plumbing connections spread throughout various locations on the locker
Handles on front and sides for easy removal from rack	No handles and no attachment to the rack

Table 5: Design Differences Between Idealized and Prototype Payload Locker Designs

There were no handles or front door, and no connection to the sliding rails. We created an 18.125 x 10.5 x 20.5 inch box made out of 80/20 and acrylic panels. We used straight brackets to connect the 80/20 and silicone and hot glue to seal the edges and corners.

Some components not shown on the CAD include the holes on the back and sides to connect all the other subsystems. Also, the top panel has a removable smaller panel with a handle, allowing us to open the box and place the payloads inside.

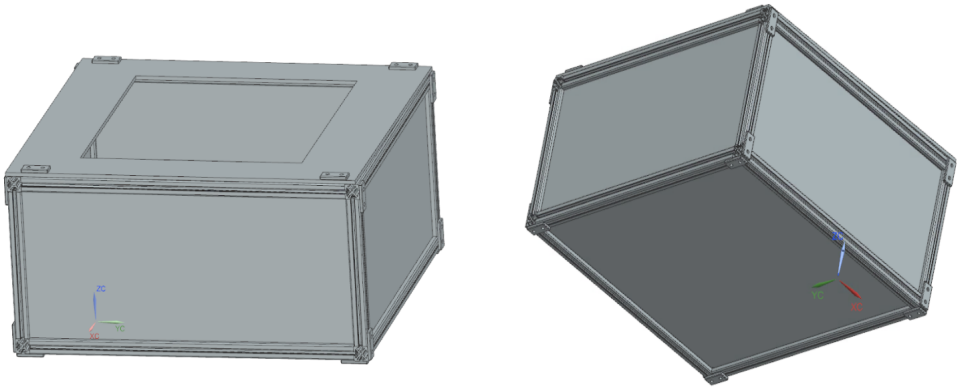

Figure 48: Top and Bottom Views of Payload Locker Prototype

4.2.2 Subsystem Design and Capabilities

This section will describe in greater detail the electrical and habitation subsystems as designed, built, and tested for the bench-top prototype.

Overall, the bench-top system is constructed with heating, cooling, liquid waste removal, feedwater, air circulation and dehumidification, payload lighting, and fire detection subsystems. These systems were secured to a wooden test bench as displayed in Figures 50 and 49. Withholding the liquid waste removal, air circulation systems, and feedwater, the systems are supported by a combination of microcontrollers, sensors, and power relays that facilitate the real-time monitoring and automated control of the locker's environment as is modeled in Figure 51.

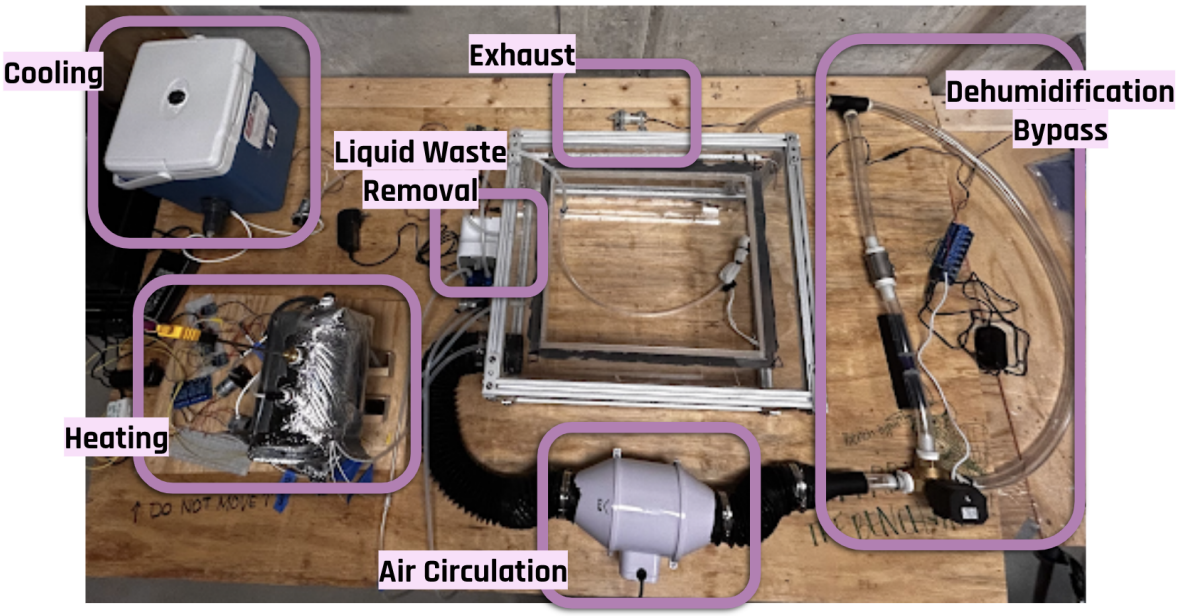

Figure 49: Bench-top Subsystems

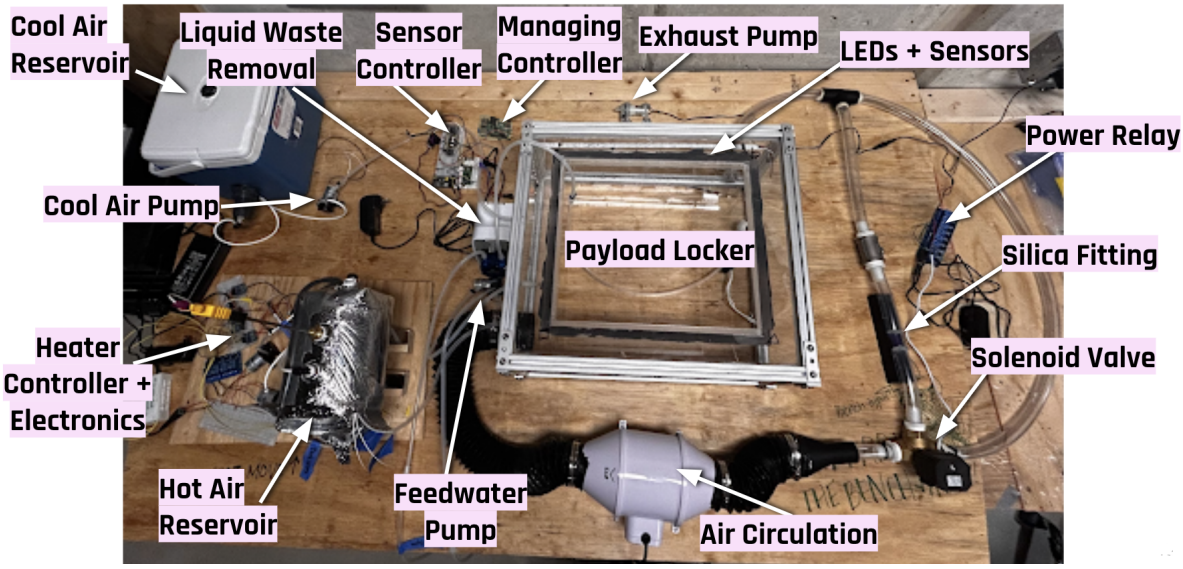

Figure 50: Bench-top Key Components

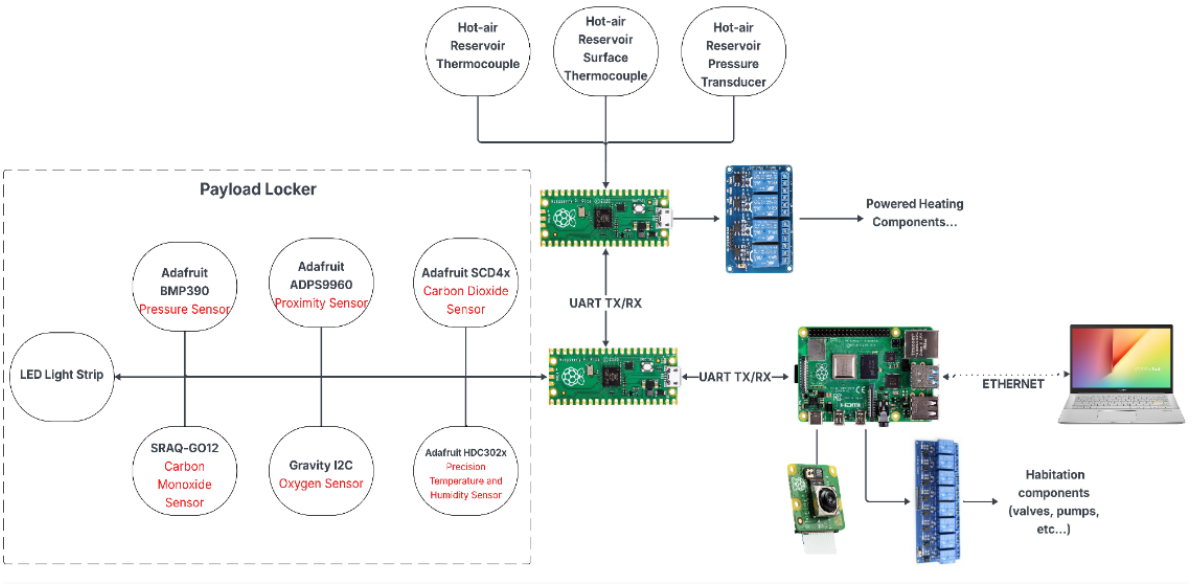

Figure 51: Bench-top Electrical Components

Microcontrollers The bench-top prototype is made up of three microcontrollers: one Raspberry Pi Pico dedicated to monitoring and controlling heating system, a second Raspberry Pi Pico dedicated to reading and forwarding the values from the sensor suite within the payload, and a Raspberry Pi 4, which activates environmental controls based on sensor readings and hosts the web server that the user interface uses to send commands and retrieve data.

Sensors To enable comprehensive monitoring of the locker's environment, the interior of the locker is equipped with a robust sensor suite that monitors pressure, air composition (carbon dioxide, carbon monoxide, and oxygen), temperature, and humidity. These values are read and relayed to our Raspberry Pi 4 which is responsible for the toggling of each data point's respective environment controller via a logic-driven power relay.

Heating For prototype testing, an external heating reservoir was used to transfer heated air to the payload locker prototype. The heating reservoir was a one liter stainless steel tank with four ports. Each of these ports had a fitting to support attachments of other components. In Figure 52, you can see the air tank and the various attached components.

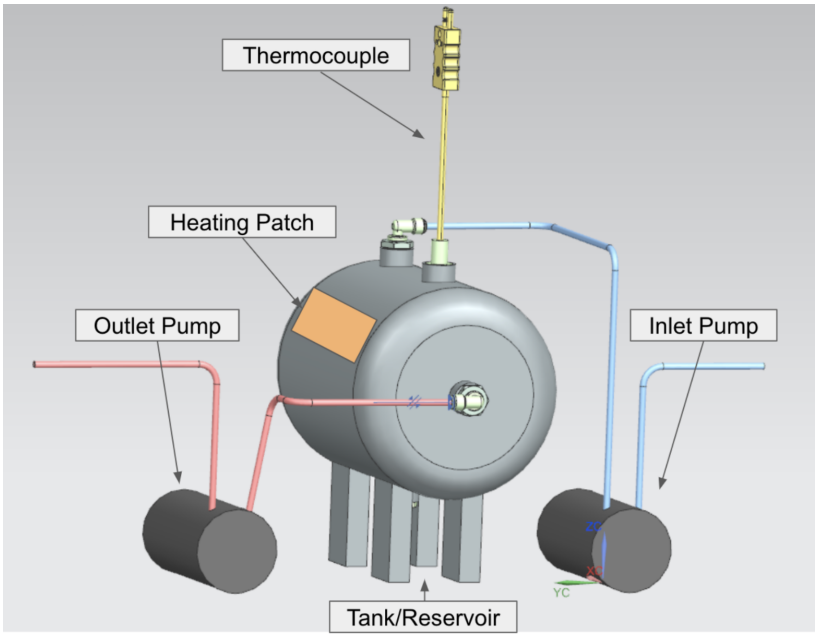

Figure 52: The payload heating subsystem CAD

There are also a few components that are not depicted in the CAD, such as the surface thermocouple which is located under the heating patch, and the pressure transducer which is located in the bottom port of the air tank, between the legs. Also not included are the Raspberry Pi microcontroller and power relay, facilitating the autonomous control of the system's electrical components.

The surface thermocouple is meant to measure the temperature of the heating patch. The purpose of the thermocouple inside the air tank is to measure the temperature of the air inside the reservoir. The pressure transducer is responsible for measuring the pressure inside the air tank as needed.

The heating patch was one of the most critical components, and was needed to supply the heat to the reservoir and warm the air. The heating patch was 5 inches by 6 inches, and required 150 Watts of power. The patch was capable of reaching 180 °C. The other critical component for this subsystem was the pumps. There were two pumps, the inlet and outlet pump. The inlet pump was responsible for filling the air tank with air when the tank was empty. The outlet pump was responsible for transporting the air out of the tank and into the payload locker. The pumps were rated for 17 mL/min, though testing showed that this flow rate was too little for the designed capabilities.

All of these components make up the complex heating payload subsystem, in order to support maintaining a habitable environment. The logic of our system ensures that each component is triggered at the correct time, and that flow of processes is in sequential order. To begin, the inlet pump turns on and fills the air tank until the pressure transducer reads the set point. Then when the payload locker temperature sensor reads that the temperature is too low inside the locker, the heating patch turns on to prepare delivering warmed air to the locker.

Once the heating reservoir has reached the correct temperature which is being read by the air tank thermocouple, the outlet pump turns on and delivers the warmed air to the payload locker.

The outlet pump stays on until the temperature inside the payload locker reaches the set point.

Cooling For prototype testing, a beverage cooler was filled with ice and used as the source from which to pump cool air into the payload. To do this, a bulkhead fitting on the side of the cooler attached tubing to a pump that routed cool air to the payload locker. Not included in the CAD model (Fig. 53) is the thermocouple, probed through the top of the cooler, which was used to test the efficacy of the cooler.

Also not depicted in the CAD are the electrical components that allow for the autonomous control over the outlet pump. Similar to the heating system, the logic of the cooling system ensures that the cool-air pump is triggered at the appropriate time. When the payload locker temperature reads that the temperature is too high inside the locker, the cool-air pump is toggled on until the temperature returns to its set point.

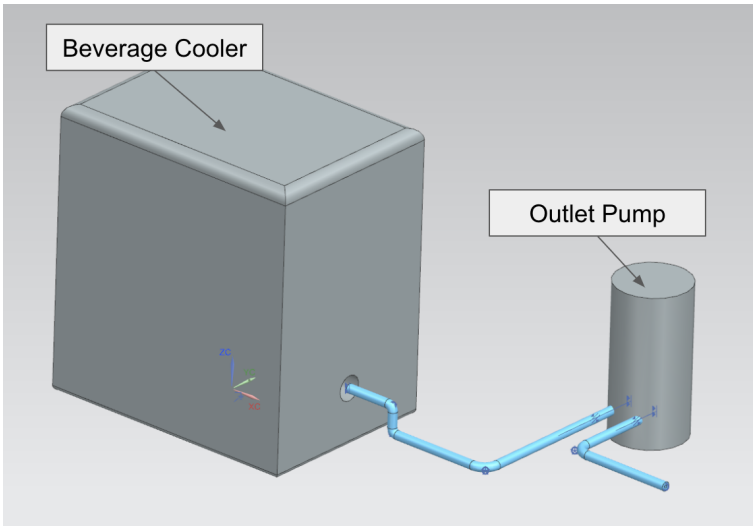

Figure 53: The payload cooling subsystem CAD

Liquid Waste Removal For our prototype design, we used a peristaltic pump due to its simplicity to implement. Peristaltic pumps perform well with liquids and can better tolerate particulates and larger debris in comparison to other traded components.

In the prototype, tubing extends from the ports located underneath the dial, one end of which is placed in a waste container the liquid waste would travel into, and the other end meant to physically remove the liquid waste. At the end of the waste removal tube is a mesh used to filter large particulates that may travel through the pump, causing a failure. A CAD model of the liquid waste removal pump is displayed in Figure 54.

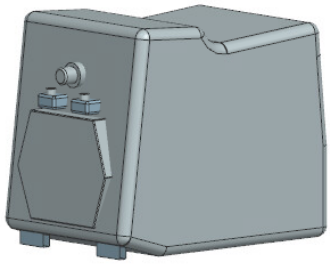

Figure 54: Liquid Waste Removal Pump CAD

Feedwater The prototype design used for bench-top testing consisted of a peristaltic pump with tubing connected to a spray interface. The other end of tubing would be connected to the potable water source, which was, in this case, a container full of water. The flow rate for our pump was dependent on the voltage supplied to the pump, which was capped at 12 volts. The key difference between our idealized and prototyped design was that our prototyped design was fully manual. A CAD model of the feedwater assembly is displayed in Figure 55.

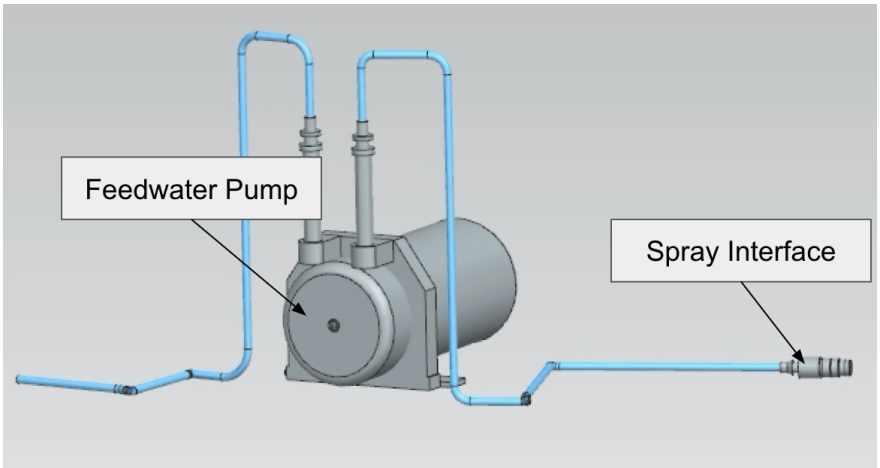

Figure 55: Feedwater System CAD

Air Circulation and Dehumidification Our benchtop prototype design consists of a fan with ductwork and a three-way solenoid valve that can circulate air through the dehumidification line with a custom desiccant fitting or the bypass line. The desiccant fitting is made out of a section of 1 inch PVC tubing, around a length of 1 and $\frac{3}{4}$ inches, with steel mesh on each end and filled part way with silica gel beads. The fan has 3 inch connections that correspond with the 3 inch duct. To reduce down from the duct to the 1 inch PVC tubing used for the rest of the system, there is a custom plastic reducer downstream of the fan. The ductwork upstream of the fan provides for the inlet of air to the system from the payload locker. A custom T-shaped connector also connects the dehumidifying line, bypass line, and outlet into the payload. Within our bench-top design we also chose to leave a pressure transducer inline and downstream of the desiccant. This can allow us to take pressure recordings when needed. The key differences between the bench-top and idealized

designs and are outlined below in Table 6.

Idealized Design	**Prototype Design**
Integrated exhaust line with fan	Separate exhaust line a pump
Three-way solenoid valves downstream and upstream of the desiccant	Three-way solenoid valve upstream of the desiccant fitting
Check valves downstream of desiccant line and bypass line	No integrated check-valves
Inline pressure relief valve for fault tolerance	No pressure relief valve

Table 6: Design Differences Between Idealized and Prototype Air Circulation System

For the bench-top prototype, the peristaltic pump used for exhaust is separated from the air circulation loop. The exhaust pump is used when our air composition sensors in the system read undesirable conditions. The pump has a maximum flow rate of 1.3 Liters Per Minute (LPM) and is self-sealing. This piece connects to the payload locker with its included silicon tubing that can withstand high temperatures if needed.

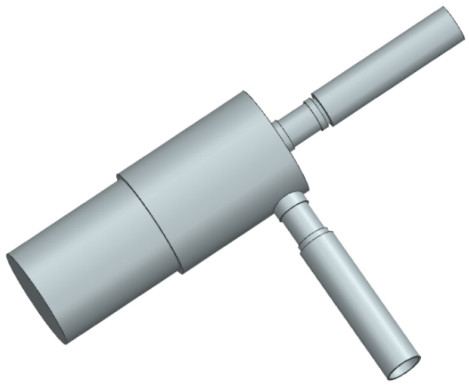

Figure 56: Exhaust Pump CAD

Additionally, the air circulation system makes use of a fan. The role of the fan is to circulate air in the payload through either the dehumidifying line or bypass line as necessary. The fan for our bench-top prototype is made of plastic, has adjustable air speed, and has 3 inch connections. The fan itself has a diameter of 4 inches. Through testing, we determined that the strongest flow rate of the fan corresponding with the last notch on the potentiometer of the fan's controller was 23.19 SCFM. The surrounding ductwork is attached to the fan with hose clamps.

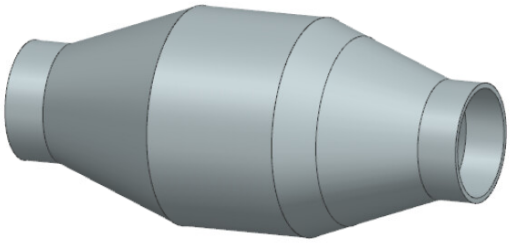

Figure 57: Air Circulation Fan CAD

A three-way solenoid valve is used to direct air through the dehumidifying line when payload humidity levels are not as specified or through the bypass line when humidity levels are equal to a set point. The three-way valve is made of brass with 1 inch female NPT connections. It can withstand temperatures from 2-90 degrees Celsius and pressure up to 185 PSI with no minimum value. It has a height of 4.50 inches, a width of 3.35 inches, and a length of 3.35 inches. It weighs 2 pounds and has a manufacturer-reported position switch time of 5 seconds.

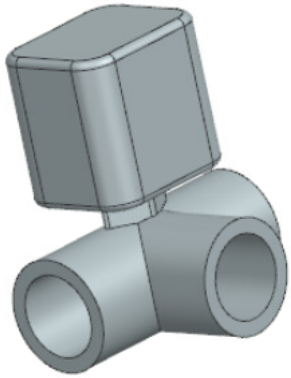

Figure 58: Air Circulation Three-way Solenoid Valve CAD

In order to scrub humidity within the payload, a custom desiccant fitting is used to remove water from the circulating air while payload humidity levels are above a set point.

The desiccant of our bench-top prototype is made up of a section of 1 inch tubing with mesh attached to each end and filled with silica gel.

As shown in the CAD per Figure 59, PVC sleeves were designed to reinforce the intersections between the mesh and the 1 inch PVC sleeve for a secure fit. However, in our bench-top prototype, we found this method difficult to implement effectively given poor tolerances in the fit we were able to manufacture. The sleeve proved more cumbersome and less beneficial to the system than initially anticipated. Thus, it was removed in the bench-top design.

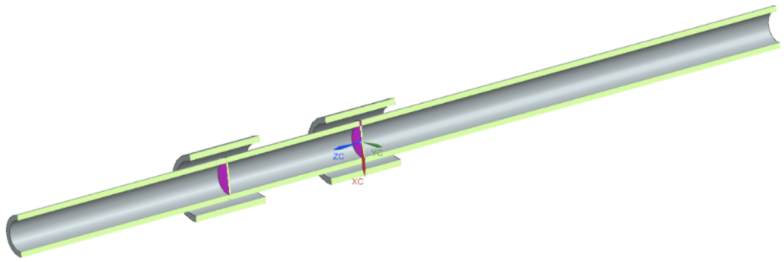

Figure 59: Desiccant Fitting Line CAD

Overall, our system cooperates with electronics to service the payload. The three-way solenoid valve changes positions depending on the readings from the humidity sensor located inside the payload locker. Through the payload user interface, the user is able to set the relative humidity to a desired point. At nominal condition, the valve is set to circulate air through the bypass line. When the relative humidity is sensed to be higher than the set point, the valve switches to circulate air through the dehumidifying line.

In our idealized design, the exhaust line would be fully integrated with the air circulation and dehumidification system through another three-way solenoid valve downstream of the bypass and desiccant lines. When the air composition sensor located inside the locker reads values greater than a set point, the valve would switch positions to carry air away from the payload using a fan.

The air circulation and dehumidification system operates independently of most other habitation systems as it runs continuously under nominal conditions. When the fire detection system senses carbon monoxide values greater than a set point, however, the fan is ideally turned off and air is prevented from leaving the payload locker.

Fire Detection Our detection system is a very small system. We decided to use a detector able to identify a combustion gas, which would be a byproduct of fire. This was a singular carbon monoxide detector. Our primary reason for using this detector instead of an optical smoke detector was that the smoke detector is not necessarily as sensitive a detector as a combustion gas detector. However, it is able to detect multiple gases, but would not provide us with a qualitative or quantitative result when gas is detected. This component's role within the payload is to provide a reading of the amount of CO within the payload, and is able to do so between 10 and 10000 ppm. Our system is relatively independent, as it just needs a power source, and it is then able to relay information regarding gas within the payload.

Payload Lighting For our prototype, we used LED strips and placed them directly above the plants within our payload locker. Through our user interface, the LED's can be configured to a specified brightness and color.

Camera Connected to our Raspberry Pi 4 and mounted on the side of the locker, capturing the interior of the locker, is a Raspberry Pi camera module. This live video feed is displayed and can be stored via our user interface.

4.3 Experimental Payload

To demonstrate the prototype system's capabilities, we designed a biomining experiment involving extraction of metals using living organisms. These capabilities include control of temperature, atmospheric conditions (gas concentration, humidity, pressure), water temperature and pressure, and lighting. We aimed to determine whether plants are able to utilize metal ions from simulated regolith as they do from soil. We planned to grow radishes in a lunar regolith simulant with minimal metal ion contamination from water and fertilizer, then harvest the planets and measure their uptake of metal ions. This experiment demonstrates how long-term lunar habitats can potentially utilize living organisms for processes such as recovery of metals from refined ores for higher mining yields, and bioremediation to filter metal contaminants from soil, groundwater, and wastewater.

Small containers with drainage holes were filled with mixtures of soil and volcanic ash ranging from 100% soil to 100% volcanic ash in 10% increments. A 2% solution of nitrogen-phosphorous-potassium (NPK) fertilizer dissolved in distilled water was added, followed by the planting of 4-5 radish seeds in each container. The plants were grown under a lamp to simulate 24-hour daylight and additional distilled water was added as necessary. After 36-40 days, the plants were harvested, weighed, and ground using a mortar and pestle. The plant matter was dissolved in 1 mL of distilled water per 20 mg of mass. Test strips detecting iron ($Fe^{2+/3+}$), calcium (Ca^{2+}), and magnesium (Mg^{2+}) were submerged briefly in the dissolved plant matter and read according to the colorimetric scales provided with the test strips. For full system testing, the plants were grown in the bench top payload rack system under LEDs emitting red light at a wavelength of 700 nm.

5 Trade Studies

5.1 Structures

5.1.1 Frame

There was a trade study performed to evaluate the material used for the frame. The trade study compared aluminum 6061, titanium, and 400 series steel to be used for the frame. The main wants in the trade study were that the material is affordable and low cost, lightweight, and durable. Aluminum 6061 is well known to be lightweight, relatively low cost, strong, and is resistant to degradation. Because aluminum 6061 best met all of these requirements, it was selected for the frame material.

5.1.2 Shell

Different materials were looked at in evaluation of the shell, including aluminum, acrylic, polycarbonate, and steel. Assessed properties were cost, moduli of elasticity and shear, and density. Density was ultimately the most important factor as the optimal material should minimize mass, while all of the given choices are guaranteed to add stability for the magnitude of forces to which the rack should be subjected. With a heavier weighting of the importance of density, acrylic was chosen as the shell material. While the metal choices would operate under a thickness of $\frac{1}{16}$", the plastic choices can be increased to $\frac{1}{8}$" with their lesser density, adding to the structural stability. It is important to note that the acrylic must be black/opaque in coloring as to not permit light to enter and interfere with the payloads inside, and that specific acrylic should be chosen such that electrical charge does not build up on the shell over time.

5.1.3 Rack Handle

The primary trade decisions in selecting the rack handles centered around heritage designs—specifically, what experienced users in similar environments are already familiar with. This was particularly influential in determining the shape and width of the handles to ensure intuitive and ergonomic use. Additionally, material selection was carefully considered to align with the materials already chosen for the rack structure. The goal was to ensure durability and compatibility, particularly in withstanding the forces exerted during movement and transport.

The trade decisions were evaluated through a combination of historical research and engineering analysis. We studied previous rack designs from NASA to understand what has been successful in similar environments, focusing on factors like user ergonomics and material selection. In addition, we performed calculations to ensure the handles could withstand expected forces, specifically analyzing how loads would be distributed through the screws and interface points. This approach allowed us to balance performance, reliability, and ease of integration with the rest of the rack system.

We decided to use aluminum as the handle material due to its compatibility with the rest of the rack structure. The handle dimensions of 65" in length, 0.75" in width, and 1.5" in depth, with rounded edges for safety and user comfort were set in accordance to NASA's standards for handle shape and size to ensure ergonomic compliance, basing our design on heritage models. Each handle is attached using four $\frac{1}{4}$"-20 thread size cap screws for structural integrity.

These decisions were based on several key assumptions: that the load applied during movement would not exceed the expected forces from our requirements and that legacy NASA designs reflect best practices for human interaction in aerospace environments.

5.1.4 Mobility

The primary trade study for the mobility system was done for the main movement and locking method for the rack. The trade study looked at rubber wheels, a magnet system, treads, wire mesh wheels, wheels with disk brakes, and wheels with smart lock mechanisms.

The trade study focused on the simplicity of the mechanism, the ease of use, maintenance, and noise concerns. For the simplicity of the mechanism, less components meant less parts that could fail. This was important for our design and construction since it made it less complex for the team and astronauts using the rack. The ease of use was important since moving the rack may be a frequent action performed by astronauts. The team needed to make sure that it was easy to move since astronauts must be able to perform the task without tipping the rack over or damaging it. For ease of maintenance, space habitats often have limited resources on them, so the maintenance must be easy. The tools to maintain it must be easily accessible and the rack mobility system itself must be easily fixable. For the low creation of noise, rattling, and vibrations, the want was low since the vibrations should be pretty small regardless of which system we picked and this would only cause a minor inconvenience compared to the other wants if it's not fulfilled. Based on these wants, the team ultimately went with rubber wheels with locks because it was simple, easy to implement and maintain, and did not create a large amount of vibrations.

5.1.5 Sliding Rails

The key trade decisions focused on whether the payload insertion/removal options could support a 60.3 kg load in lunar gravity and be operated by a single person. Once these requirements were met, we prioritized system "wants" to improve engineering success. These included ease of handling, mechanism simplicity, manufacturability, potential failure modes, space usage, insertion/removal speed, and durability.

Ease of manufacturing and simplicity were rated as the most important "wants" and thus weighed more heavily in scoring. We considered these most impactful because all options were sufficiently durable, compact, and quick, making differences in those areas negligible. In contrast, user interaction and manufacturing ease had a greater effect on mission success for astronaut research.

Alternatives considered included 80/20 slotted rails, ball bearing sliders, latching clamp platforms, pulley belt systems, and motor/actuator mechanisms. Velcro and strap systems were excluded early due to prior failures at low loads and difficulty with payload removal. Ultimately, 80/20 slotted rails were selected as the best option due to ease of use, mechanical simplicity, availability of pre-made components, proven reliability, and team experience from previous BLiSS projects. The variety of rail options also offered flexibility in load capacity and travel length, supporting easy assembly and compatibility.

5.1.6 Desk

Material cost versus structural stiffness (bending) was a key factor in the trade study for the desk and rail system. Various material options and support configurations were evaluated based on their ability to limit deflection under expected loading conditions while maintaining a low overall cost. The analysis showed that using a thicker aluminum sheet alone would meet structural requirements but significantly increase system weight and cost. To address this, the team selected a thin $\frac{1}{16}$" 6061 aluminum sheet for the desk surface, supported by a structural frame made from 80/20 aluminum extrusion. This configuration provided the necessary stiffness while keeping material costs and system mass within acceptable limits. Assumptions made during the trade study included estimated loading from astronaut interaction and constraints on volume and mass due to integration within a confined habitat environment.

5.1.7 Roller Rails

The payload lockers needed a subsystem set up supporting both movement and alignment of each respective capsule, and the roller rails best served that purpose. The movement is supported by the line of wheels along the rails, which slide alongside the payload locker side. There is then an extruded set of material to line up and lock into the crevices between the wheels, ensuring alignment during movement.

5.1.8 Latch

Trade decisions were made through consideration of requirements, as well as consideration of wants. Requirements were mainly: UI-2.1: The payload shall be physically prevented from being unsecured from the rack, unless purposeful action is taken to unsecure it. PC-1.1, partially, mainly that the securing mechanism must not interfere with other components and interfaces accompanying the payload. Trade decisions were made with a trade study matrix, with weights assigned to the

wants. The highest weighted wants were “ease of use”, and “unlikely to jam/get stuck”. Factors that determine the aforementioned wants would be factors such as whether or not the mechanism is commonly seen, or have a simple mechanism. The main assumption through the study is that for each latching mechanism the user is trained in its operation. Outside of the trade study matrix, further discussion was deliberated, and the main concerns were physical space requirements, as well as price and lead time. We decided that the purchase of a latch was ideal. The final decision was that the latch was to be a mechanism that could exist on the external area of the payload locker, and utilize a relatively low complexity mechanism. Some alternative choices we were considering were cam latches, draw latches, and slide-bolt latches.

5.1.9 Payload Locker

The payload locker frame did not rely on any trade studies. For manufacturing simplicity, the final decision for the major material for the locker is 80/20 aluminum.

The primary trade decisions in selecting the payload handles centered around heritage designs—specifically, what experienced users in similar environments are already familiar with. This was particularly influential in determining the shape and width of the handles to ensure intuitive and ergonomic use. Additionally, material selection was carefully considered to align with the materials already chosen for the rack handles. The goal was to ensure durability and compatibility, particularly in withstanding the forces exerted during movement and transport.

In addition to this, designs for vertical and horizontal handles for the lockers differ in attachment brackets with the horizontal payload handles having four screws per attachment instead of two for more stability.

The trade decisions were evaluated through a combination of historical research and engineering analysis. We studied previous rack designs from NASA to understand what has been successful in similar environments, focusing on factors like user ergonomics and material selection. In addition, we performed calculations to ensure the handles could withstand expected forces, specifically analyzing how loads would be distributed through the screws and interface points. This approach allowed us to balance performance, reliability, and ease of integration with the rest of the locker.

We selected aluminum as the material for the payload handles due to its compatibility with the rack’s overall structure. The handle dimensions of 8” in length, 0.75” in width, and 1.5” in depth, with rounded edges for safety and user comfort were set in accordance to NASA’s standards for handle shape and size to ensure ergonomic compliance, basing our design on heritage models. To meet ergonomic requirements for gloved astronaut hands, a 3” gap was incorporated between the handle and the mounting surface. The design follows NASA standards for handle geometry and size, drawing from heritage configurations to ensure usability in lunar environments. Horizontal payload handles are mounted using eight $\frac{1}{4}$”-20 thread size cap screws to maintain secure attachment to address the increased torque loads expected during movement. Vertical payload handles are mounted using four $\frac{1}{4}$”-20 thread size cap screws to maintain secure attachment.

5.2 Electrical

To support the development of the electrical subsystem, we completed trade studies focused on selecting components that could realistically be implemented within the bench-top prototype.

These studies focused on criteria that would help the electrical subsystem be sufficient and integrate smoothly with the rest of the rack's system. In particular, we evaluated multiple options for programming languages, environmental sensors, and cameras.

5.2.1 Software Language and Hardware Integration

A trade study was conducted to determine which software language would be the most appropriate for the electrical subsystem. This study focused on multiple criteria, including accessibility, team familiarity, support for data visualization, and speed. We weighted these criteria based on how relevant they were to the development of the project. Accessibility and team familiarity were determined to be the highest of importance. We compared four different languages: Python, C, C++, and Java.

After evaluating all options, we found that Python was the best choice. Python was the most familiar language among members, and the easiest to learn and implement, making it highly accessible. The only shortfall was that Python executes programs slower compared to the other options, given the right implementation. This was not a critical drawback since the electrical subsystem did not demand extremely intensive tasks. Data visualization was also not heavily considered, since this criteria more so relies on how the user interface was implemented. Ultimately, Python's benefits in accessibility and familiarity made it the preferred choice for the project.

Following the choice of utilizing Python as our programming language, our preceding decisions were made to allow for a unified Python environment and simplified communication throughout the system. Regarding the choice for a Python-based microcontroller, a trade study was not conducted for this, as Raspberry Pi was the trivial option when considering the goals of the bench-top system—a functional proof-of-concept with lack of regard toward efficiency and resiliency.

Two Raspberry Pi Pico boards were chosen for the bench-top prototype due to their simplicity, compact design, and reliable all-around performance. One was allocated for the telemetry within the locker, and the other for the heating and cooling systems. Furthermore, we chose a Raspberry Pi 4 as our laptop-facing controller due to its versatile and robust Linux-based operating system, Raspberry Pi OS. Additionally, there is a large amount of GPIO pins that allows for easy integration of control relays and sensors. The Pi 4 is also equipped with an Ethernet port which allows for reliable computer-to-Pi communication.

5.2.2 Temperature and Humidity Sensor

A trade study was conducted for selecting a temperature and humidity sensor to be used in the payload locker. Options were evaluated based on size, cost, precision in measurement, and Raspberry Pi compatibility. Overall, a total of five sensors were compared: DFRobot's SHT30, Digilent's Pmod HYGRO, SparkFun's SHTC3, and Adafruit's Sensirion SHT45 and HDC3022. While the SHT30 had long-term stability, it relied on an analog interface, whereas I^2C was preferred for its digital reliability when working with Raspberry Pi. The remaining four sensors utilized I^2C communication, were precise in measurement, compatible with Raspberry Pi, and were compact enough for use in the payload locker. Adafruit's HDC3022 was ultimately chosen for being the most cost-effective option with very precise readings of temperature in degrees Celsius and relative humidity in percentage.

5.2.3 Oxygen Sensor

A trade study was conducted for selecting an oxygen sensor to be used in the payload locker. The criteria that we based this study on were size, cost, precision in measurement, and Raspberry Pi compatibility. Overall, a total of two sensors were compared: DFRobot's I^2C Oxygen Sensor and Tinkersphere's Oxygen Sensor. Tinkersphere's Oxygen Sensor was only compatible with Arduino, so this would not work with our system as we had decided on using Raspberry Pi. DFRobot's I^2C Oxygen Sensor was ultimately chosen for this reason, along with the fact that it was more cost effective, was compact enough for use in the payload locker, Raspberry Pi compatible, and has very precise measurements for oxygen concentration in percentage.

5.2.4 Carbon Dioxide Sensor

A trade study was conducted for selecting a carbon dioxide sensor to be used in the payload locker. The criteria that we based this study on were cost, size, precision in measurement, and Raspberry Pi compatibility. Overall, a total of two sensors were compared: Adafruit's SCD40 and SparkFun's SCD41. Both sensors were Raspberry Pi compatible and were compact enough for use in the payload locker. However, Adafruit's sensor had an accuracy of ± 10 ppm more than SparkFun's. Adafruit's SCD40 was ultimately chosen for this reason, along with the fact that it was more cost effective.

5.2.5 Pressure Sensor

A trade study was conducted for selecting a pressure sensor to be used in the payload locker. The selection criteria included cost, size, precision in measurement, and Raspberry Pi compatibility. Three sensors were compared: Adafruit's BMP390, AUTEX's 150 PSI Pressure Transducer, and DwyerOmega's 100 PSI Pressure Transducer. All three sensors were Raspberry Pi compatible and compact enough for use within the payload locker. While the pressure transducers from AUTEX and DwyerOmega offered higher precision, they were significantly more expensive than Adafruit's sensor - being $35 and $370 each, respectively. Adafruit's BMP390 was ultimately chosen for this reason, along with the fact that it was still very precise when measuring pressure in millibars.

5.2.6 Camera

A trade study was conducted to select a camera that would stream and record video of the interior of the payload locker. The system required the camera be able to record in 1080p resolution as well as be compatible with the selected microcontrollers (Raspberry Pi). Additionally, the cameras were rated based on their size and cost. The two cameras compared in our trade study were the Raspberry Pi camera module and a Power-over-Ethernet (PoE) camera. Though both cameras were compatible with the system and could record with the desired resolution, the Raspberry Pi camera module's small size and affordable price ($20 versus the PoE Camera's $50) made it the best choice for implementation into the bench-top prototype.

5.3 Habitation

Trade studies on each subsystem and components were used to select the architecture types used for the prototype. This section will outline the trade studies as they pertain to each habitation subsystem.

5.3.1 Heating

The first trade decision evaluated was for the basic architecture of the payload heating source for the prototype system. This trade study helped determine how many components would be needed for the system.

This trade decision was evaluated using the criteria of cost, ease of installation, practicality, and effectiveness. The criteria was then given weights, and then each option was given a value out of ten for how well it met the given criteria. The options evaluated were heating patches, a heating fan, or coils. After evaluating each option the heating patches resulted in the highest score, and therefore the winner of the trade study. This decision then resulted in sourcing other components for the subsystem.

To determine the mode of transportation for the air, a trade study was done. This trade study evaluated fans, a diaphragm pump, or a peristaltic pump. These were evaluated on self-sealing capability, ease of maintenance, long lifespan, ease of installation, and practicality/simplicity. After evaluation, it was determined that a peristaltic pump would best meet our needs. Another component that had to be sourced was the air reservoir. This did not require a formal trade study, but we made assumptions that the reservoir had to be conductive, small in volume, and easily connect to tubing for transporting the air.

5.3.2 Cooling

The trade options that were evaluated were evaporative cooling (swamp cooling), mini fans, liquid coolant (air conditioning), and water cooling. These would each provide cool air sources to the payload locker. Initially, the evaporative cooling fan was selected due to its minimal complexity and cost. Evaporative cooling works by evaporating a liquid, typically water. This evaporation removes latent heat from the volume where evaporation takes place, resulting in cool air. However, there were concerns about the evaporative cooling leaving excess humidity within the payload locker. Thus, we decided to shift gears towards the beverage cooler which would provide us with cool air without the undesired humidity for a simple and cost effective design.

5.3.3 Liquid Waste Removal

Trade studies were conducted to determine which pump would be best to act as the suction pump for this system. This component would act, with the addition of tubing, to suction waste out of the payload locker.

We evaluated components on the criteria of ability to work in a closed system, small size, ability to handle various fluid types based on viscosity, ease of maintenance, and suction power. Each of the criteria were weighted in terms of importance to the final design. The most weight was placed on the ability to handle varying fluids, as it cannot be determined how muddy, or full of sediment, liquids handled by our pump may be. For that reason, it was essential that the selected component must be able to handle liquid with sediment or particulate in it. The least weight was placed on ease of maintenance, as we did not imagine that our options for the suction system would greatly differ in terms of maintenance.

The options we evaluated in this trade study were diaphragm pumps, capillary action system, bladder systems, and canned motor pumps. Canned motor pumps ranked first, mostly due to their

small size and ability to handle different fluid types. However, within the trade, diaphragm pumps received identical scores to canned motor pumps in all categories except small size and ability to work in closed systems.

Upon further research, it was realized that an additional trade should be conducted evaluating pumps and their ability to handle liquid with particulates. With this in mind, we evaluated diaphragm pumps, peristaltic pumps, and canned motor pumps, as canned motor pumps and diaphragm pumps had scored highest in ability to handle fluids of different types. Once we evaluated based on ability to handle sediment within liquid, it was found that peristaltic pumps would work best, as diaphragm and canned motor pumps would be clogged by liquids that contained more than fine particulates. Peristaltic pumps would be the best option to handle slurries, and thus became the first choice.

Assumptions made throughout our trade studies were that each of these pumps would be able to work in a microgravity environment. This assumption was made due to the mechanism by which each of these options currently works on Earth. Testing would need to be conducted to ensure that that is the case.

5.3.4 Feedwater

Trade studies were conducted to determine the pump that would be used to deliver water to our system, as well as the means by which we planned to do it. Instead of one stream in particular, trade studies evaluated the complexity needed for our system, specifically, the number of components we would use.

For our first trade study regarding the pump we would use for our feedwater system, we evaluated a mechanical pump, pressurized air system, and capillary action system. These were evaluated using the criteria of ease of maintenance, lifespan, ease of installation, and complexity. All criteria were given almost the same weight, as they were all deemed to be nearly equally important. Ease of installation and complexity were given slightly more importance, as we wanted this system to be easy for crew members to use and understand, and viewed installation as being important because we did not want for it to be difficult to implement within the payload.

The assumption made for this trade study was that these pumps would work identically in whatever environment they are in to how they do in 1G. Naturally, further research would have to be done to ensure that is the case.

Another, more in-depth trade study was conducted to determine which interface would be used to deliver the potable water to our payload locker. Since this system would primarily be used to deliver water to botany, we would have to consider the pressure and stream would hit the inside of the payload locker, and wanted to ensure that, regardless of flow, the output would not be too aggressive for biological life. To do this, we examined multiple irrigation systems, deciding on a mist interface after conducting a low-scale trade study.

5.3.5 Air Circulation and Dehumidification

For the design of our system, we did a trade study on the method of air circulation. The options we evaluated were a ventilation grill, cooling plates with air circulation, a fan, and an

integrated air system with sensors. The criteria dictating this study were efficiency of circulation, noise production, temperature regulation, ease of maintenance, and complexity. Considering these traits for each option, we ultimately decided on using a fan to circulate air within the payload.

5.3.6 Payload Lighting

Trade studies were conducted to determine which component would be best to act as our payload lighting mechanism. The criteria by which we evaluated our options were ease of installation, maintenance time needed, lifespan, ability to support biological life, and complexity. We also wanted for our lighting to work for extended periods of time. Further, the ability to support biological life would require for our component to utilize specific wavelengths to optimize photosynthesis.

Out of our criteria, the most consideration was given to minimal maintenance time, and the least was complexity and ability to support biological life. We thought it important to have a component within the payload that did not need constant monitoring, and that would not require multiple additional components in the case that it stopped functioning.

The options for our trade study were LEDs, fiber optics, and fluorescent lighting. LEDs ranked highest overall, as well as in the category for the support of biological life. After this, we considered the different types of LEDs, and conducted an additional trade on whether we wanted to use LED bulbs, strips, or panels. We evaluated each of these options on the criteria of how much space they would use within the payload, lifespan, and energy consumed. We found that LED strips ranked highest overall. The LED strips would take up minimal volume and use the least amount of energy.

5.3.7 Fire Detection

Trade studies were conducted to determine which component would be used to detect fire within the payload. Criteria for our fire detection trade study included sensitivity to small fires, ability to detect a fire that produces smoke, real-time alerting, and ability to work in different conditions. The listed criteria were chosen because we wanted to ensure that our method of fire detection had the ability to detect all kinds of fire, regardless of size and gas patterns that may occur in different gravity environments.

Each criteria were weighted differently, with the most importance placed on the ability to work in different conditions, and the least on sensitivity to small fires. We viewed it more important that a larger fire would always be identified, rather than the ability to detect small fires under certain conditions. However, the ability to detect small fires was still given importance.

For this trade, we evaluated an optical smoke detector, gas detector, heat detector, and infrared camera for implementation in this system. Based on the criteria, the optical smoke detector ranked first, and infrared camera second. Gas and heat detectors tied for last place.

While the optical smoke detector was ranked first, we chose to not use it due to its large volume. Additionally, the optical detector had the potential to produce false indications when if humidity is detected. We could not implement the infrared detector due to cost constraints. We then decided to use a gas detector to detect combustion gases produced by fire, as it would ensure that false alarms did not occur and was well within budget.

5.4 Human Factors

Trade studies in human factors focused on evaluating different methods of interfacing and loading payloads into the rack. A majority of human factors design decisions did not require trade studies, but instead required experimental analysis which will be highlighted in Sections 6 and 7. This section will outline the trade studies conducted.

5.4.1 Payload Handleability for Loading

A trade study was conducted to evaluate different methods of loading the payloads into the slots on the rack. This trade study was important to conduct as extra resources can be used to mitigate the risk of injury from biomechanical stress when loading payloads into the uppermost or lowermost slots on the rack. Options included handles on the side of the payload, manual hoist, electric hoist, and a scissor lift platform. Criteria evaluated include strain on the lower back, probability of failure, build difficulty, and cost. Handles on the side of the payload locker won as payload weights should not be significantly heavy enough to warrant external assistance.

5.4.2 Handle Placements

A trade study was conducted to evaluate payload handle placements on the locker and rack used to assist inserting and removing payloads. This trade study was important to conduct as there are significant tradeoffs between handleability and added weight and surface area. Options included two vertical bars on the payload locker and side bars on the rack, one horizontal bar on the bottom of the payload locker, two vertical bars on the payload locker, two vertical bars and two horizontal bars on the payload locker, one horizontal bar on the bottom of the payload locker and side bars on the rack, and two horizontal bars on the payload locker and side bars on the rack. Criteria evaluated handleability, biomechanical stress or risk of injury, added weight to payload locker, and intrusion on potential payload locker UI space. Two vertical bars on the payload locker and side bars on the rack won as vertical handles support a neutral wrist posture and side bars support stability and decrease the risk of slips while manipulating payloads.

5.5 Experimental Payload

Trade studies conducted to design the payload experiment included decisions on which plants to grow, how to measure metal ion uptake, and what material to use as a lunar regolith simulant. Radishes were selected as the subject of the study due to their ability to grow under low intensity LED lights and relevance to a long-term space habitat. Test strips were chosen as the method of metal measurement over more complex methods due to their insusceptibility to false results and high reproducibility. Initial trade studies selected a high-fidelity lunar south pole regolith simulant for use in exploring the ability of plants to utilize the metal content of regolith. However, due to safety and logistical concerns, the decision was made to replace the lunar regolith simulant with volcanic ash as a low fidelity version of our original design.

6 Testing and Results

6.1 Structural Prototype

In order to test the designed capabilities of the rack, validation testing was performed on the full-system prototype. All tests are outlined in this section, and are broken down by subsystem.

6.1.1 Frame

The following outlines the full system verification and validation testing that was performed for the rack frame subsystem.

Test 1: Frame Loading

Purpose To verify that the rack frame can support a payload load up to 60.3 kg in earth gravity.

Test Requirements

- SSI-1.7: The system shall support a payload of up to 60.3 kg on Earth scaled to lunar gravity.

Test Materials The materials used for testing were as follows:

- Complete rack frame
- Weight equal to roughly 60.3 kg (must be at least 60.3 kg)
- Additional weights up to 90.6 kg

Test Procedure The following test procedure was used to fulfill the test objectives:

1. Add weight to payload
2. Once minimum weight of 60.3 kg is reached, stop adding weight
3. Allow weight to sit in payload and perform "normal" rack functions (roll rack, open payload lockers, etc) and watch for signs of failure to hold weight
4. Continue to add weight up to 90.45 kg into the payloads. Add weight to payload in increments of 5-10 kg (if possible) and allow weight to sit in payload for a minimum of 10 seconds between weight increments. Watch for signs of failure to hold weight
5. At maximum weight, perform "normal" rack functions (roll rack, open payload lockers, etc) and watch for signs of failure to hold weight
6. Once evaluation is complete, remove weight from rack

Test Results and Analysis The test was completed and was able to successfully verify that the rack frame can support the required minimum load of 60.3 kg. The test also verified that the frame can support the 1.5 factor of safety load of 90.45 kg. There were no signs of displacement or failure during the test. A picture of one section of the test can be seen in Figure 60.

Figure 60: Rack Frame Load Test

6.1.2 Shell

The following outlines the full system verification and validation testing that was performed for the shell subsystem.

Test 1: FEA

Purpose The goal is to verify that the shell adds stability to the frame. The addition of the $\frac{1}{8}$" acrylic shell around 4 faces of the frame exterior should prevent some displacement in all directions.

Test Requirements

- R-01: The system shall be contained within the dimensions of the heritage EXPRESS racks.
  - The rack shall not displace out of these dimensions when subjected to expected forces in usage
- R-11: The placement of the system shall be rearrangeable within the planetary habitat.
  - The frame components shall not displace largely or deform plastically when rearranging components

Test Materials The materials used for testing were as follows:

- FEA software
- Shell and frame CAD

Test Procedure The following test procedure was used to fulfill the test objectives:

1. Load frame CAD into FEA solver
2. Constrain at relevant locations
3. Apply point forces at rack ends
4. Record displacement/deformation/stress
5. Add in shell CAD
6. Constrain to exterior frame faces
7. Repeat point force analyses

Test Results and Analysis Unfortunately, the FEA testing was not able to be completed. The model was able to be loaded into Ansys-the FEA solver-but the model was not able to be solved. The model required long run times that ended in the software crashing while the model was being solved.

The issue was attempted to be solved by reducing the number of parts within the assembly and changing some settings within the software, but ultimately this did not work. After numerous attempts to run the model, it was concluded that it would not be able to be completed by the deadline.

It is believed that the reason for these issues may have been due to a large, complex assembly, and that the computer labs provided by the University are not able to handle a model of this magnitude. If more time was allocated for this project, the FEA model may be able to go through additional diagnostics to allow for the model to be completed.

6.1.3 Rack Handle

Validation testing was not performed with this subsystem, since we designed the handle according to previously determined dimensions that are deemed industry standard. The rack handle is designed according to NASA standards, and our physical prototype validates the size, shape, and orientation of these handles.

6.1.4 Mobility

The following outlines the full system verification and validation testing that was performed for the mobility subsystem.

Test 1: Mobility Loading

Purpose To verify that the rack mobility can support a payload load up to 60.3 kg in earth gravity along with the load of the rack itself.

Test Requirements

- SSI-1.7: The system shall support a payload of up to 60.3 kg on Earth scaled to lunar gravity.

Test Materials The materials used for testing were as follows:

- Completed prototype rack
- Weight equal to roughly 60.3 kg (must be at least 60.3 kg)
- Additional weights up to 90.6 kg

Test Procedure The following test procedure was used to fulfill the test objectives:

1. Add weight to prototype rack
2. Once minimum weight of 60.3 kg is reached, stop adding weight
3. Allow weight to sit in payload and perform "normal" rack functions (roll rack, open payload lockers, etc) and watch for signs of failure to hold weight by the mobility subsystem
4. Continue to add weight up to 90.45 kg into the Prototype Rack. Add weight to Prototype Rack in increments of 5 - 10 kg (if possible) and allow weight to sit in it for a minimum of 10 seconds between weight increments. Watch for signs of failure to hold weight by the mobility subsystem
5. At maximum weight, perform "normal" rack functions (Roll rack, Open payload lockers, etc) and watch for signs of failure to hold weight by the mobility subsystem
6. Once evaluation is complete, remove weight from rack

Test Results and Analysis The test was completed and was able to successfully verify that the mobility subsystem can support the required minimum load of 60.3 kg. The test also verified that the subsystem can support the 1.5 factor of safety load of 90.45 kg. There were no signs of displacement or failure during the test. Additionally, the test conductors found no issues with moving the rack at the desired loads.

6.1.5 Sliding Rails

The following outlines the full system verification and validation testing that was performed for the sliding rails subsystem.

Test 1: Payload Locker Loading

Purpose To verify that the rails can properly support the weight requirements for the payloads and in the orientations that we intend to use them in. This also serves as a subsystem/-component test as well for the payload locker's rails in regards to load testing.

Test Requirements

- SSI-1.7: The system shall support a payload of up to 60.3 kg on Earth scaled to lunar gravity.

Test Materials The materials used for testing were as follows:

- O18.125" x 10.5" x 20.5" Payload Locker
- Pair of FL-COU14-100lbs Rails ordered from 8020.net
- Spring scale capable of measuring at least 40lbs
- Complete rack prototype
- Screwdriver
- Allen wrench
- 20 Count, 8-32 $\frac{3}{8}$in depth screws
- Compact masses to place within the payload locker that add up to 40 pounds along with the weight of the payload

Test Procedure The following test procedure was used to fulfill the test objectives:

1. Weigh the assembled payload locker itself (ours was 10lbs) using a spring scale
2. Attach the large payload to the rails with the screws in the orientation in which the payload is suspended from the rails
3. Fill the payload with 10lb marked bag weights until it all weighs 40 lbs (load to fit requirement will weigh 20lbs, but we wanted a 1.5 safety factor for the load and and the payload locker itself is 10lbs), ensuring that the weight is along the edges of the payload to simulate a distributed load, and make sure the rail is pushed all the way in
4. Measure displacement of the rail and watch for any snapping of the rail for 10 minutes
5. Extend the payload to full extension and run trials for this as well, making sure to measure displacement after 10 minutes of observing the behavior
6. Once evaluation is complete, remove weight from payload

Test Results and Analysis This load testing revealed that the roller rails worked for the large payloads when holding the load of the payload from above. The exact observation and data are recorded in Table 7.

Orientation	Trial 1 (mm)	Trial 2 (mm)	Time Broken At	Notes
Large payload, rails above - pushed in	~0mm	~0mm	N/A - withstood the 10 minutes	No measurable displacement with the caliper, but the bolts do seem to weaken compared to before the load was introduced
Large payload, rails above - full extension	15.93	11.79	N/A - withstood the 10 minutes	Displacement does not seem to be increasing over time, but the displacement is noticeable compared to how the rails rest unloaded.

Table 7: Results from Sliding Rail Load Testing

Importantly, the first test with the rails pushed in showed no noticeable displacement. This result also makes sense because when they are pushed in, each rail is supported by 10 bolts each and the load is evenly distributed along the rail as opposed to when it is extended and only some of the bolts are able to support the payload, while the others are connecting it to the 80/20. Figures 61 and 62 show the testing performed.

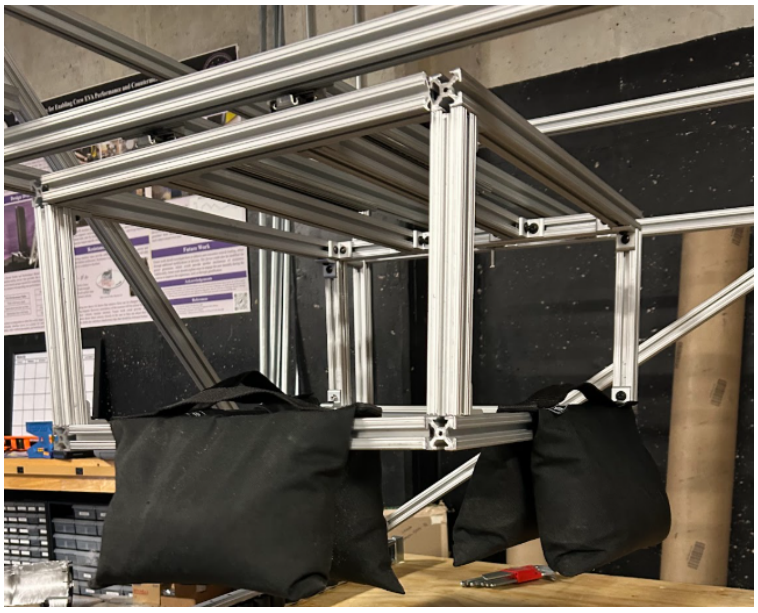

Figure 61: Load Testing Setup with Payload Pushed In

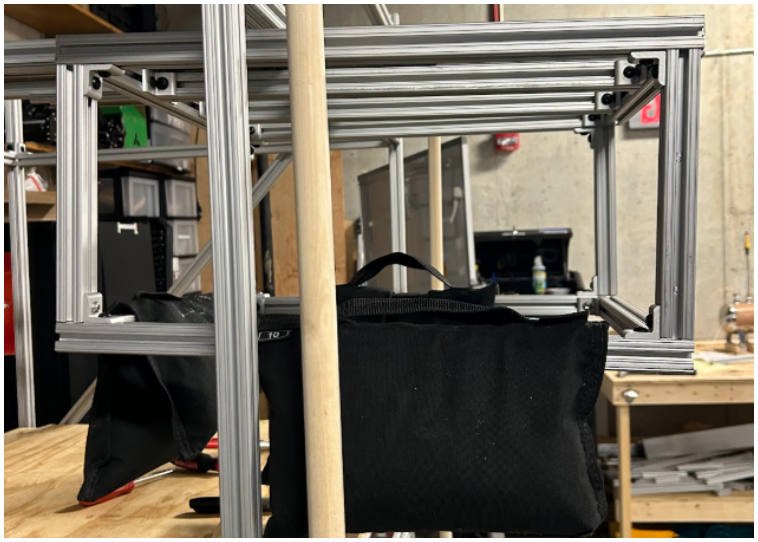

Figure 62: Load Testing Setup with Payload Fully Extended

We deemed 10 minutes as sufficient for testing because we believe that a researcher would not want to leave the payload open for too long at one point in time. Still, the factor of safety we used was 1.5, which is 10 pounds over the capacity stated in requirement SSI-1.07. As long as astronauts adhere to this limit and are trained properly not to overload the weight of the payload, then this displacement should be even less and the rails will hold the load properly. The noticed loosening of the bolts will also be lessened, and can also be checked with simple routine maintenance and/or thread locker. Additionally, since the rack is expected to hold the payloads stationary for a long period of time, the test showing that there was very little displacement when fully loaded and pushed in, is a promising result.

We were unable to test other payload orientations, but since the rails held the payload from above successfully, we are confident that support from below would work as well. We also were not able to test the other standard payload size, but the rails for those should be capable of withstanding a smaller payload because the weight is less dispersed. With more time, and resources, it would be a good idea to test all configurations, and also different geometries, such as the small payload, and also a longer payload that can take up the space of two payloads horizontally or vertically. Lastly, we briefly considered front loading the payload to see if this would break, but determined that this would be a hazard for tipping since we were testing on the frame without the other payloads in it, and were more susceptible to this load tipping it. However, from briefly placing the weight towards the front, and from intuition about bending moments, users should be advised against putting all the weight in the front for extended periods of time.

6.1.6 Desk

The following outlines the full system verification and validation testing that was performed for the desk and rail subsystem.

Test 1: Loading

Purpose To verify that the desk and rail subsystem can support the intended payload (20 lbs, or up to 40 lbs when testing with two payloads) without deformation or structural failure. It also verifies the stability and mechanical integrity of the rail movement post-loading.

Test Requirements

- SSI-1.7: The system shall support a payload of up to 60.3 kg on Earth scaled to lunar gravity.

Test Materials The materials used for testing were as follows:

- 6061 Aluminum Desk (24" x 39" x $\frac{1}{16}$" thick)
- 8020 Aluminum Support Frame
- Sliding rails with fasteners
- Incremental load sets: pairs of weights summing to 30 lbs, 40 lbs, 50 lbs, and 60 lbs
- Ruler or dial indicator for tracking deformation

Test Procedure The following test procedure was used to fulfill the test objectives:

1. Secure the desk and rail system to the 8020 frame using all mounting fasteners.
2. Fully extend the desk to its maximum operational length.
3. Place 30 lbs of weight at the outermost edge of the desk surface.
4. Hold the load in place for 2–3 minutes while observing for deformation.
5. Measure and record any vertical displacement or bending.
6. Repeat the process for 40 lbs, 50 lbs, and 60 lbs, increasing the total weight with each iteration.
7. After each load, check for visible signs of deformation or structural strain.
8. After completing all loading steps, push the desk back into its retracted position.
9. Confirm smooth rail movement and alignment.

Test Results and Analysis The test was completed and was able to successfully verify that the desk subsystem can support the required minimum load of 40 lbs. The test also verified that the subsystem can support the 1.5 factor of safety load of 60 lbs. There were signs of displacement during the test above the minimum required load. The desk experienced noticeable deflection under higher loads up to a safety factor of 1.5 (50–60 lbs). So while the requirement was somewhat met, additionally reinforcement will need to be added in order to fully pass. Table 8 shows the results of the test, and a supporting picture can also be seen in Figure 63.

Load Applied	Observed Deformation	Structural Performance	Rail Functionality
30 lbs	No visible deformation	Maintained full structural integrity	Smooth retraction and extension
40 lbs	Minimal deformation, within tolerance (0.08in)	Met structural requirements	Smooth retraction and extension
50 lbs	Noticeable deflection near center (0.2in)	Approaching structural limits	Rail motion unaffected
60 lbs	Significant bending observed (0.5in)	Structural integrity compromised	Rail still functional post-test

Table 8: Results from Desk Load Test

Figure 63: Desk Load Test

6.1.7 Roller Rails

Verification and validation testing was not performed on the roller rail subsystem. The prototype was constructed in order to determine the clearance needed between the roller rails and the payload locker.

6.1.8 Latch

The following outlines the full system verification and validation testing that was performed for the latch subsystem.

Test 1: Disturbance Tests

Purpose The purpose of this test is to determine if the latch can keep the payload lockers secured in face of impulses, disturbances, and movement.

Test Requirements

- PC-1.3: The payload shall have a locking mechanism securing its position in place to the rack when not in use.

Test Materials The materials used for testing were as follows:

- Frame with singular payload and latches

Test Procedure The following test procedure was used to fulfill the test objectives:

1. Secure latches to the payload locker.
2. Move the entire rack a total of 10 yards. Determine if the latch is still secured or not.
3. Impact locker door with a light impulses, front and back. Determine if the latch is still secured or not.
4. Pull on handles with the latch secured.

Test Results and Analysis Testing results are largely observational data, because the requirements are mostly qualitative by nature. The latch successfully secured the payload locker, and did not disengage through disturbances and brute actions. The latch can secure the locker in place, and can keep the payload locker secure in face of disturbances or movement, meaning that the latch can only successfully unlatch through deliberate, correct, effort.

Test 2: Physical Test

Purpose The purpose of this test is to determine if latch operations can be done with one hand, as well as comfortably by the user.

Test Requirements

- UI-2.11: Force requirement to lift guarding mechanism should not exceed 13 Newtons.
- UI-2.4: Control interfaces shall be separated between minimum and maximum distances that support one handed usage.

Test Materials The materials used for testing were as follows:

- Frame with singular payload and latches
- Force spring meter

Test Procedure The following test procedure was used to fulfill the test objectives:

1. Using force spring meter, pull on the latch to disengage, while reading the gauge number.
2. Repeat 3 times.
3. Using one hand, unlatch the latch, and then relatch it.

Test Results and Analysis Average force needed to operate the latch was between 2.9 and 3.9 Newtons, which is less than the 13 Newton maximum as determined by UI-2.11. The latch is also operable by one hand, though due to the physical mechanical characteristics of the latch it is slightly difficult to do. The results show that the latch could be operated by one hand, and that the force needed to do so is not exceeding what we determined to be ideal. This data is slightly limited due to the fact that the force is not completely homogeneous throughout the motion. However, since the mechanism is a torsion spring, the data is still good for a general understanding.

Test 3: Human Usability Test

Purpose The purpose of this test is to have multiple operators of different characteristics attempt to use the latch, as well as operate the latch in conjunction with the payload locker. This test will determine if the latch interferes with the payload when the latter is traversing and gather human input on physical implementation.

Test Requirements

- UI-1.10: User interfaces shall be interpretable to users with corrected 20/20 vision under nominal illuminations levels.
- UI-2.4: Control interfaces shall be separated between minimum and maximum distances that support one handed usage.

Test Materials The materials used for testing were as follows:

- Frame with singular payload and latches

Test Procedure The following test procedure was used to fulfill the test objectives:

1. Unlatch the latch.
2. Extend the payload.
3. Secure the payload.
4. Secure the latch.
5. While the latch is secured, pull on the payload locker. Varying impulses are good.
6. Repeat for each human subject.

Test Results and Analysis The results of this test are qualitative by nature. Users were able to successfully operate the latch, although some users grabbed the hoop first, instead of lifting the lever. The payload traversal also was not impacted by the latches, and users did not need to take extra precautions to ensure that. Various impulses also did not impact the latch's securing capabilities. Most users responded positively to the mechanism, although there were also some comments about how the latches were somewhat difficult to use. The latches don't get in the way of the payload's traversal, and the latches are somewhat easy to use and intuitive to users.

6.1.9 Payload Locker

The locker itself did not undergo direct testing, but it was used in multiple other subsystems' tests, most notably in the sliding rails subsystem.

6.2 Bench-Top Prototype

The bench-top testing tailored the traditional systems engineering process by separating testing into unit testing and full-system testing. Unit testing was used to verify nominal operation of the individual components. Additionally, unit testing was done to create calibration curves and learn more about the operation of the selected components to allow for rapid prototyping in the designs. Some full-system testing was used in tandem with the unit testing to check system compliance with the identified requirements.

It is important to note that unit testing in systems with few components worked to validate full-system performance. This is because these subsystems did not interact with other subsystems. Examples of this are seen on the exhaust, lighting, and feedwater subsystems. Subsystems such as air circulation and temperature regulation required more extensive testing within the fully-fleshed out bench-top prototype.

6.2.1 Heating

The following outlines the testing that was performed on the payload heating subsystem.

Test 1: Pump Capability Testing This unit-test plan was used to verify the capability of the pump to allow airflow. There is no specific requirement needed for this part. However, it is expected that our system can push air at a rate that allows for a controlled increase in temperature in the payload locker.

Test Objectives The test objectives highlight important information towards verifying functionality and determining relevant parameters of the peristaltic pump to be used for moving air in the payload heating subsystem. The three primary objectives of this test are as follows:

- **Objective 1:** Inspect the power on/off of the pump
- **Objective 2:** Inspect whether our system pushes air when turned on
- **Objective 3:** Collect flow rates for different supply voltages in the 2- 12V range

Test Materials The materials used for testing were as follows:

- DC power supply
- Banana to Alligator Clip Test Leads
- 12V DC Dosing Peristaltic Pump
- High-Temperature Silicone Tubing, Durometer 35A, Opaque White, 3mm ID, 5mm OD
- Rotameter with Valve Adjustable, LZM-6T Flowmeter, 6-600 ml/min

Test Procedure The following test procedure was used to fulfill the test objectives:

1. Assemble the peristaltic pump, ensuring all pieces are installed correctly
2. Connect a piece of the high-temperature tubing to the peristaltic pump ends
3. Connect the pump to the DC power supply using the test leads
4. Supply 12V to ensure the pump can be turned on, as well as pushes air
5. Adjust the input voltage between 2-12V
6. Read the flow rate off of the rotameter and record it

Test Results and Analysis Upon completion of this testing, all test objectives were met. It can be noted that the unit test concluded that the peristaltic pumps are indeed functional and do push air. Between supply voltages of 0-8V the flow was minimal and not detected by the rotameter. The full results of the test are shown below in Table 11.

Voltage (V)	Air Flow Rate (mL/min)
2	No Flow Detected
4	No Flow Detected
6	No Flow Detected
8	No Flow Detected
10	7
12	17

Table 9: Heating: Air Pump Testing Values

Full system testing will later show that the flow rate of 17 mL/min was insufficient. Supplier data stated that the pumps could reach approximately 100 mL/min. Although the flow rate at the operating voltage was lower than expected, the pumps were used in the subsystem due to there being no relevant requirements for how much air should be pushed through the system. Although this does directly affect the time taken to heat the payload, if more air needs to be pushed, pumps with higher flow rates can be purchased and integrated in future testing or design iterations. Additionally, flow rate requirements must be added to ensure the proper pumps are sourced for future work.

Test 2: Heated Air Tank Capability Testing This unit-test plan was used to measure the time it takes for the temperature inside the air tank to reach 100 °C. This 100 °C temperature was the determined setpoint that would be needed to achieve requirement PC-2.02 that would allow for the dispensed air to raise the temperature to at least 28 °C.

Test Objectives The test objectives highlight important information towards verifying functionality and determining relevant parameters of the hot air reservoir to be used for storing hot air in the payload heating subsystem. The three primary objectives of this test are as follows:

- **Objective 1:** Ensure the heating patch's intended functionality
- **Objective 2:** Observe the time the air takes to reach 100 °C
- **Objective 3:** Measure the time it takes for the air inside the tank and the tank to reach room temperature after the heating patch is turned off

Test Materials The materials used for testing were as follows:

- DC power supply
- TurboFlex Standard Flexible Heating patch, Teflon, 5 x 6 in, 150 W
- 1 Gallon 304 Stainless Steel Air Tank
- Thermocouple Type J, Round-Pin Connector, 12" Long x 3/16" Diameter Probe
- Thermocouple Type K, Surface, 40 Gage Micro Diameter Wire, PFA Insulated with Miniature Connector
- Adjustable Thermocouple Compression Fitting, Brass, 3/16" Probe OD x $\frac{1}{2}$ NPT Male 3mm Thick Polyethylene Insulative Layer, Foam Core Radiant Barrier
- Laptop with Code to Read Temperature Data

Figure 64 below shows the test set-up.

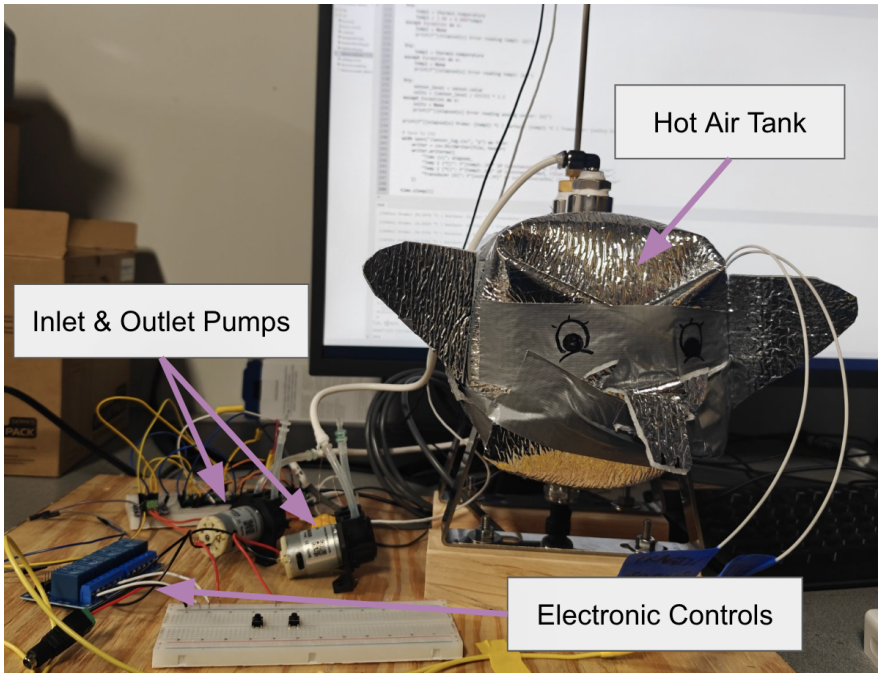

Figure 64: Dumbo the Hot Air Tank during Heating Testing

Test Procedure The following test procedure was used to fulfill the test objectives:

1. Ensure tank is fully assembled (sensors installed and functioning, insulation on)
2. Turn on the heating patch
3. Record temperature from surface thermocouple and reservoir thermocouple at every time step until the air target temperature of 100°C within the tank is reached
4. When the air target temperature of 100°C within the tank is reached, turn the patch off
5. Observe the temperature of the air tank at every time step until the temperature reaches approximately room temperature

Test Results and Analysis Upon completion of this testing, all test objectives were met. As shown in Figure 65, the heating patch stagnates at approximately 18 minutes around a temperature of 180°C and that the air tank reaches the target temperature of 100°C at approximately 45 minutes.

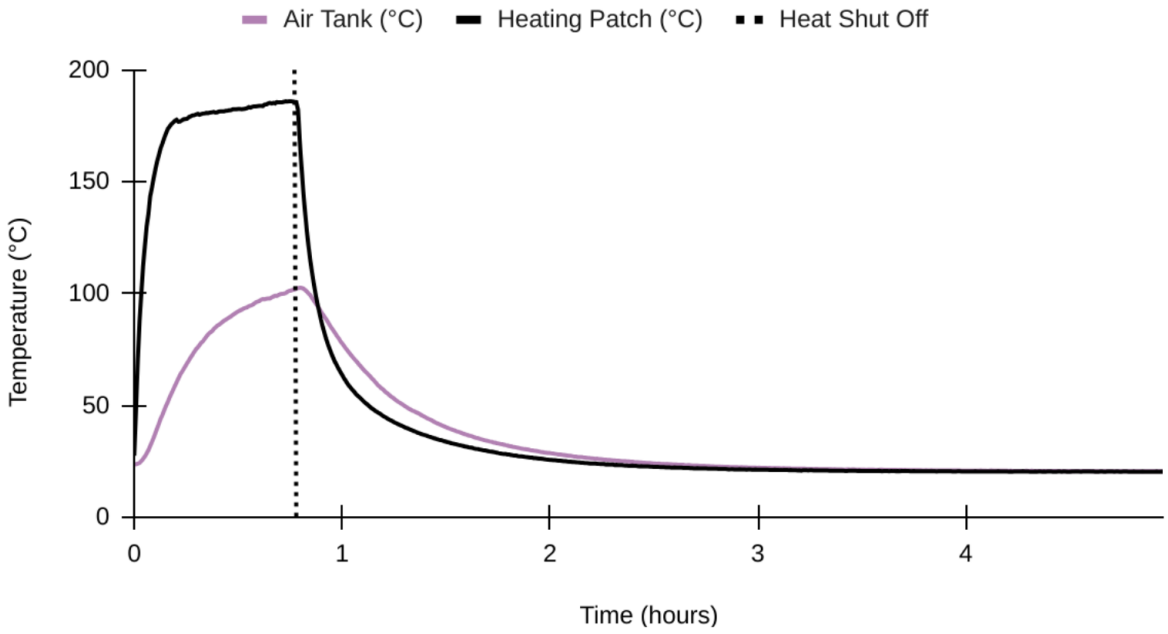

Figure 65: Tank Reservoir and Surface Temperature as a Function of Time

After the heating patch is turned off, it can also be noted that it takes approximately 2.5 hours for the heating reservoir to cool back down to room temperature. The primary takeaway from this unit test is that the heating reservoir functions as intended and will have the capability to reach air temperatures satisfactory for raising the payload temperature to at least 28°C. An additional takeaway is that for a future design iteration, a more reliable heating patch would be ideal, as during testing with temperatures above 100°C, the heating patch adhesives for the surface and wiring began to noticeably degrade.

Test 3: Full System Payload Heating This is a full system test to run the payload heating pumps and record the temperature increase.

Test Objectives The primary objective of this test is as follows:

- **Objective 1:** Determine the time (pump outlet run time) needed for the payload heating subsystem to increase the payload locker temperature to 28 °C.

Test Materials The materials used for testing were as follows:

- DC power supply
- TurboFlex Standard Flexible Heating patch, Teflon, 5 x 6 in, 150 W
- 1 Gallon 304 Stainless Steel Air Tank
- Thermocouple Type J, Round-Pin Connector, 12” Long x 3/16” Diameter Probe

- Thermocouple Type K, Surface, 40 Gage Micro Diameter Wire, PFA Insulated with Miniature Connector
- Polyethylene Insulative Layer, Foam Core Radiant Barrier
- High-temperature Silicone Rubber Tubing, Durometer 35A, 3mm ID, 5mm OD
- 12V DC Dosing Peristaltic Pump
- 150 PSI Pressure Transducer Sensor, $\frac{1}{4}$" NPT, Stainless Steel
- 3mm Thick Polyethylene Insulative Layer, Foam Core Radiant Barrier
- Breadboard
- Male-to-Male Jumper Wires
- Electrical Tape
- Teflon Tape

Test Procedure The following test procedure was used to fulfill the test objectives:

1. Turn on the heating patch
2. Allow the temperature from the reservoir thermocouple to go to 100 °C
3. Turn on the outlet pump
4. Record the temperature in the payload until the payload locker reaches 28 °C
5. Turn the heating patch off

Test Results and Analysis At this time, no results have been obtained for the full system heating payload test. It was realized upon completion of assembly and initial attempts to run the unit-test, that the pump operating flow rate of 17 mL/min was too low for transporting air from the heating reservoir to the payload. Under project time constraints, this test was unable to be completed. If this testing was to continue towards completion under this design iteration, a pump or fan system with a larger flow rate would be recommended for transporting the hot air to the payload.

Testing Summary The payload heating subsystem successfully demonstrated its ability to warm a reservoir of air to 100°C, which was intended to be circulated to the payload compartment in order to maintain a habitable environment. However, despite this initial success, the system as a whole is currently nonfunctional. The primary limitation lies in the air pump, which lacks the necessary capacity to deliver the required flow rate. As a result, the heated air is not transported efficiently enough to raise the temperature within the payload volume over time. This bottleneck highlights the need for either a more powerful pump or an alternative air delivery method to ensure effective thermal regulation across the intended space.

6.2.2 Cooling

The following outlines the testing that was performed on the payload cooling subsystem.

Test 1: Cooler Temperature Stabilization This unit-test plan was used to determine how long the beverage cooler can maintain cool air before it stabilizes to room temperature. There is no specific requirement needed for this part. However, it is expected that our prototype cooler can last for extended periods.

Test Objectives The primary objective of this test is as follows:

- **Objective 1:** Determine the temperature within the beverage cooler as a function of time

Test Materials The materials used for testing were as follows:

- Nine Quart Portable Cooler
- Thermocouple Type J, Round-Pin Connector, 12" Long x 3/16" Diameter Probe
- Thermocouple Fitting Brass, for 3/16" Probe OD x 1/2 NPT Male
- Large bag of ice
- Thick-Wall Connector, 1/2 NPT Female, for 2-5/64" Maximum Wall
- Adafruit Max 31856 Temperature Sensor
- Pico Board Microcontroller

Figure 66 below shows the test set-up.

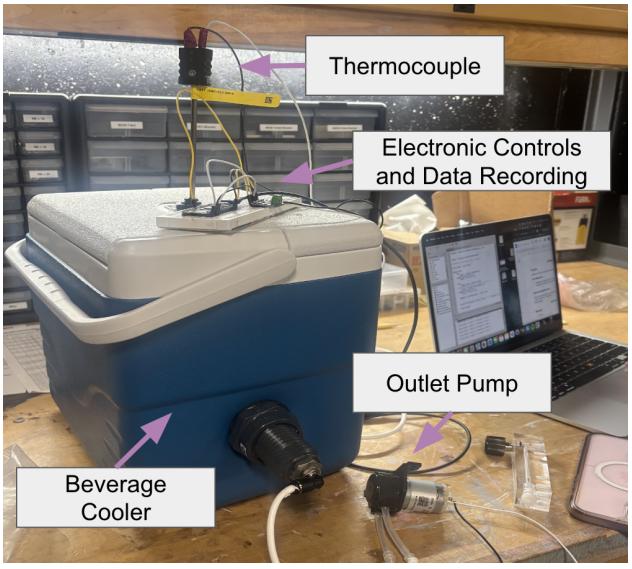

Figure 66: Cooler Temperature Testing

Test Procedure The following test procedure was used to fulfill the test objectives:

1. Place ice in the cooler until the cooler reaches approximately 8 degrees C
2. Record the temperature every 5 seconds
3. End the test when the temperature inside the cooler reaches approximately room temperature

Test Results and Analysis Upon completion of this testing, all test objectives were met. As shown in Figure 67, the cooler will stay below room temperature for approximately 50 hours. The temperature will remain between 5-10 degrees Celsius for 17 hours. After 17 hours it is recommended that the ice in the cooler be replaced for full-system testing.

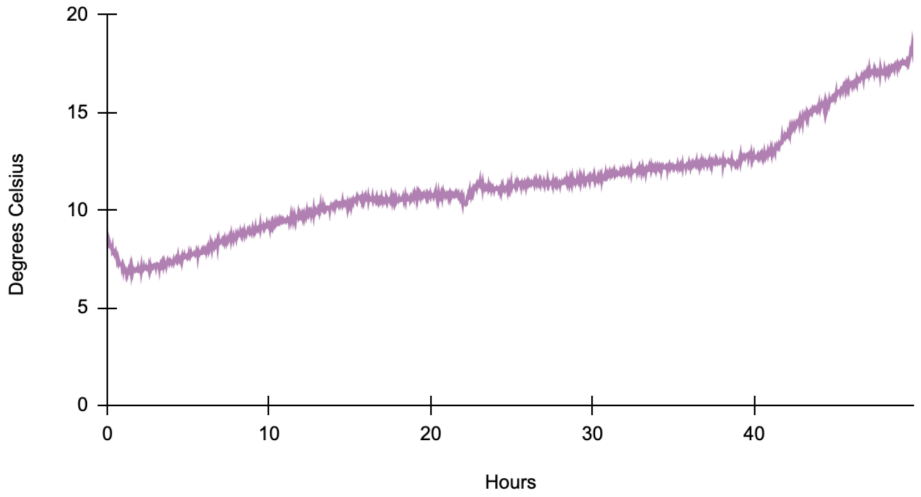

Figure 67: Beverage Cooler Temperature as a Function of Time

Test 2: Full System Payload Cooling This is a full system test to run the payload cooling pumps and record the temperature decrease.

Test Objectives The primary objective of this test is as follows:

- **Objective 1:** Determine the time (pump outlet run time) needed for the payload coooling subsystem to decrease the payload locker temperature to 17 °C.

Test Materials The materials used for testing were as follows:

- DC power supply
- Nine Quart Portable Cooler
- Thermocouple Type J, Round-Pin Connector, 12" Long x 3/16" Diameter Probe
- Thermocouple Fitting Brass, for 3/16" Probe OD x 1/2 NPT Male
- Large bag of ice
- Thick-Wall Connector, 1/2 NPT Female, for 2-5/64" Maximum Wall
- Adafruit Max 31856 Temperature Sensor
- Pico Board Microcontroller

Test Procedure The following test procedure was used to fulfill the test objectives:

1. Put ice in the cooler
2. Allow the temperature in the cooler to go to approximately 8 degrees Celsius
3. Turn on the outlet pump
4. Record the temperature in the payload until the payload locker reaches 17 °C

Test Results and Analysis Similar to the heating subsystem, at this time, no results have been obtained for the full system cooling payload test. Since the cooling subsystem uses the same pumps as the heating subsystem, it was determined that the pump operating flow rate of 17 mL/min was too low for transporting air from the heating reservoir to the payload. Under project time constraints, this test was unable to be completed. If this testing was to continue towards completion under this design iteration, a pump or fan system with a larger flow rate would be recommended for transporting the cool air to the payload.

Testing Summary Overall, it takes about 50 hours for the cooler temperature to come to room temperature. In order to fullt validate the system, a larger pump will be needed.

6.2.3 Liquid Waste Removal

The following outlines the testing that was performed on the payload liquid waste removal subsystem.

Test 1: Angled Flow Rate This unit-test plan was used to determine the flow rate of our liquid waste removal system when the tubing is held at different angles.

Test Objectives The primary objective of this test is as follows:

- **Objective 1:** Inspect flow rate while tubing is held at different angles and determine the optimal angle at which the tubing should be held by the user

Test Materials The materials used for testing were as follows:

- Kamoer KCPA600 24V peristaltic pump
- 4mm ID x 7.2 mm OD Neoprene tubing
- 200 mL beaker
- Protractor
- Waste cup
- Stopwatch

Test Procedure The following test procedure was used to fulfill the test objectives:

1. Fill the 200 mL beaker
2. Attach tubing to the peristaltic pump
3. place outlet tubing into waste container
4. Hold tubing at specified angles by measuring with a protractor
5. Use the stopwatch to time how long it takes to fill the waste cup
6. Measure the volume of water in the waste cup
7. Repeat the test for various tubing angles and trials

Test Results and Analysis It was expected that there would be a uniform decrease in the amount of water displaced by the pump as the angles from horizontal increased. We were able to see that that was not the case in any of our trials. In fact, in each trial, the tubing being held at an angle of 45 degrees actually caused more water to be produced in 30 seconds than when held at 30 degrees. This can be noted from Table 10. In trials A and C, we see an increase in volume when the tubing is held at 60 degrees, and the only case in which this does not occur is trial B, with it being a sharp enough decrease in volume that it affects the average.

Tube Angle (Degrees)	**Trial A (mL/s)**	**Trial B (mL/s)**	**Trial C (mL/s)**	**Average (mL/s)**
30	3.50	4.17	2.85	3.51
45	3.67	4.33	3.33	3.78
60	3.83	3.33	3.50	3.55
90	1.50	3.50	1.67	2.22

Table 10: Pump Flow Rate and Tube Angle

This test allowed us to understand whether this system would be effective at removing liquid waste within the payload. We were able to see that it may take longer when held at a larger angle, our pump is still able to work efficiently.

Test 2: Maximum Particulate Amount The purpose of this test is to investigate the particulate amounts that can pass through the peristaltic pump and mesh opening without clogging the pump.

Test Objectives The primary objective of this test is as follows:

- **Objective 1:** Quantify the maximum particulate amount able to progress through the peristaltic pump and mesh opening.

Test Materials The materials used for testing were as follows:

- Kamoer KCPA600 24V peristaltic pump
- 4mm ID x 7.2 mm OD Neoprene tubing
- Zip Ties
- Polyester Fabric Mesh Storage Bag
- Waste cup
- Potting Soil Sediment
- 500 mL beaker

Test Procedure The following test procedure was used to fulfill the test objectives:

1. Mix 100 mL of water with 100 mL of sediment in the 500 mL beaker
2. Attach the mesh bag to the tubing inlet using the zip tie
3. Place inlet tubing into the water-sediment semiliquid

4. Place outline tubing into the waste cup
5. Run liquid waste pump for 90 seconds
6. Examine the resulting waste cup and sediment beaker

Test Results and Analysis Our testing was conducted all while our pump was at a medium speed, more so a measure of how much sediment is able to be removed by our component. In all three trials, we were left with liquid that was not clear, but was free of sediment. This ensured that our component and system were able to fully rid our semiliquid of sediment, returning water that was not clear, but also did not contain visible contaminants. For that reason, our test objectives were met, as our pump was able to handle semiliquid, and we were able to determine that spills that are primarily liquid are able to be suctioned by our system.

Figure 68: The 200 ml mixture containing 100 ml of sediment and 100 ml of water, which was replenished and used for all 3 trials

Figure 69: Waste Cup Results After the First Trial

As aforementioned, it is notable that almost no visible particulate matter is present. After our first trial, we noted that essentially all sediment had been filtered.

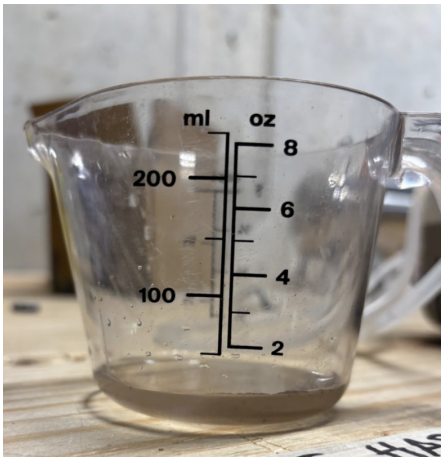

Figure 70: Waste Cup Results After the Second Trial

In addition to obtaining the same result as our first trial, we were able to note during a second trial that approximately 20 ml of water was able to travel through our system and be processed during the 90 seconds that each trial lasted. This was verified by measuring the liquid output after each trial ran, with the same approximate amount of water being measured each time.

Figure 71: Waste Cup Results After the Third Trial

Notably, there is slightly more particulate matter present in this trial. We were able to conclude that this could be a source of error, as we did not clean the tubing or pump between each trial, which meant that it could have been sediment from a previous trial. This did allow us to note that the pump may need to be emptied after a few minutes of use between runs, something that we would have to further test to ensure.

Testing Summary In summary, we are able to conclude that our system does serve its purpose, as it would be fully able to be manually used to remove liquid waste within our payload locker.

Seeing as our requirement for bench-top testing is that this system is able to remove liquid waste, we can say with certainty that our system works, especially because it is able to work at different angles.

6.2.4 Feedwater

The following outlines the testing that was performed on the feedwater subsystem.

Test 1: Pump Flow Rate The purpose of this test is to create a calibration curve for the feedwater pump.

Test Objectives The primary objective of this test is as follows:

- **Objective 1:** Determine pump flow rate as a function of input voltage.

Test Materials The materials used for testing were as follows:

- 2PCS 12V DC Dosing Peristaltic Pump
- 5mm ID x 7mm OD Silicone Tubing
- Water Container
- Outlet Water Container
- Stopwatch

Figure 72 below shows the pump used for testing.

Figure 72: Pump Used For Feedwater Testing

Test Procedure The following test procedure was used to fulfill the test objectives:

1. Connect tubing to the pump
2. Fill container with 200 mL of water
3. Place the inlet end of the tubing into the water container and the outlet end of the tubing into the outlet water contianer
4. Power the pump with a given voltage
5. Measure water dispensed after 2 minutes
6. Calculate the flow rate and record the value
7. repeat for a second trial and calculate the average

Test Results and Analysis The resulting calibration curve from testing is shown below in Figure 73.

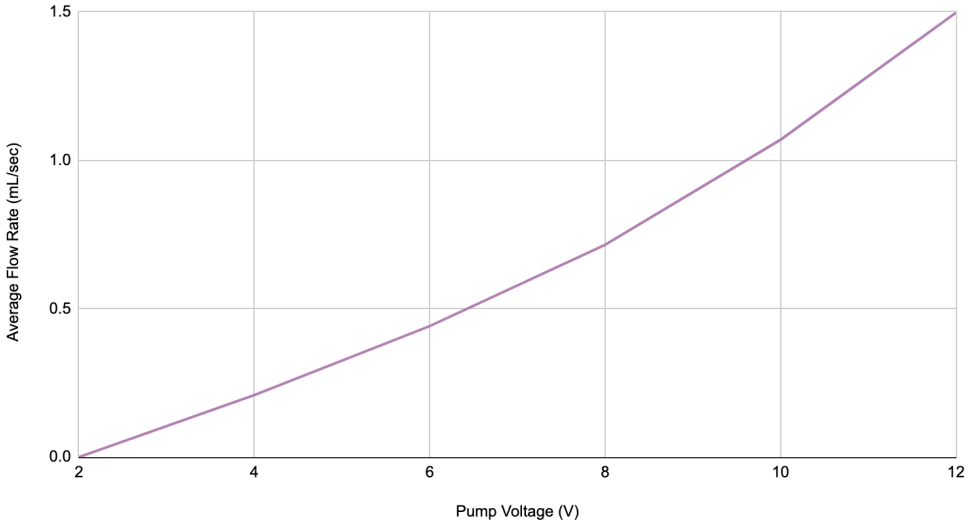

Figure 73: Feedwater Pump Calibration Curve

Test 2: Pump Consistency Flow Rate The purpose of this test is to determine the pump voltage and thus flow rate needed to establish the maximum consistent flow at the feedwater spray interface. We have characterized a consistent flow rate as having a steady stream of water that is able to turn into mist by the time it reaches the mist interface, whether water does not stop, or drip, and the flow is not intense. A non-intense flow means, to us, that the water pressure is not so high that the mist is nonuniform or so aggressive that it may damage the payload inside the locker.

Test Objectives The primary objective of this test is as follows:

- **Objective 1:** Determine the pump flow rate and input voltage needed to establish consistent flow

Test Materials The materials used for testing were as follows:

- 2PCS 12V DC Dosing Peristaltic Pump
- 5mm ID x 7mm OD Silicone Tubing
- Water Container
- Outlet Water Container
- Stopwatch
- Spray Interface

Figure 74 below shows the pump used for testing.

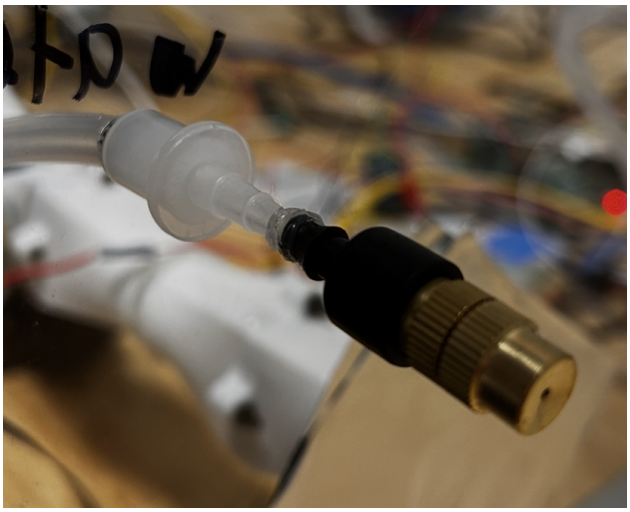

Figure 74: Spray Interface Used For Feedwater Testing

Test Procedure The following test procedure was used to fulfill the test objectives:

1. Connect tubing to the pump
2. Fill container with 200 mL of water
3. Place the inlet end of the tubing into the water container
4. Power the pump with a given voltage
5. Use average flow rate calibration curve to determine approximate flow rate
6. Record qualitative descriptors outlined in Table **??**

Test Results and Analysis This test allowed us to determine that an input voltage of between 8-12 V for a flow rate of between 0.46-1.07 mL/sec will result in a mist that does not have dripping, is not too intense, and provides a steady stream.

Voltage (V)	Flow Rate (mL/min)	Qualitative Descriptors			
		Automatic Mist?	Drip?	Too Intense?	Steady Stream?
2	0	No	No	No	No
4	0	No	Yes	No	No
6	0.21	No	Yes	No	No
8	0.46	Yes	No	No	Yes
10	0.72	Yes	No	No	Yes
12	1.07	Yes	No	No	Yes

Table 11: Feedwater Flow Consistency Results

Testing Summary In conclusion, our design does work as intended. It is able to deliver potable water to our payload locker provided 8-12V, as well as deliver a consistent flow with a mist at 0.46-1.07 mL/sec.

6.2.5 Air Circulation and Dehumidification

The following outlines the testing that was performed on the air circulation and dehumidification subsystem.

Test 1: Desiccant Pressure Drop The purpose of this test was to determine the severity of the pressure drop across the desiccant fitting.

Test Objectives The primary objective of this test is as follows:

- **Objective 1:** Characterize the pressure drop across the desiccant

Test Materials The materials used for testing were as follows:

- Custom desiccant fitting with 1 inch PVC tubing with 4 grams of silica gel
- Hon&Guan Quiet 3 Inch Duct Fan
- 1/4" Male NPT Pressure Transducer 10-32 VDC
- 1 inch PVC Tubing

Test Procedure The following test procedure was used to fulfill the test objectives:

1. Install pressure transducer and fittings downstream of the fan and desiccant fitting
2. Run the fan at 23.19 SCFM and measure readings from the transducer

Test Results and Analysis At a flow rate of 23.19 SCFM the pressure transducers read an inlet voltage of 0.482V and an outlet voltage of 0.481V. The working pressure transducer outputs from a range of 0.5V to 4.5V defined by the specifications. The pressure transducer reads to an accuracy of 1% of the full scale. Therefore, it can determined that the results of this test show a pressure drop of the noise of the sensor.

While there is no requirement for the pressure flow rate needed by the fan and a maximum pressure drop given by the desiccant fitting, the value will need to be determined for future applications.

Test 2: Fan Air Flow Rate The purpose of this test is to quantify the volumetric air flow at each notch of our controllable fan's potentiometer.

Test Objectives The primary objective of this test is as follows:

- **Objective 1:** Place quantitative values at every notch identified on the fan's controller in units of SCFM

Test Materials The materials used for testing were as follows:

- NICE-POWDER Anemometer
- Hon&Guan Quiet 3 Inch Duct Fan

Test Procedure The following test procedure was used to fulfill the test objectives:

1. Place anemometer in front of the fan
2. Run the fan at each notch and record the flow rate (m/s) displayed on the anemometer
3. Calculate and record the volumetric flow rate by using the cross sectional area of the fan

Test Results and Analysis Table 12 below outlines the associated flow rates and volumetric flow rates for each notch on the fan.

Notch Number	Flow Rate (m/s)	Volumetric Flow Rate (SCFM)
1	2.4	23.19
2	2.1	20.29
3	1.9	18.36
4	1.8	17.39
5	1.7	16.43
6	1.5	14.49
7	1.4	13.53

Table 12: Fan Flow Rates and Volumetric Flow Rates

Test 3: Full System Dehumidification This is a full system test meant to evaluate the capability of the dehumidifying system.

Test Objectives The primary objective of this test is as follows:

- **Objective 1:** Determine the amount of silica needed to decrease the humidity within the payload locker from 90% to 60%

Test Materials The materials used for testing were as follows:

- Feedwater Subsystem
- Payload Locker
- Air Circulation Subsystem
- Desiccant Silica Gel (4 grams)
- Adafruit HDC3022 Precision Temperature & Humidity Sensor
- Stopwatch

Figure 75 shows the dehumidifying bypass line. Additionally, figure 76 shows the dehumidifying line (the desiccant fitting is not shown in the image).

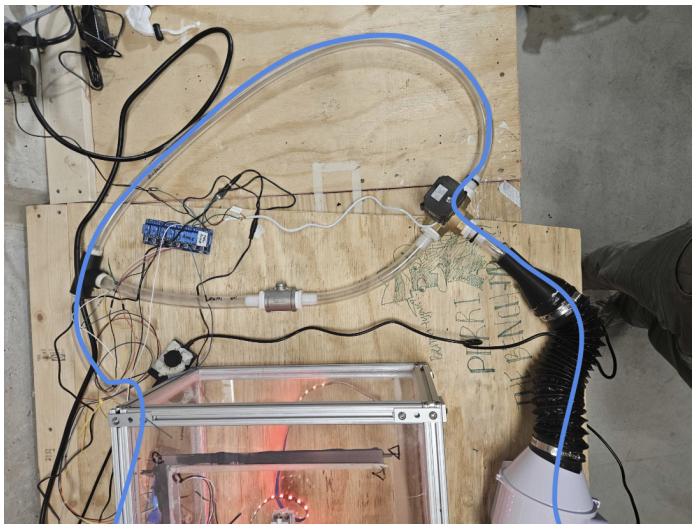

Figure 75: Dehumidifying Bypass Line (Blue)

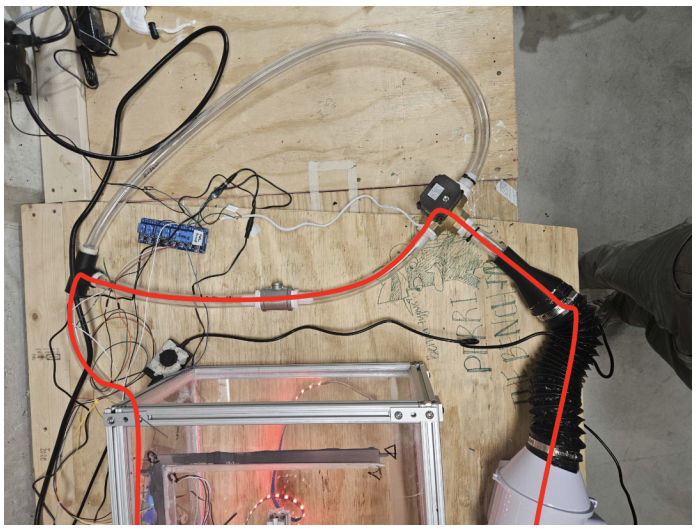

Figure 76: Dehumidifying Desiccant Line (Red)

Test Procedure The following test procedure was used to fulfill the test objectives:

1. Use the feedwater system to spray water into the payload locker until 90% relative humidity is read on the humidity sensors
2. Turn on the air circulation fan and record time
3. Record humidity until a stable value is read and the silica gel beads become pink in appearance

Test Results and Analysis As shown below in Figure 77, the silica gel did lower the relative humidity in the payload locker. The humidity, when 4 grams of silica gel was used showed a drop from 90% humidity to 60% humidity. This drop, however, does not mean that 30% relative humidity was absorbed. In the beginning of this test, we see a huge drop in humidity, and then a rapid decline. However this is attributed to the moisture being dispensed into the system and then immediately dispersed. Thus, by cutting down the window we are viewing our humidity changes in, shown in the graph below, we observe around 5% absorption of relative humidity using 4 grams of silica gel beads (65%-60%).

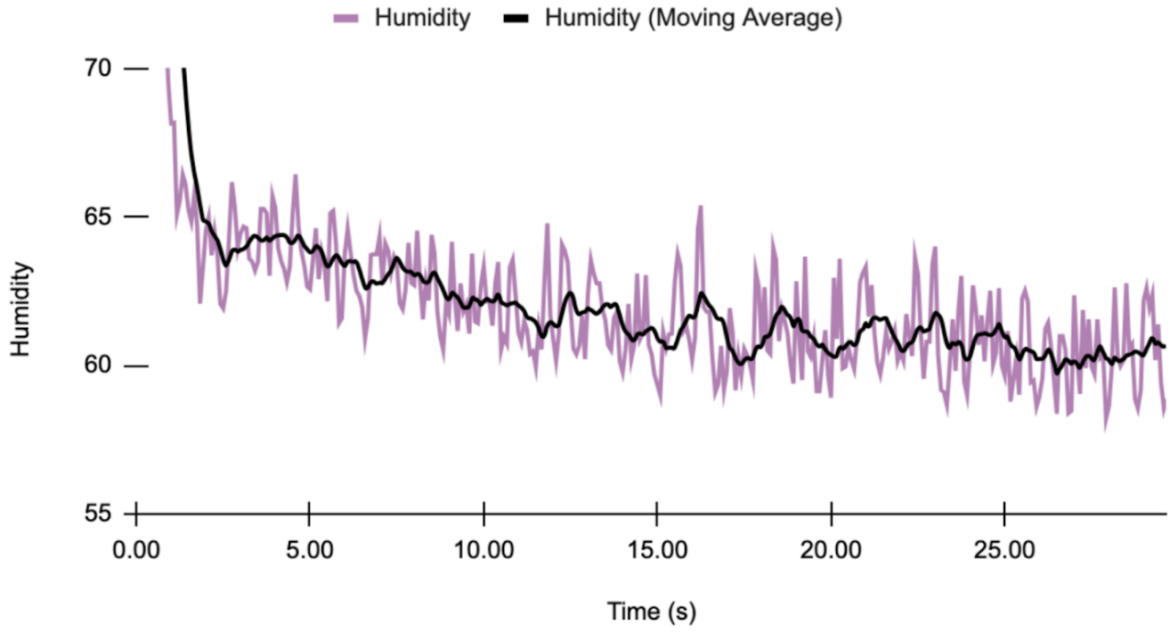

Figure 77: Humidity Absorption of 5% Relative Humidity

The relative humidity decreased by 5% in 30 seconds. This means that the system can scrub approximately 0.17% relative humidity per second. Additionally, in order to scrub 60% relative humidity, 48g of silica will be needed within the custom desiccant fitting.

Testing Summary There were several key takeaways from our system testing, verification and validation, and overall bench-top setup of the air circulation and dehumidification line. First, we looked at tests involving our 3-way solenoid and volumetric air calculations. These tests gave us valuable insight into what settings would be most optimal for the system, such as which notch or SCFM rate to use, as well as confirming that electronic components like the solenoid are operational and functional. The average time it took for the solenoid to complete its L-shaped movement

helped us evaluate whether the switching time is practical in real-world use when dehumidification or bypass is needed. Based on our results, we concluded that the values were acceptable for our current system.

The pressure drop test was another key part of our validation process. Our data showed only a minimal pressure drop across the desiccant, which made sense given how small our desiccant is. However, we also had to consider the limitations of our pressure transducers. The sensors we used operate over a wide range (0 to 150 PSI) which likely reduces accuracy at the extreme low end of that range, where our voltage readings fell. Especially considering they fell outside of the expected output range (0.5V-4.5V). This doesn't invalidate our test results as we noticed no backflow and air output did not seem as different from air input. But it's an important limitation to keep in mind. Again, the desiccant showed no signs of blockage or pressure buildup, which indicates successful integration of the custom desiccant into our system.

Finally, we tested the effectiveness of the desiccant through full system testing, which gave us insight into how the design might perform in real-life conditions. In our setup, the feedwater system can increase humidity inside the payload. This triggers the humidity sensors, which signal the solenoid to open the dehumidification line. Once activated, the desiccant begins absorbing moisture until humidity drops below our target threshold of 30%.

We did not test the exhaust line, as no additional validation was necessary. The peristaltic pump associated with this line functions reliably in coordination with the electronics, and its flow rate is well-documented in the technical specifications. Overall, our system performed as intended. While there are areas where testing could be improved to yield more precise data, these limitations were primarily due to constraints in time and resources, not flaws in the design itself.

6.2.6 Payload Lighting

The following outlines the testing that was performed on the payload lighting subsystem.

Test 1: Brightness Calibration The purpose of this test is to ensure that the LED strips are able to accommodate for low, medium, and high levels of lighting, per our system requirements. Additionally, this test will check to ensure that the brightness of our LED strips will not wane after 30 minutes of use.

Test Objectives The primary objectives of this test is as follows:

- **Objective 1:** System Requirement PC-2.5: The payload locker shall accommodate low, medium, and high lighting with wavelengths within the visible and UV spectrum
- **Objective 2:** Record the brightness of the LEDs as a function of control input

Test Materials The materials used for testing were as follows:

- Luxmeter
- BTF-LIGHTING WS2812B IC RGB 5050SMD LED Strips
- Power Supply

Figure 78 shows the LED strips as powered during testing.

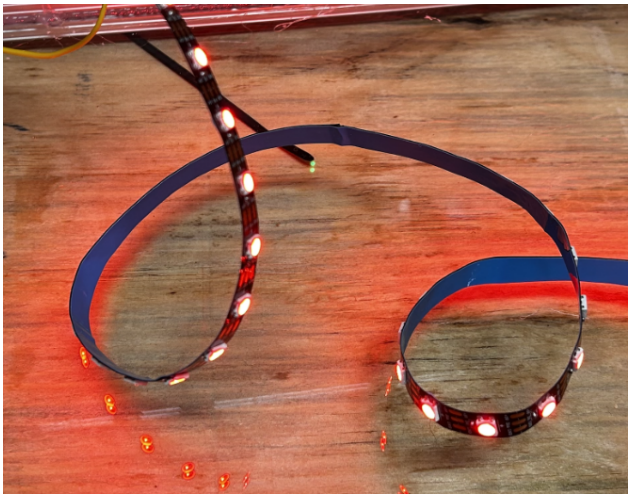

Figure 78: LED Strips Used During Testing

Test Procedure The following test procedure was used to fulfill the test objectives:

1. Power on the LED strip
2. Adjust the LED strip to different levels of brighness using control input values between 0 to 1
3. Let the LEDs sit for 30 minutes
4. Record the brightness of the LEDs

Test Results and Analysis Tables 13, 14, and 15 below outlines the brightness of the LEDs as a function of the light input.

LED Command Input	Brightness (lux)
0.01	14
0.17	23
0.33	35

Table 13: Low Brightness LED Calibration

LED Command Input	Brightness (lux)
0.34	35
0.50	45
0.66	70

Table 14: Medium Brightness LED Calibration

LED Command Input	Brightness (lux)
0.67	70
0.84	80
1.00	100

Table 15: High Brightness LED Calibration

We can conclude from this test that brightness increases as levels increase, and that the lux does not dip below the expected amount when it is set to a particular number, even after it is on for 30 minutes. This allows us to understand that brightness will remain constant while the lights are on within the payload, and that they will not wane. We can then assume that when we set our lights to a particular brightness, that that is the brightness reaching the plants for the duration of time that they are on.

Test 2: LED Heat Generation The purpose of this test is to evaluate the heat generation of the LEDs.

Test Objectives The primary objectives of this test is as follows:

- **Objective 1:** Record the temperature of the LED strips as a function of distance
- **Objective 2:** Record the temperature of the LED strips as a function of time

Test Materials The materials used for testing were as follows:

- Luxmeter
- BTF-LIGHTING WS2812B IC RGB 5050SMD LED Strips
- Thermocouple
- Power Supply

Test Procedure The following test procedure was used to fulfill the test objectives:

1. Power on the LED strip
2. Measure the heat emitted using a thermocouple from 0 to 18 inches
3. Repeat the previous step every 5 minutes for 15 minutes

Test Results and Analysis The test results show per Figure 79, there is a gradual increase in temperature, approximately a quarter of a degree Celsius every 5 minutes. The amount of time the lights within the payload will be on is dependent on the kind of botany within the payload, and a test such as this allows us to understand at what point the lights may generate enough heat to have an effect on the payload within the payload locker.

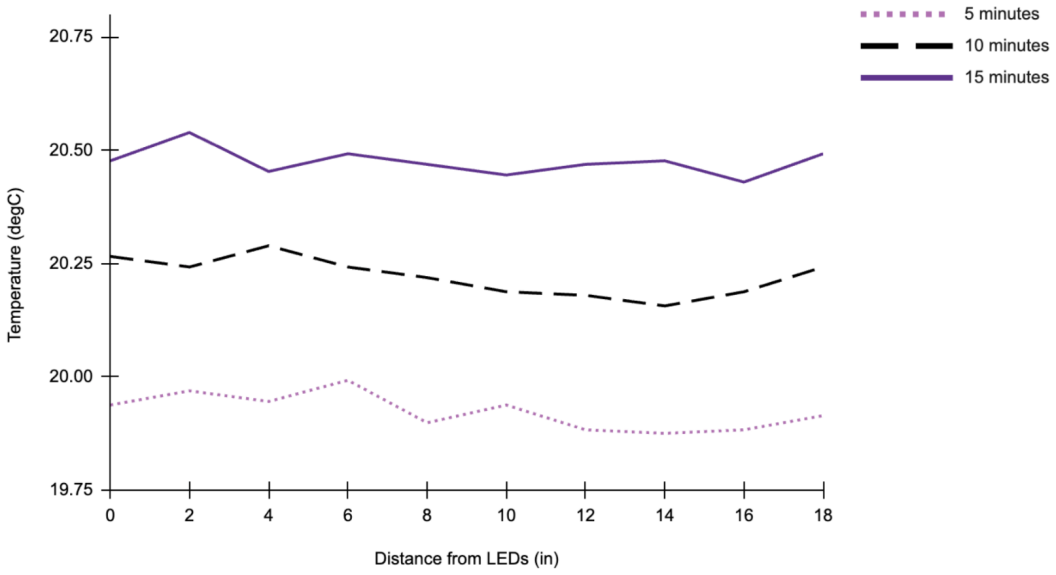

Figure 79: Heat Generation of the LEDs

Testing Summary Our design does, in fact, work as intended. We are able to note that as time goes on, as does the amount of heat emitted by our lights. The temperature increase is something that we noted, as we originally wanted to ensure that the distance between the plants and lights would not cause a significant amount of heat to reach the plants. Our design does work, especially since brightness remains the same over time, meaning that we are able to ensure that the amount of light delivered to botany within the payload will remain the same. However, we are able to take away that these lights would not be an ideal component within our payload locker due to the increase in temperature over time. While this would likely not be a concern for shorter periods of time, if we were to have life within the payload that were extremely heat-sensitive, tall enough to be in close proximity to the lights, or required lots of light, the temperature would then be a concern.

6.2.7 Fire Detection

The following outlines the testing that was performed on the fire detection subsystem.

Test 1: Carbon Monoxide Edge Test The purpose of this test is to evaluate the detector's ability to detect carbon monoxide within the payload and determine if CO readings can help in fire detection.

Test Objectives The primary objective of this test is as follows:

- **Objective 1:** Determine the point at which our CO detector will be able to detect the emission of carbon monoxide, verifying this occurs at approximately 10 ppm.

Test Materials The materials used for testing were as follows:

- Household Candle (Fire Source)
- SRAQ-G012 CO Detector Module

- Breadboard
- Power Supply
- Raspberry Pi Pico

Figure 80 shows the CO sensor as powered during testing

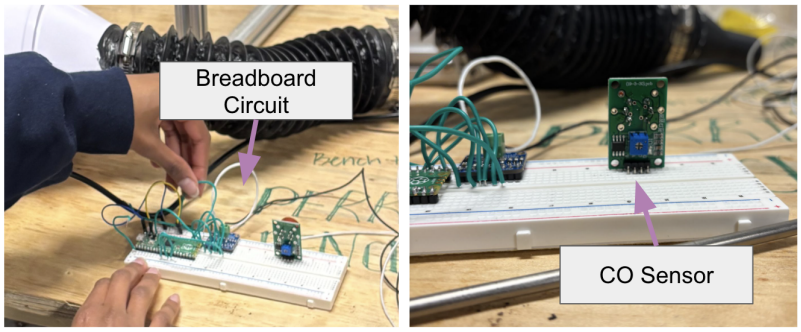

Figure 80: CO Sensor Configurating

Test Procedure The following test procedure was used to fulfill the test objectives:

1. Light the candle in a closed environment.
2. Place the candle 10 inches from the CO detector.
3. Take readings every 10 seconds for 2 minutes.

Test Results and Analysis The Rs value was the amount of carbon monoxide said to be in the present area, and the Ro value is the amount of carbon monoxide within a clean, ventilated environment. An increase in the ratio corresponds to an increase in carbon monoxide within the area.

The baseline indoor ratio is approximately 0.78. The values given by Figure 81 show that there was an overall increase in the amount of carbon monoxide detected when a fire was present, thus validating our detection system.

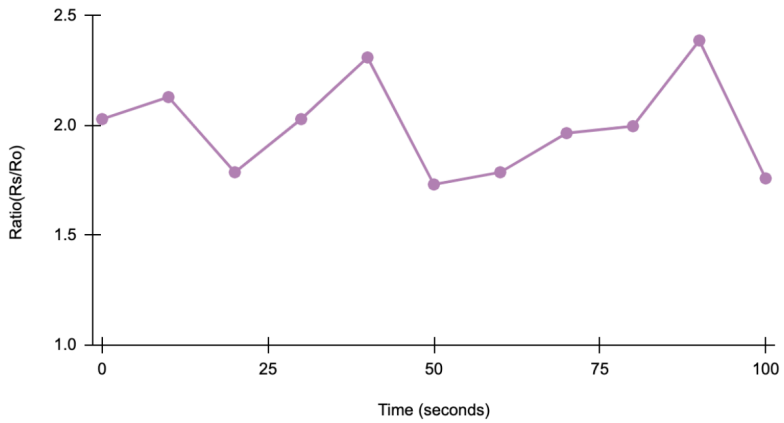

Figure 81: Carbon Monoxide Detection 10 inches from the sensor

Testing Summary In conclusion, we are able to determine that our design does work. Thus, we are able to conclude that small fires produced within 10 inches of the detector, or approximately the length of our payload, will be detected by our device. We can then use this information to decide what location we would like to put this component to make it most useful.

6.2.8 Temperature and Humidity Sensor

The following outlines the testing that was performed with the Adafruit HDC3022 Temperature and Humidity Sensor.

Test 1: Sensor Verification The purpose of this test is to verify that the sensor can measure the temperature of an environment within accuracy of ±2°C, confirm that the data from the sensor can be retrieved and stored, and validate the sensor can measure temperatures within the expected range of 17-28°C for the payload rack.

Test Objectives The primary objectives of this test are as follows:

- **Objective 1:** Ensure the sensor can be powered through the micro controller.
- **Objective 2:** Ensure the temperature measurement has an accuracy within ±2°C.
- **Objective 3:** Retrieve and store the data from the sensor.

Test Materials The materials used for testing were as follows:

- Adafruit HDC3022 Sensor
- Raspberry Pi Pico
- Breadboard
- Computer with Thonny IDE
- Jumper Wires
- USB to Micro-USB Cable

Figure 82 shows the temperature and humidity sensor powered during testing.

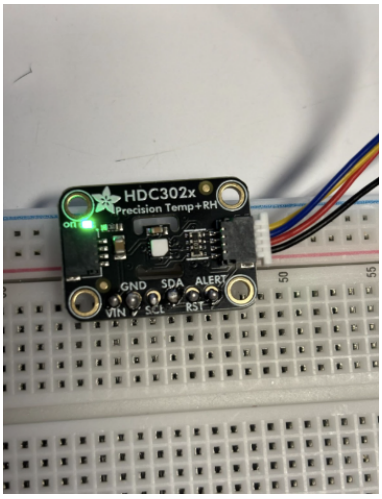

Figure 82: Temperature and Humidity Sensor

Test Procedure The following test procedure was used to fulfill the test objectives:

1. Connect the sensor to the Raspberry Pi Pico using jumper wires.
2. Power the Pico by connecting it to a computer using a USB to micro-USB cable.
3. Place the sensor in an indoor room.
4. Open Thonny IDE and run the pre-written test script for the sensor.
5. Display and record the temperature and humidity readings displayed on the serial monitor.
6. Compare the recorded values to the true indoor temperature and humidity.
7. Move the sensor outdoors and re-run the test script on Thonny IDE.
8. Compare the recorded values to the true outdoor temperature and humidity.
9. Move the sensor to a second indoor room, and re-run the test script on Thonny IDE.
10. Compare the recorded values to the true indoor temperature and humidity.

Test Results and Analysis Testing was done in three environments: Room 1, Room 2, and outdoors. For each environment, the test was run for 30 seconds every 5 seconds while data was being read onto the serial monitor using Thonny IDE. These values were also compared to the true temperature and humidity conditions measured previously using a thermometer and hygrometer in their respective environments.

In Room 1, the true conditions measured were 20°C and 17% humidity. The values given in Table 16 show that the temperature readings stayed consistent at 21°C, and the humidity readings varied between 16.7-17.1%.

Similarly, in Room 2 the true conditions measured were 18.5°C and 18% humidity. The values given in Table 16 show that the temperature readings stayed consistent at 18.5°C, and the humidity readings varied between 18.2-18.4%.

Time (s)	**Temp (°C) Room 1**	**Humidity (%) Room 1**	**Temp (°C) Room 2**	**Humidity (%) Room 2**
0	21.0	17.0	18.5	18.2
5	21.0	16.7	18.5	18.3
10	21.0	16.8	18.5	18.4
15	21.0	16.8	18.5	18.4
20	21.0	16.7	18.5	18.4
25	21.0	17.1	18.5	18.4
30	21.0	16.9	18.5	18.4

Table 16: Temperature and Humidity Sensor Measurements in Room 1 and Room 2.

In the outdoor environment, the true conditions measured were 0.56°C and 57% humidity. The values given in Table 17 show that the temperature readings varied between 1.4-1.5°C, and humidity remained consistent at 53.5%.

Time (s)	Temp (°C)	Humidity (%)
0	1.4	53.5
5	1.4	53.5
10	1.4	53.5
15	1.4	53.5
20	1.5	53.5
25	1.5	53.5
30	1.4	53.5

Table 17: Temperature and Humidity Sensor Measurements in the Outdoor Environment.

Testing Summary After testing, we verified that the Adafruit HDC3022 Temperature and Humidity Sensor met all three testing objectives outlined for this test. Thus, we are able to conclude that this sensor is suitable for our system and that accurate temperature and humidity data can be monitored and stored.

6.2.9 Oxygen Sensor

The following outlines the testing that was performed with the DFRobot I²C Oxygen Sensor.

Test 1: Sensor Verification The purpose of this test is to verify that the sensor can measure the oxygen concentration of an environment in percentage and confirm that the data from the sensor can be retrieved and stored.

Test Objectives The primary objectives of this test are as follows:

- **Objective 1:** Ensure the sensor can be powered through the micro controller.
- **Objective 2:** Verify readings are within range of 1% normal oxygen composition per the NOAA (20.9% O2 concentration).
- **Objective 3:** Retrieve and store the data from the sensor.

Test Materials The materials used for testing were as follows:

- DFRobot I²C Oxygen Sensor
- Raspberry Pi Pico
- Breadboard
- Computer with Thonny IDE
- Jumper Wires
- USB to Micro-USB Cable

Figure 83 shows the oxygen sensor powered during testing.

Figure 83: Oxygen Sensor

Test Procedure The following test procedure was used to fulfill the test objectives:

1. Connect the sensor to the Raspberry Pi Pico using jumper wires.
2. Power the Pico by connecting it to a computer using a USB to micro-USB cable.
3. Open Thonny IDE and run the pre-written test script for the sensor.
4. Record the oxygen readings displayed on the serial monitor.
5. Compare the recorded values to the normal concentration of 20.9%.
6. Repeat until three trials have been completed.

Test Results and Analysis Testing ran for 30 seconds every 5 seconds for all three trials while data was being read onto the serial monitor using Thonny IDE. These values were also compared to the normal oxygen concentration of 20.9%, according to the NOAA.

The values given in Table 18 show that the oxygen readings stayed within the range of 20.45-20.95% across all three trials. Some of the values in Trials 2 and 3 did not fall within 1% of 20.9% oxygen concentration due to human error. This was because the sensor was not re-calibrated before attempting to collect new data.

Time (s)	**O_2 (%) Trial 1**	**O_2 (%) Trial 2**	**O_2 (%) Trial 3**
0	20.82	20.72	20.50
5	20.92	20.73	20.47
10	20.88	20.73	20.45
15	20.95	20.69	20.45
20	20.89	20.65	20.46
25	20.88	20.62	20.49
30	20.86	20.69	20.58

Table 18: Oxygen Concentration across Three Trials.

Testing Summary After testing, we determined that the DFRobot I^2C Oxygen Sensor met all three test objectives outlined for this test, despite the human error that caused Objective

2 not to be fully met for Trials 2 and 3. Overall, we are able to conclude that this sensor is suitable for our system and that accurate oxygen concentration data can be monitored and stored.

6.2.10 Carbon Dioxide Sensor

The following outlines the testing that was performed with the Adafruit SCD40 Carbon Dioxide Sensor.

Test 1: Sensor Verification The purpose of this test is to verify that the sensor can measure the carbon dioxide concentration of an environment in ppm and confirm that the data from the sensor can be retrieved and stored.

Test Objectives The primary objectives of this test are as follows:

- **Objective 1:** Ensure the sensor can be powered through the micro controller.
- **Objective 2:** Verify readings are within range of 400-1000 ppm, and are realistic for the current environment.
- **Objective 3:** Retrieve and store the data from the sensor.

Test Materials The materials used for testing were as follows:

- Adafruit SCD40 Carbon Dioxide Sensor
- Raspberry Pi Pico
- Breadboard
- Computer with Thonny IDE
- Jumper Wires
- USB to Micro-USB Cable

Figure 84 shows the carbon dioxide sensor powered during testing.

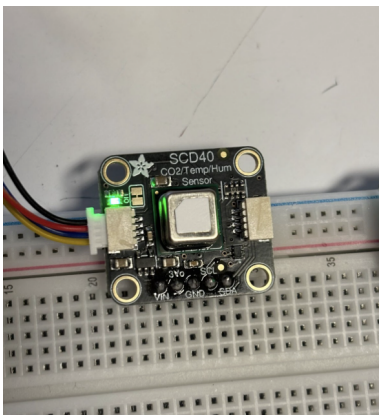

Figure 84: Carbon Dioxide Sensor

Test Procedure The following test procedure was used to fulfill the test objectives:

1. Place the sensor indoors.
2. Connect the sensor to the Raspberry Pi Pico using jumper wires.
3. Power the Pico by connecting it to a computer using a USB to micro-USB cable.
4. Open Thonny IDE and run the pre-written test script for the sensor.
5. Record the carbon dioxide readings displayed on the serial monitor.
6. Compare the recorded values to the range of 400-1000 ppm.
7. Repeat until four trials have been completed.

Test Results and Analysis Testing ran for 60 seconds every 5 seconds for all four trials while data was being read onto the serial monitor using Thonny IDE. These values were also compared to recommended indoor carbon dioxide levels of 400-1000 ppm.

The values given in Table 19 show that all of the readings for trials 1, 2, and 4 stayed within the healthy range of 400-1000 ppm. However, some of the values in trial 3 went above 1000 ppm, the highest recorded reading being 1103. This is likely due to the testing being conducted in a small, confined room with multiple people, not an actual issue with the sensor.

Time (s)	**CO_2 (ppm) Trial 1**	**CO_2 (ppm) Trial 2**	**CO_2 (ppm) Trial 3**	**CO_2 (ppm) Trial 4**
0	648	844	1103	788
5	652	852	1052	790
10	656	854	1005	804
15	648	850	975	816
20	641	841	952	824
25	634	841	934	829
30	633	839	925	831
35	634	835	915	828
40	632	833	911	827
45	631	827	902	825
50	629	820	889	823
55	627	817	883	820
60	624	818	866	817

Table 19: Carbon Dioxide Concentration across Four Trials.

Testing Summary After testing, we determined that the Adafruit SCD40 Carbon Dioxide Sensor met all three test objectives outlined for this test, despite the environmental error that occurred in trial 3. Overall, we are able to conclude that this sensor is suitable for our system and that accurate carbon dioxide concentration data can be monitored and stored.

6.2.11 Pressure Sensor

The following outlines the testing that was performed with the Adafruit BMP390 Pressure Sensor.

Test 1: Sensor Verification The purpose of this test is to verify that the sensor can measure the pressure of an environment in millibars and confirm that the data from the sensor can be retrieved and stored.

Test Objectives The primary objectives of this test are as follows:

- **Objective 1:** Ensure the sensor can be powered through the micro controller.
- **Objective 2:** Verify readings are within range of ±20 mb of the true room pressure.
- **Objective 3:** Retrieve and store the data from the sensor.

Test Materials The materials used for testing were as follows:

- Adafruit BMP390 Pressure Sensor
- Raspberry Pi Pico
- Breadboard
- Computer with Thonny IDE
- Jumper Wires
- USB to Micro-USB Cable

Figure 85 shows the pressure sensor powered during testing.

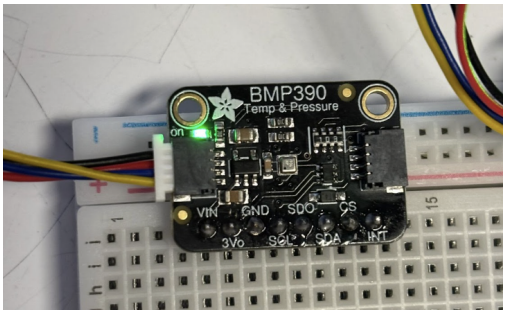

Figure 85: Pressure Sensor

Test Procedure The following test procedure was used to fulfill the test objectives:

1. Place the sensor indoors.
2. Connect the sensor to the Raspberry Pi Pico using jumper wires.
3. Power the Pico by connecting it to a computer using a USB to micro-USB cable.
4. Open Thonny IDE and run the pre-written test script for the sensor.
5. Record the pressure readings displayed on the serial monitor.
6. Compare the recorded values to the true pressure values.
7. Repeat until three trials have been completed.

Test Results and Analysis Testing ran for 10 seconds every 1 second for all three trials while data was being read onto the serial monitor using Thonny IDE. These values were also compared to the true pressure of the room using an online app.

The values given in Table 20 show that all of the readings for all three trials were within ±20 mb of the true room pressure. All recorded values also stayed very precise around 997 mb.

Time (s)	Pressure (mb) Trial 1	Pressure (mb) Trial 2	Pressure (mb) Trial 3
0	997.0	997.0	997.0
1	996.9	997.0	997.0
2	997.0	997.0	997.0
3	997.0	997.0	997.0
4	996.9	997.0	997.0
5	996.9	997.0	997.0
6	996.9	996.9	997.0
7	996.9	997.0	997.1
8	997.0	997.0	997.0
9	996.9	997.0	997.0
10	996.9	997.0	997.0

Table 20: Pressure across Three Trials.

Testing Summary After testing, we determined that the Adafruit BMP390 Pressure Sensor met all three test objectives outlined for this test. Overall, we are able to conclude that this sensor is suitable for our system and that accurate pressure data can be monitored and stored.

6.2.12 Camera

The following outlines the testing that was performed with the Raspberry Pi Camera Module 3.

Test 1: Camera Verification The purpose of this test is to verify that the camera can capture quality image and video quality.

Test Objectives The primary objectives of this test are as follows:

- **Objective 1:** Acquire images from the camera with at least 800x600 pixels.
- **Objective 2:** Acquire video from the camera with at least 720p100 quality.
- **Objective 3:** Verify the capture latency is within 5 seconds when run from command.
- **Objective 4:** Verify that the camera's footage can be retrieved and stored.

Test Materials The materials used for testing were as follows:

- Raspberry Pi Camera Module 3
- Raspberry Pi 4 Module B

- Monitor
- Insignia HDMI to Micro-HDMI Cable

Figure 86 shows the camera powered during testing.

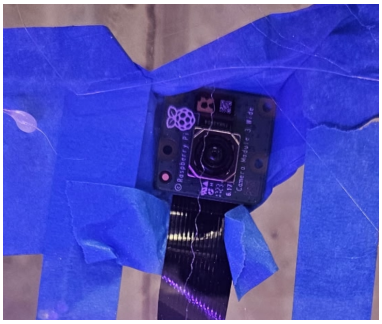

Figure 86: Raspberry Pi Camera

Test Procedure The following test procedure was used to fulfill the test objectives:

1. Connect the camera to the Raspberry Pi 4.
2. Power the Pico by connecting it to a computer using a USB to micro-USB cable.
3. Restart the Pi 4 to activate the camera module.
4. Start timer.
5. Capture and store an image using the command window.
6. End timer.
7. Start timer.
8. Capture and store a video using the command window.
9. End timer.
10. Check the captured image and video quality, as well as the time of the capture.

Test Results and Analysis Ten trials were conducted while capturing images, and ten trials were conducted when capturing video. The latency and quality for these trials were observed.

The values given in Table 21 show that all of the readings for all ten trials had a latency within 5 seconds.

Trial	Image Latency (sec)	Video Latency (sec)
1	3.82	3.76
2	3.77	3.51
3	3.87	3.81
4	3.65	3.72
5	3.91	3.75
6	3.86	3.70
7	3.56	3.59
8	3.82	3.90
9	3.76	3.99
10	3.82	3.94

Table 21: Camera Latency across Ten Trials.

The values given in Table 22 show that all of the readings for all ten trials had an image quality of 800x600 pixels and a video quality of 720p100.

Trial	Image Quality (pixels)	Video Quality (resolution)
1	800x600	720p100
2	800x600	720p100
3	800x600	720p100
4	800x600	720p100
5	800x600	720p100
6	800x600	720p100
7	800x600	720p100
8	800x600	720p100
9	800x600	720p100
10	800x600	720p100

Table 22: Camera Quality across Ten Trials.

Testing Summary After testing, we determined that the Raspberry Pi Module 3 Camera met all four test objectives outlined for this test. Overall, we are able to conclude that this camera is suitable for our system and that good image and video quality can be retrieved and stored.

6.3 Experimental Payload Prototype

The results from the payload metal uptake experiments are presented in Table 23. It is worthy of note that four sets of radishes were planted and consistently resulted in growth of healthy plants in up to 60% volcanic ash, indicating that this level of low-fidelity regolith simulant is capable of supporting plant life. Our results show that no iron ions were detected in the plants grown in any condition. Both the calcium and magnesium concentrations remain

fairly consistent between each soil condition, indicating that there is adequate uptake of metals even from the source with minimal soil present (60% volcanic ash, 40% soil). The lack of iron detected in the plants is likely due to the actual concentration being outside of the detection limit of the test strips, rather than any deficiency in iron uptake, since the plants appeared healthy throughout their growth cycle and iron is a crucial component in the cellular respiration of plants. The calcium and magnesium concentrations could not be measured more precisely than those presented due to the sensitivity of the test strip method. Growing the plants overnight in the bench top system demonstrated adequate short-term support of botanical life using the LED lighting and air circulation systems.

Condition	**$Fe^{2+/3+}$ mg/ml**	**Ca^{2+} mg/mL**	**Mg^{2+} mg/mL**
100% soil	0	0.8-0.16	0-2.4
90% soil, 10% volcanic ash	0	0.08-0.16	0-2.4
80% soil, 20% volcanic ash	0	0.16-0.24	0-2.4
70% soil, 30% volcanic ash	0	0.08-0.16	0-2.4
60% soil, 40% volcanic ash	0	0.08-0.16	0-2.4
50% soil, 50% volcanic ash	0	0.08-0.16	0-2.4
40% soil, 60% volcanic ash	0	0.08-0.16	0-2.4

Table 23: Results from Metal Ion Uptake Experiment.

6.4 User Interface

Objective In order to characterize and iterate on our user interface design, we conducted an institutional review board approved usability study to inform emerging design decisions. Results from this study aim to inform best practices for designing intuitive and effective user interfaces in high-stakes, space exploration environments, where ease of use is critical for mission success.

Procedure Before performing usability testing, verbal consent was obtained from participants using the IRB exempt consent form. If consent was obtained, then each participant went through five pre-designed scenarios using a mockup of the UI on a laptop. Participants' screens were recorded using Apple's MacBook native screen capture application during usability testing. Screen recordings enabled task completion time and common interface patterns to be assessed during data analysis. Upon completion of the usability testing scenarios, participants completed the NASA Modified System Usability Scale (NMSUS) and were asked a series of questions to obtain qualitative feedback on the UI design. Audio recordings of participant responses to the post-test interview questions were captured using an audio recording device, but responses were deidentified and converted to transcripts using OpenAI's Whisper.

It is important to note that the participants were not asked about each task individually. To evaluate their experiences, we relied on the NMSUS questionnaire, qualitative feedback,

and screen recordings. As a result, low mention counts do not indicate disagreement, but rather that participants did not bring up those aspects unprompted.

Scenario 1 Experimenter: "Please tell me what the fourth most recent change to the rack was, who made the change, and what the note they left said".

Objective: The goal of this scenario is to identify whether the (1) timeline layout is intuitive, (2) the horizontal scroll feature is intuitive, (3) users understand that there is a full timeline page, (4) the full timeline page is easy to navigate, and (5) understand.

Results: Out of 24 participants, five explicitly mentioned the timeline when asked what they liked about the UI, highlighting the ability to view dates, notes, processed thoughts, and updates—even after they had been pushed.

When asked about UI elements they disliked, only two participants mentioned the chronological order (from least recent to most recent). However, screen recordings showed that all participants, except two, were able to immediately and correctly interpret the order in which payloads were pushed. Based on this, we added an arrow to further clarify the visual representation of chronological order.

In addition, three participants mentioned problems with the timeline's design, highlighting aspects such as "super small text" on the main page. In response, we reduced the amount of information shown in the preview cards, increased their size, and simplified the overall design.

Scenario 2 Experimenter: "Please tell me all the current rack parameters for the upper left most payload".

Objective: The goal of this scenario is to (1) determine whether the steps to navigate to the full payload information is intuitive and (2) the layout of the rack parameters is understandable to the point where users can easily edit the various parameters.

Results: Twelve out of 24 participants noted that navigation between pages, including the view page, was straightforward. They described the interface as "organized," "cohesive," "simple," and "intuitive." One participant specifically mentioned appreciating the uniformity of information between different payloads. Additionally, three participants commented on the clarity of the parameter observation page, liking both the amount and the quality of information presented for each payload.

In contrast, two participants mentioned difficulty in locating the back button. However, screen recordings showed that participants generally found it quickly. Since the back button's placement (in the upper left corner) aligns with common user expectations, and users were ultimately able to locate it despite initial hesitation, we chose to leave it unchanged.

Scenario 3 Experimenter: "Under the profile of Jakob Swilley, navigate to orbital middeck 4, and change the temperature to 10 degrees celsius, wavelength to 35 nanometers, brightness to 68 lumens, and leave a short note about your changes".

Objective: The goal of this scenario is to (1) determine whether the navigation to edit the rack information is intuitive, (2) the edit mode layout is understandable, and (3) determine whether the account login is understandable.

Results: Three out of 24 participants commented on the clarity of the editing page, mentioning that it was simple to use but required users to be intentional with their changes.

However, another three participants reported difficulty in locating the edit mode. This was an intentional design choice, as we wanted users to be deliberate when making edits. As such, the edit mode button was intentionally kept away from the normal space of interaction within the screen. Once astronauts locate the edit page, they are unlikely to forget its location, so we decided to keep the edit mode button as it was.

In addition, three participants suggested that the popup should also indicate whether a user has been selected. This feature, and the indication of whether a note was entered, was therefore implemented in the second iteration of the design.

Scenario 4 Experimenter: "Return to the home page".
Objective: The goal of this scenario is to (1) determine whether users can easily return to the home screen from inside a payload and (2) whether users understand what the landing page is.

Results: Since the GUI automatically returns users to the front page after an edit is pushed, this scenario was designed to test whether users recognized the landing page as the default, main view. This was largely successful: five participants noted that the layout was clear, and eight specifically mentioned appreciating the alignment of the visual display with the physical rack.

Scenario 5 Experimenter: "Now, there is suddenly an error with orbital middeck 8. Tell me what the error is and how to fix it".

Objective: The goal of this scenario is to (1) determine if users can locate the anomaly tracker, (2) are able to interpret which payload(s)/features of the rack is causing the anomaly, and (3) determine if the error call in the anomaly tracker stack is intuitive and interpretable (users must pay close attention to the dates to get this correct).

Results: Five out of 24 participants mentioned features they appreciated about the anomaly page. These included its ability to display past issues, the use of color to indicate severity, the flashing alert when an anomaly was present, and the inclusion of advice on how to resolve the issue.

However, 6 participants reported difficulty interpreting the anomaly page. Specifically, there was confusion about the meaning of the colors, especially gray. A few participants admitted to not reading the error messages, especially if they were unfamiliar with the software or the technical style of error reporting. To address this, we revised the anomaly page to display only current errors, moving gray (resolved) errors to the full anomaly log. We also

darkened the yellow color for increased readability and re-ordered the message so that the recommended action appears first. The technical language of the recommendation was kept, given the astronauts' technical background and the information such language provides.

There was also a specific question in the qualitative feedback section about the participants' thoughts on what each color indicated:

- Red: 12/24 believed it indicated the most urgent error, 3/24 thought it marked an error exceeding a threshold, and another 3/24 associated it with something specific being broken.
- Yellow: 18/24 interpreted it as a medium-level emergency, 2/24 as a warning with the system still operational, 1/24 linked it to a flow rate issue, and 1/24 was unsure.
- Gray: 10/24 believed it represented the least urgent error, 3/24 said it indicated an error without a safety threat, 1/24 considered it a normal error, 1/24 a measurement error, and 1/24 thought it meant the system was unplugged. Only 4/24 correctly identified gray as indicating a resolved issue with the system functioning normally.

Due to the ambiguity in the interpretation of colors, we introduced explicit text markers such as "RESOLVED" at the beginning of messages in the second iteration.

Qualitative Feedback Questions

1. Describe what you liked about the UI.
2. Describe what you disliked or felt was missing in the UI.
3. Of the tasks you completed, which do you think would be easier with a touchscreen instead of a trackpad and keyboard?
4. Were there any tasks you think would have been easier with manual controls (e.g., switches, dials, buttons)?
5. What do you think the colors of the error messages on the anomaly tracker represented?

7 Ergonomic Study

7.1 Introduction

This research study investigates the injury risks associated with manually loading scientific payloads into a lunar payload rack, focusing on the effects of vertical loading height on astronaut biomechanics and musculoskeletal strain across a range of body types. Simulated loading scenarios were analyzed using Rapid Upper Limb Assessment (RULA) and 3D Static Strength Prediction Program (3DSSPP) software. Key metrics included spinal compression, joint load, reach capability, and the percentage of the population able to perform the task safely.

The purpose of this study is to evaluate potential scientific payload loads and their associated injury risks for astronauts when manually loading payloads into a lunar payload rack. Specifically, this study examines the impact of loading tasks performed at various vertical heights on crew biomechanics and musculoskeletal strain across a range of astronaut anthropometries. The parameters measured through the simulations include spinal compression, joint

load, percent of population capable of the maneuver, and maximum stable reach distance. By analyzing these factors, the study aims to identify height-related trends in injury risk and to develop recommendations for future payload loading procedures and lunar payload rack designs. These recommendations will minimize biomechanical stress and reduce the likelihood of crew injury during lunar missions.

This study employed a combination of analytical and ergonomic assessment methods to evaluate the safety of manually loading scientific payloads into a lunar payload rack. First, an anatomical payload dimension analysis was conducted to determine appropriate payload sizes and handle placements relative to astronaut anthropometry. Next, a Rapid Upper Limb Assessment (RULA) was used to conservatively evaluate postural risk during various lifting scenarios; identifying musculoskeletal strain based on joint angles and expected exertion levels. Finally, the 3D Static Strength Prediction Program (3DSSPP) was utilized to simulate lifting tasks and estimate spinal compression, joint loading, and the percentage of the population capable of safely performing each maneuver. Together, these methods provided a comprehensive evaluation of biomechanical risk factors and informed design recommendations.

7.2 Strength Degradation with Long Duration Space Missions

The NASA Human Integration Design Handbook (HIDH) [4] provides key guidelines for designing human-in-the-loop systems that account for the physiological degradation astronauts experience following long-duration spaceflight. Prolonged exposure to microgravity increases the risk of muscle atrophy, particularly in the lower limbs and trunk, and the risk of bone mineral density loss. Both of these risks contribute to reduced physical strength and stability upon reentry to a gravity environment such as the Moon or Mars.

To help designers predict astronaut performance post-mission, the HIDH offers empirical strength degradation data and models derived from International Space Station (ISS) studies. These models indicate that maximum voluntary force production—especially in the lower body—can decline by 30% to 40% after six months in space, even with rigorous in-flight exercise countermeasures.

Importantly, the HIDH differentiates strength expectations based on operational scenario severity. It categorizes task urgency into three levels:

1. Routine operations: Require conservative force limits to ensure long-term crew health, typically not exceeding 25–50% of preflight maximum strength.
2. Contingency or degraded operations: Permit moderate increases in physical demand if necessary to complete mission objectives, with load limits approaching 60–70% of baseline capacity.
3. Emergency scenarios: Assume that an astronaut may need to exceed safe biomechanical thresholds temporarily (e.g., lifting or dragging a crewmember or payload), possibly using up to 80–100% of their reduced capacity, but with a higher risk of injury.

To mitigate risk, the HIDH advises that critical tasks should be designed to stay well within reduced strength capabilities, particularly during the initial 72-hour recovery window after reentry. Assistive technologies, paired operations, and ergonomic design principles are emphasized to prevent overexertion and support safe task execution during early surface operations.

7.3 Anatomical Payload Dimension Analysis

An Anatomical Payload Dimension Analysis was used to evaluate how human body dimensions influence an individual's ability to safely and effectively interact with a scientific payload during manual loading tasks. This method involves applying anthropometric data collected from the 2012 anthropometric survey of U.S. Army Personnel: Methods and summary statistics [5] and Human body proportions explained on the basis of biomechanical principles [6]. The data collected is on limb lengths, joint locations, body masses, and ranges of motion from a representative population (e.g., 5th percentile female, 50th percentile male, and 95th percentile male) to inform the spatial design of future payloads and handling procedures.

By mapping key anthropometric measurements to task parameters, such as handle height, limb limits, and lift zones, the analysis helps define ergonomic boundaries that accommodate a wide range of body types. This ensures that the design of payload interfaces, including handle placement and load height, aligns with the physical capabilities of the astronaut population. The goal is to avoid impossible to handle payloads, reduce musculoskeletal strain, and maximize the percentage of individuals who can safely perform the task without assistance. This analysis served as a foundational step in guiding the RULA and 3DSSPP simulations by establishing realistic and inclusive payload expectations.

Assumptions for the payload dimension analysis:

1. The task is performed against Lunar gravity ($1.62 m/s^2$).
2. Only 5% Female, 50% Male, and 95% Male data sets were observed.
3. The center of mass can exist anywhere inside the payload.
4. The individual is using a perfect lifting form.
5. The astronaut is in a standing position with no additional support.

7.3.1 Results

The analysis identified that the maximum allowable dimensions of a manually loaded payload are directly constrained by human body proportions, specifically those of the target astronaut population. Two primary anthropometric limitations were found to govern payload design:

1. The depth of the payload (distance from front to back) is restricted by the location of the payload's center of mass and the individual's ability to place their hands on either side of that center of mass during a lift. If the payload is too deep, (assuming the center of mass may be anywhere inside the payload) it will increase joint strain and reducing control, thereby raising the risk of injury or task failure.
2. The width of the payload (side-to-side dimension) is constrained by the individual's arm span, joint positioning, and forward reach capacity. To safely lift the payload, individuals must be able to reach across the width and still insert their hands deeply enough along the sides to maintain grip aligned with the center of mass. Excessive width forces the arms into unsupported and extended or impossible positions, compromising lifting mechanics and stability.

To ensure the payload is safely manageable by the intended astronaut population (defined as the 5th percentile female to the 95th percentile male) the most conservative anthropometric values must guide the design. As the 5th percentile female represents the lower limit in terms of reach, arm span, and upper body dimensions, payloads must be designed around these populations' capabilities. Due to the current payload rack design's maximum payload size still being compatible with a 5% female's anthropometry the results do not affect our overall design.

7.4 Reach Analysis

Assumptions for the reach analysis:

1. The task is performed in Lunar gravity ($1.62 m/s^2$).
2. Loads greater than 500 N have no effect on the results.
3. The score applies to all human populations and anthropometries.
4. The individual is using a perfect lifting form.
5. The payload is a constant standard width 46.04 cm wide.
6. The loads have not been adjusted to reflect a weakened astronaut.

7.4.1 Results

Analysis results revealed that lunar gravity greatly reduces an individual's ability to maintain balance and control while reaching with a weighted payload. Unlike on Earth, where the gravitational force reduces the maximum mass a person can lift based on their strength, lunar conditions allow individuals to lift much greater masses with an equivalent earth load due to the Moon's lower gravity (approximately $\frac{1}{6}$th of Earth's). However, this reduction in gravitational force also leads to a critical finding, the payloads that are easily liftable in lunar gravity can have a mass nearly equivalent to the individual's own, shifting the center of mass dangerously and compromising balance. As a result, when a crewmember extends to lift or maneuver a heavy payload, the body's base of support is quickly destabilized, increasing the risk of tipping, stumbling, falling, or damaging the payload.

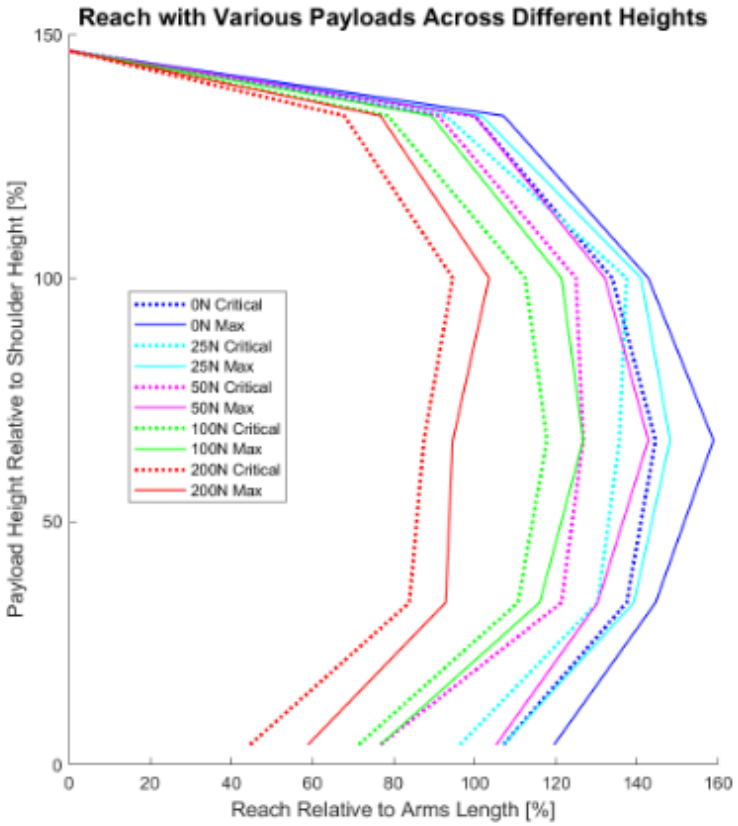

Figure 87: Reach Results

From Figure 87, we also see traditional strength-based safety assessments alone are insufficient in reduced gravity environments. Balance, reach stability, and inertial control become dominant safety factors, necessitating careful mass distribution, adjusted lifting heights, and improved posture guidance to prevent injury and damage during manual handling tasks on the lunar surface.

While the study identified that lunar gravity reduces an individual's ability to balance and reach when handling heavy scientific payloads, these findings do not directly apply to the design or operation of our specific scientific payload rack. The general concern in lunar environments arises from the fact that payloads, although lighter in weight due to reduced gravity, retain their original mass and inertia, making it easier to lose balance when reaching or maneuvering objects with significant mass. However, our system design effectively mitigates these risks through a combination of enforced lifting technique and hardware integration.

A key element of our payload handling procedure is the use of proper lifting form, which requires the astronaut to bring the scientific payload as close to the body as possible before lifting. This technique minimizes the torque on the spine and joints, improves stability, and helps maintain control—critical factors when operating in reduced gravity. By ensuring that payloads are lifted close to the body, the risk associated with mass-induced balance loss is reduced.

Additionally, the design of the payload rack itself further addresses reach and balance

challenges. Payloads are placed onto extended support rails that allow the user to slide or guide the payload into position without the need to reach deeply into the rack unit. This design eliminates the unstable body positions that would typically be required when loading payloads into enclosed or recessed compartments. As a result, users can maintain a stable stance and keep their center of gravity aligned throughout the loading process.

7.5 Rapid Upper Limb Assessment (RULA)

The Rapid Upper Limb Assessment (RULA) is an ergonomic screening tool designed to evaluate the risk of musculoskeletal injury associated with upper body postures during work tasks. It is particularly useful for assessing static or repetitive activities involving the arms, neck, trunk, and legs, such as manual lifting. This assessment was used to provide a very conservative estimate of an astronaut's risk of injury while lifting a payload of any weight off the ground up to a given height.

To determine if a lifting procedure is safe using RULA, an evaluator observes and scores the worker's posture during the lift. Key body segments—including the upper arms, lower arms, wrists, neck, trunk, and legs—are each assigned posture scores based on their angles and positions during the task. Additional modifiers are added for factors such as muscle use (static loading) and the amount of force or load involved. The values used for the assessment were gathered from the 3DSSPP software and assumed the individual maintained perfected posture.

These individual scores are combined into a final RULA score ranging from 1 to 7, which corresponds to a level of musculoskeletal risk:
1–2: Acceptable posture; no action needed.
3–4: Low risk; change may be needed.
5–6: Medium risk; investigation and change are required soon.
7: High risk; immediate investigation and changes are required.

By applying RULA to a full lifting procedure, we determined whether the posture and physical effort required during the lift places the individual at a risk of injury. If the RULA score is high, it indicates the need to redesign the task—such as adjusting the load height, improving lifting technique, or reducing the weight—to reduce ergonomic risk and enhance crew safety.

Assumptions for the RULA analysis:

1. The payload is a constant standard width 46.04 cm wide.
2. The task is performed in Earth's gravity.
3. The task is performed 3x a minute for the duration of a 8 hour work day.
4. Loads greater than 500 N have no effect on the results.
5. The score applies to all human populations and anthropometries.
6. The individual is using a perfect lifting form.
7. The loads have not been adjusted to reflect a weakened astronaut.

7.5.1 Results

The RULA analysis indicates that individuals or pairs of astronauts are unlikely to experience injury when lifting payloads under 98 newtons per person, assuming proper posture is used. However, the only way to further reduce injury risk is to eliminate the need to lift payloads from floor level and far above the head, where joint strain is highest. When the individual load exceeds 98 Newtons, the risk of musculoskeletal injury drastically increases, especially under poor posture or repeated lifting conditions.

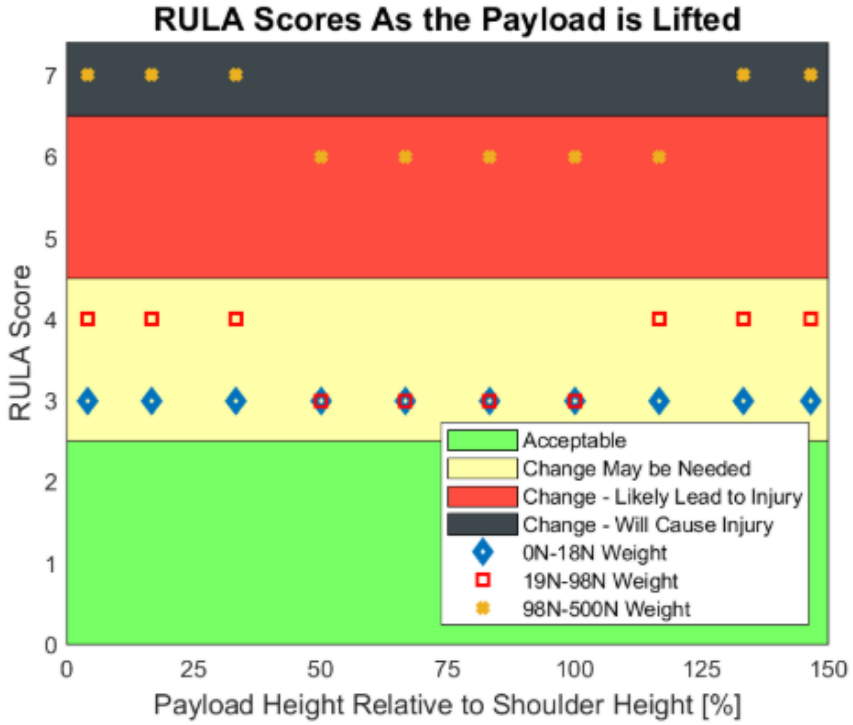

Figure 88: RULA Results

The Rapid Upper Limb Assessment (RULA) conducted in this study provided important insights into the musculoskeletal risk associated with lifting scientific payloads under lunar mission constraints. The analysis led to three primary findings: First, an individual or pair of astronauts is unlikely to experience injury if their individual lifting load is kept below 98 Newtons. Second, the only method shown to further reduce injury risk is to eliminate the need to lift payloads from floor level, as low lifts inherently produce more extreme joint angles and postural strain. Third, if an individual's lifting load exceeds 98 Newtons, the RULA results indicate a significantly increased risk of musculoskeletal injury.

While these findings suggest clear design thresholds, it is important to contextualize them. RULA was originally developed for industrial work environments, where tasks are performed repetitively for 8 or more hours per day. As such, the RULA scoring system represents a highly conservative, worst-case risk assessment that assumes continuous, repetitive action. In contrast, manual payload loading during a lunar mission is a short-duration, intermittent task, performed with significant attention to posture, coordination, and safety protocols with a likely maximum of 16 loading maneuvers in a day.

Therefore, while the RULA analysis indicates a higher risk category for loads just under 98 Newtons, this must be interpreted in light of its built-in conservatism. In fact, even under these stringent conditions, the simulated task still falls within a low to moderate risk range, which further supports the viability of the procedure. The findings reinforce the importance of minimizing load weight and avoiding low lifting heights but also suggest that with proper technique and task pacing, the risk of acute musculoskeletal injury remains acceptably low for the expected operational context.

7.6 3D Static Strength Prediction Program (3DSSPP) Analysis

The 3D Static Strength Prediction Program (3DSSPP) is a biomechanical modeling tool developed by the University of Michigan that estimates the physical demands of various manual tasks on the human body. It is particularly effective for evaluating lifting procedures by simulating the postures, joint forces, and spinal loads experienced during a lift. This makes it an ideal tool to model an astronaut's ability to load a scientific payload with high fidelity.

Assumptions for the 3DSSPP analysis:

1. The task is performed in Lunar gravity ($1.62 m/s^2$).
2. The data values reflect an individual holding a static load throughout a lift.
3. Only 5% Female, 50% Male, and 95% Male data sets were observed.
4. The individual is using a perfect lifting form.
5. The payload is a constant standard width 46.04 cm wide.
6. The individual is in a standing position with no additional support.
7. The loads have not been adjusted to reflect a weakened astronaut.

To assess a lifting task in 3DSSPP, the user inputs key parameters such as body posture (joint angles), hand load location and magnitude, and anthropometric data (e.g., height, weight, sex). The software then calculates:

- Spinal compression forces, particularly at the L5/S1 vertebral joint.
- Joint moments and forces at the shoulders, elbows, and lower back.
- The percentage of the population (based on strength capability) able to safely perform the task.
- And overall balance and reach feasibility for the posture.

Each of these values are given for a particular anthropometry in a particular position. But when these values are observed at key moments throughout a given lifting procedure the loads on the body throughout the procedure become clear, as if the entire motion was simulated.

In this simulation the safety of a maneuver is determined by comparing the simulated output values to accepted ergonomic thresholds. For example, the commonly used spinal compression low risk limit is 3,400 N at the L5/S1 disc. If the predicted forces remain below

these limits then a high percentage of the population can safely perform the lift, consequently the procedure is considered ergonomically safe. Conversely, if forces exceed safe thresholds or balance is compromised, task redesign is recommended as risk becomes high enough for an injury to be expected.

7.6.1 Results

The 3D Static Strength Prediction Program (3DSSPP) analysis revealed three key findings regarding injury risk during manual lifting tasks. First, astronauts are very unlikely to sustain back injuries if proper lifting posture is maintained. Second, the data show the individual's sex and anthropomotry such as height or weight has little effect on injury risk. Lastly, injury risk is highest when lifting from the ground, where body posture is most compromised and spinal loading is at its peak. Below are three figures which each represent the L4/L5 spinal compression throughout a well-executed lifting procedure in 5% Female, 50% Male, and 95% Male populations.

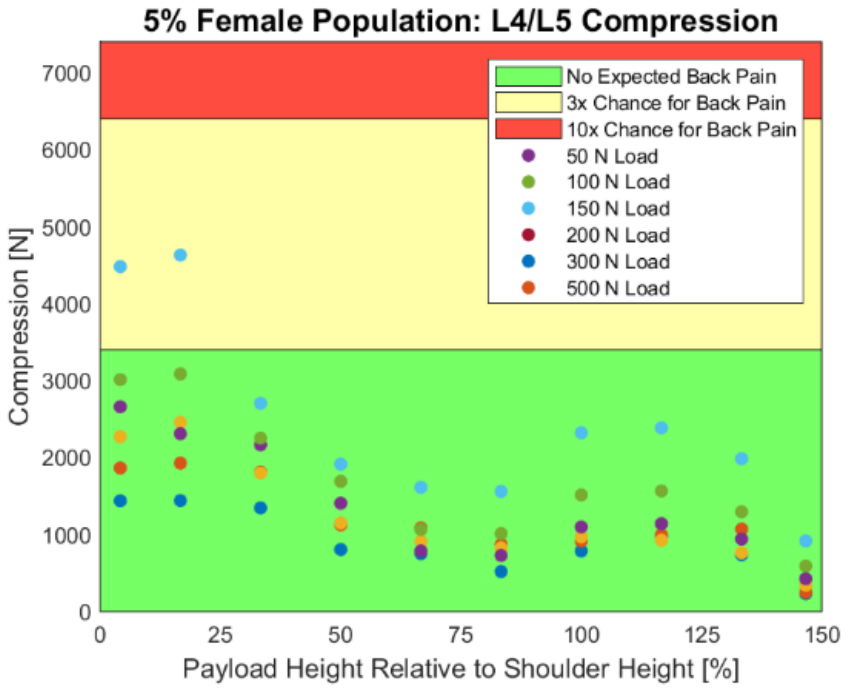

Figure 89: 3DSSPP Results for 5% Female Population

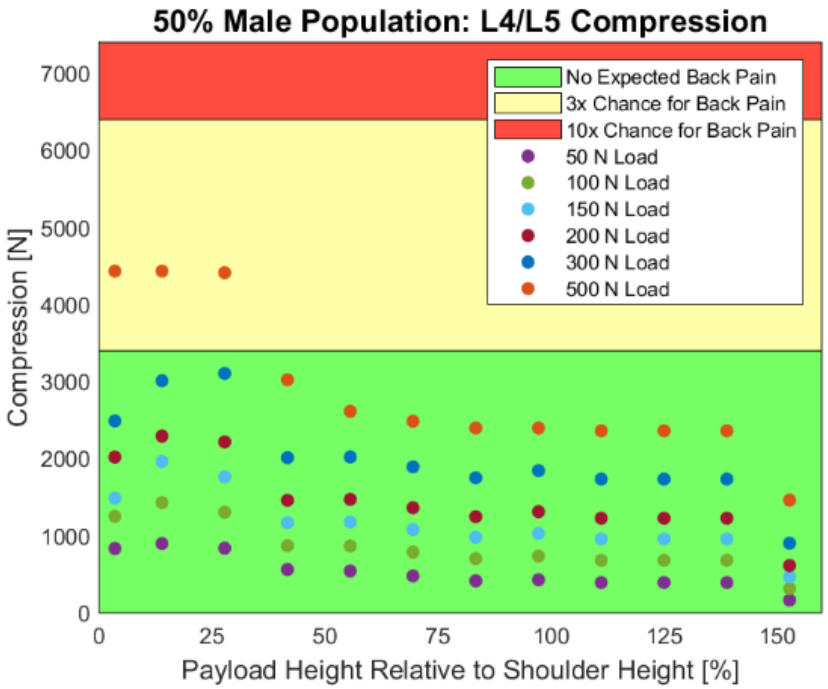

Figure 90: 3DSSPP Results for 50% Male Population

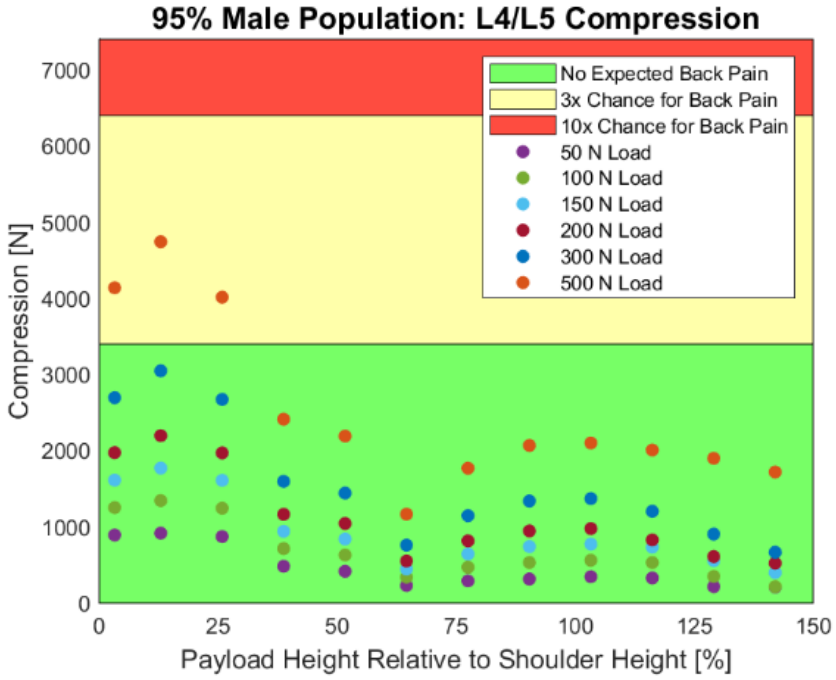

Figure 91: 3DSSPP Results for 95% Male Population

The findings from the 3D Static Strength Prediction Program (3DSSPP) simulations provide a detailed understanding of the biomechanical risks associated with manually lifting scien-

tific payloads in a lunar environment. The study confirms that astronauts are very unlikely to experience back injury when proper lifting posture is maintained, regardless of load, provided posture remains biomechanically sound. This reinforces the critical role of posture-focused training and task design in minimizing injury risk.

One of the most noteworthy outcomes is that individual anthropometry has minimal effect on the risk of back injury. While limb length, height, and body proportions naturally influence reach and load handling, these factors are far less impactful than posture when it comes to predicting injury risk. The simulations showed that poor posture (such as excessive trunk flexion or reaching away from the body) introduces far greater biomechanical strain than differences in body size. This finding supports the use of universal lifting guidelines across a diverse astronaut population, as long as posture is appropriately managed.

The results also identify that the greatest risk of back injury while using a proper lifting technique occurs when lifting from the ground up to approximately 37% of shoulder height, a zone that forces astronauts into postures that increase spinal compression and reduce balance. Above this threshold, the torso becomes more upright, joint loading decreases, and control improves, thereby reducing injury risk.

Based on these findings, several key recommendations are proposed:

1. Unloaded scientific payloads should be stored so that their handles are at least 45 cm off the ground, which corresponds to roughly 37% of a 95th percentile male's shoulder height. This minimizes exposure to the high-risk lifting zone and supports safer lifting posture for all users.
2. Individual astronauts should only lift payloads weighing less than 98 Newtons, not only to account for the increased biomechanical risk associated with posture deviations as the user's balance shifts, but also to reflect the increased risk of decline in astronaut strength after long-duration space missions.
3. Paired astronauts lifting as a team should not exceed a combined payload weight of 300 Newtons, this both protects the individual from the expected decline in strength after long-duration space missions while ensuring stability and control during the lift.

It is important to acknowledge a current limitation in the payload rack design. The lowest storage slots are just below the recommended minimum height for safe lifting, placing it within the higher-risk zone discussed in this study. While this does not invalidate the rack's usability, it introduces a biomechanical vulnerability that could be mitigated. This shortcoming can be readily addressed in a future design iteration by adjusting the height of the lowest storage location to meet or exceed the 45 cm threshold, or providing a kneeling pad to support work at lower heights.

7.7 Conclusions

This study evaluated the biomechanical risks associated with manually loading scientific payloads into a lunar payload rack, with a focus on how vertical loading height and gravitational differences affect astronaut safety across a range of anthropometries. The findings clearly indicate that one of the most effective strategies to reduce injury risk is to eliminate the need for astronauts to lift payloads from floor level. RULA assessments identified that individual

payloads exceeding 98 Newtons greatly elevate the risk of musculoskeletal injury. Meanwhile, 3DSSPP simulations suggest that while loads up to 300 Newtons may be manageable with proper posture, balance becomes a critical concern when heavy objects are handled in lunar gravity. The decreased stability and reach capacity observed under lunar conditions further emphasize the importance of minimizing loads and optimizing lifting ergonomics.

Based on these findings, several design and procedural recommendations were developed to mitigate injury risks. Unloaded payloads should be stored with handles positioned at least 45 centimeters above the ground, equivalent to approximately 37% of a 95th percentile male's shoulder height. This ensures that the majority of astronauts avoid the most hazardous lifting zone. Additionally, payload handles should extend the full length of both sides of the payload to accommodate diverse centers of gravity and reduce torsional stress on the body. To manage physical strain, individual astronauts should only be tasked with lifting payloads under 98 Newtons, while team lifts should be limited to 300 Newtons, assuming ideal posture and coordination. These recommendations aim to support safe, efficient payload handling procedures and inform future lunar payload rack designs.

The significance of this study lies in its demonstration that individual astronauts can safely perform payload loading tasks under specific weight and posture conditions, which could enhance operational flexibility within a lunar habitat. Furthermore, it highlights that lunar gravity substantially impacts an individual astronaut's balance during manual handling, reinforcing the need for caution and tailored procedural controls.

8 Risks and Mitigation

Risk management is a critical aspect of any project, particularly in endeavors as complex and multifaceted as ours. A comprehensive risk matrix has been developed to identify and assess potential hazards that could impact the success of our mission. Each risk item has been meticulously analyzed, considering its likelihood of occurrence and the severity of its consequences on a scale of 1-5. Through this process, we have identified various technical, schedule, cost, and safety-related risks that could impede our progress or compromise the functionality and safety of our equipment. Appendix D includes the missions and human risk matrices along with their respective fever charts for detailed documentation of risks. Fever charts are a visual representation of how application of mitigation strategies has a positive impact on the risks associated with the design.

One notable technical risk involves the possibility of silent payload control failure, wherein the payload controls may be unable to be executed properly and there exists no indication that this is occurring. Similarly, concerns regarding payload handling when taking lockers out of the rack pose issues to the experiments within the rack, potentially rendering it impossible to manually service them. Mitigation strategies have been proposed for each risk item to minimize their potential impact. For instance, in response to concerns about payload control failure and handling, efforts are underway to enhance electrical and resourcing robustness, as well as the removal mechanism of the lockers.

Similarly, measures to mitigate risks related to electrical system exposure to liquids have

been proposed, including the incorporation of waterproof enclosures and selecting sensors with appropriate resistance to liquid exposure. In addition to technical risks, human-level risks have also been identified and addressed in our risk management approach and evaluated on a logarithmic scale for their likelihoods of occurrences. These include risks such as user injury due to electrification on improperly housed electronics, injury from incorrect payload handling, crushing from improper rack handling, or abrasion on sharp surfaces. Mitigation strategies for these risks focus on providing proper training, instructions, and incorporating safety features to minimize the likelihood of accidents or injuries during manual rack operation.

Overall, our risk management strategy is aimed at proactively identifying and mitigating potential hazards to ensure the successful and safe execution of our mission. By implementing robust mitigation measures and continuously monitoring and reassessing risks throughout the project lifecycle, we aim to minimize disruptions and maximize the effectiveness of our payload rack in supporting experimentation during space missions.

9 Project Management

9.1 Work Breakdown Structure

The work breakdown structure (WBS) for the Rack and Stack project is roughly illustrated in Figure 92.

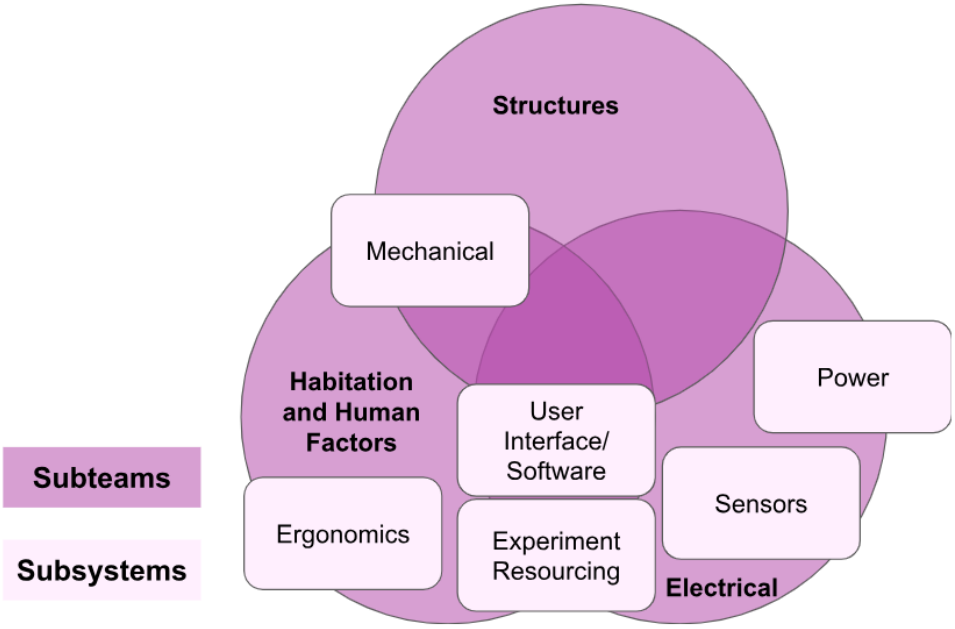

Figure 92: Work Breakdown Structure.

9.2 Project Schedule

With a complex project, such as this one, an important aspect that needs to be accounted for is the project schedule. The success of this project will be dependent on the ability of our team to stay on course with the project schedule that has been predetermined.

The key dates that our team ensured to abide by are listed below:

- **October 8, 2024:** Requirements and System Definition Review
- **November 15, 2024:** Preliminary Design Review
- **February 7, 2024:** Critical Design Review
- **March 20, 2024:** Progress Checkpoint Review
- **May 8, 2024:** Project Completion and Evaluation

Our team designed a Gantt chart so that we could have the key milestones and dates depicted in an easy-to-view manner as shown in Figure 93.

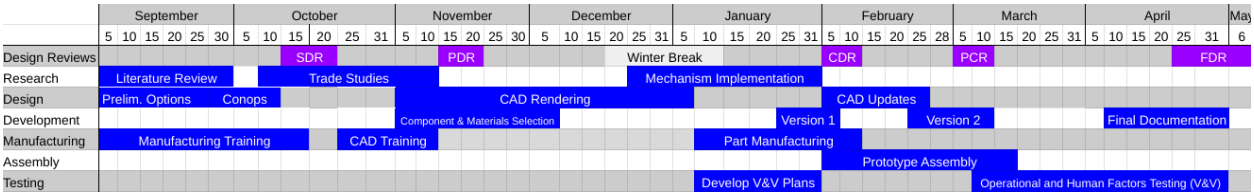

Figure 93: Year-Long Gantt Chart

To note, winter break has been scheduled into the Gantt chart due to the majority of project team members being unable to meet in person and work on the project.

For the second semester, in anticipation of a busy prototyping season, we outlined a more detailed Gantt chart as shown in Figure 94.

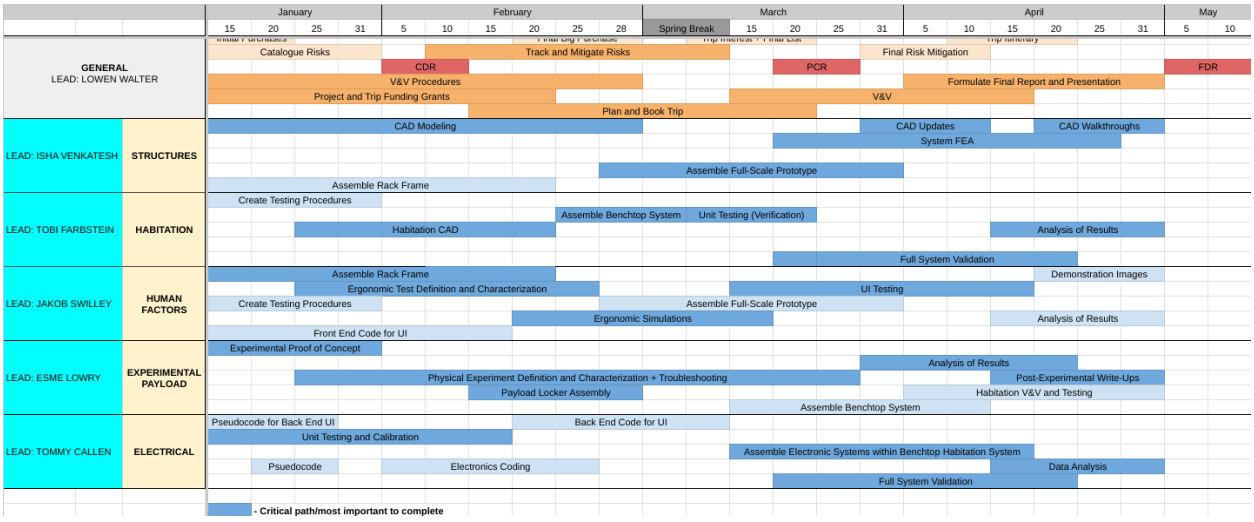

Figure 94: Second Semester Gantt Chart

The second semester Gantt chart is broken down into 6 sub-groups which correspond to each of the 5 subteams, as well as a general section in order to breakdown tasks further. The dark orange and blue tasks belong to the critical path which is composed of primary tasks for each subteam. Each of these tasks rely on one another, so it was important to track these in

particular to ensure the project would be completed on time.

9.3 Project Cost

The cost for this project is a limiting factor that will define what materials our team will be able to utilize. The preliminary budget allocation is that of $. The budget breakdown is depicted in Figure 95.

Figure 95: Preliminary Budget Allocation

Our final cost breakdown is shown in Figure 96.

Figure 96: Project Costs

To note, our team decided to go with a 10% cost margin. We also received $ in funding from the University of Michigan for our Experimental Payload subteam.

10 Suggestions for Future Exploration

10.1 Structures

With more time and resources, we would continue to build out our full rack and expand our testing to include vibration and shock testing, as well as impact testing. The following sections outline future work for each subsystem in more detail.

10.1.1 Frame

As shown from the system testing, the design works as required. The rack frame can support both the 60.3 kg payload requirement as well as the 1.5 factor of safety of 90.45 kg. As no signs of displacement of failure were observed, design changes and additional testing are not required.

While this rack frame is a good proof of concept, the overall design needs to be further refined before it would be mission-ready. In an idealized system, the rack frame would likely not be made of 80/20 profiles. Instead, a profile already machined with all of the specific attachment points needed would be used. The weight of the rack frame could be greatly reduced if a thinner profile was used. This would require additional analysis and testing that is outside the scope of this stage in the project.

The 80/20 profile relies upon friction and preloading in the T-slotted fasteners to attach all of the components. In the idealized design, T-slotted fasteners would not be used for this reason. Instead, bolts, screws, or welds would be used to attach all of the components and

rack frame together.

Further testing would also be required to verify that the rack frame can support a factor of safety of at least 1.5 times the payload weight. There are numerous different configurations for this situation that have yet to be tested. Durability testing and testing of the yield and ultimate loads that the frame could withstand would be integral for a rack that would be used on a mission. Vibration testing would also be needed to show that all fasteners would not come loose during the mission: this testing was not completed on the structural prototype as the team was unable to get access to a big enough vibration table to perform the test.

10.1.2 Shell

The shell is a necessary rack component to encase the frame and all interior components. The material will be black acrylic at $\frac{1}{8}$" thickness, with electric insulating qualities in order to block light from entering the payload lockers and to prevent charge from building on the rack exterior. As the shell is fastened along the frame, it should add structural stability to help frame displacement in rack movement. While FEA could not be completed, the shell can be tested in the final assembly for displacement prevention.

For absolute implementation, the shell should be tested physically to ensure stability is added to the frame, verifying future FEA results. As the acrylic should be ordered black and electrically insulating, tests should be conducted to ensure that no light can pass through the material and minimal charge can be stored upon the material, where the value can be determined by risk mitigation assessment of electrical systems.

10.1.3 Rack Handle

With more resources, we would recommend building a prototype from the idealized material of aluminum and conducting validation testing to verify that the handle meets all ergonomic requirements.

10.1.4 Mobility

As shown from the system testing, the design is able to meet the requirement of supporting a load of 60.3 kg. The rack mobility subsystem can support both the 60.3 kg payload requirement as well as the 1.5 factor of safety of 90.45 kg. No signs of displacement of failure were observed.

While the system clearly works under Earth gravity, the main concern the team had when designing the subsystem was how it would act while moving it in lower gravity situations. In these situations, the weight of the rack would be significantly less causing it to be more easily tippable. Some of the design changes that the team could consider would include designing or locking the back wheels so that they cannot turn. This would provide more stability while moving the rack in the event that one wheel spins due to a defect on the ground causing the rack to fall. Another change could be to make the wheels larger so that the rack has a closer center of gravity to the ground. This would increase the torque needed to tip over the rack. However, these wheels would most likely have to be internal and positioned to not affect the placements of the payload bays.

Additionally, the team would also have to do a vibration test on the mobility section while under the weight of the rack. We were unable to do this vibration test since the available vibration table was too small for the rack. This test could be analyzed to see how well the rack stays in place while in a locked position. However, it is certain that an additional separate interface would have to be added for mounting the rack during activities such as launch.

10.1.5 Sliding Rails

The load testing can be declared a success since it validated the requirement SSI-1.07, and proved the feasibility of the sliding rails subsystem. The main takeaways would be watching for wear and tear of these components, even if it will not be as dramatic as in testing since astronauts should be advised against going neat or beyond the safety factor loading weight that we tested with. For maintenance, it is important to check that the bolts stay secured, and this can be done easily by removing the payload. Also, users should be advised against putting the majority of the weight very densely towards the front of the payload locker when fully extended since this can either be a tipping hazard, or cause more stress on the rails and cause them to wear out quicker. Additionally, the success of this testing shows that the other payload configurations may work as well since the sliding rails performed when the mass was compact. Also, the other payloads have 2 sets of sliding rails supporting them instead of just one, but are still subject to the same weight requirements. Lastly, in accordance with SSI-1.08 our rails can accommodate for payloads that cover the area of two large payloads side by side, the area of two payloads on top of each other, and the area of four payloads in a grid.

Though the material of the rails, galvanized steel, is already strong, it would improve design confidence to make them even stronger by making the rails thicker. Deep analysis regarding the strength to weight trade-off to prevent the weight of the rack from becoming too much while still supporting the payload would be crucial. This would help especially if the rails are lengthened to allow for further travel distance since it would create a greater moment. Other than changes to strength to accommodate for further travel distance and greater bending moments, we think making rails that have a similar release latch, but in an easier to reach location would be helpful. Though our functionality testing showed that it could be done, it can be a bit difficult to disengage the latch to remove the payload when the rails are underneath the payload, especially the lower it is to the ground. Other design changes might reveal themselves if the other testing that we recommended were to be done, such as load testing with the underneath orientation, smaller payloads, and other payload geometries, but we expect that no major changes would be necessary.

10.1.6 Desk

The Desk & Rail subsystem successfully demonstrated its ability to support up to 40 lbs of payload under Earth gravity without deformation or structural failure. Testing confirmed that the lightweight $\frac{1}{16}$" 6061 aluminum desk, when supported by a simplified 8020 frame, meets structural and functional requirements under expected operational conditions. The system also maintained smooth rail functionality after load testing, indicating mechanical robustness. However, the desk experienced noticeable deflection under higher loads up to a safety factor of 1.5 (50–60 lbs), reinforcing the importance of additional internal support in the final design.

The current design is functional within its load limits, but structural improvements—either

through enhanced support or stronger rail systems—are necessary to meet higher safety factors or more demanding mission loads.

The path of flight for the desk includes upgrading to higher-strength sliding rails that are capable of supporting greater loads in both the deployed and retracted positions. This would prevent the structural issues seen in the load test at higher loads. Additionally, in order to improve the desk itself, designers should reintroduce internal 80/20 supports or consider alternative lightweight truss structures to enhance overall stiffness without significantly increasing the system's mass.

10.1.7 Roller Rails

The roller rails and associated end caps are used to properly ensure movement and alignment of the payload lockers by placement at the vertical midpoint of each locker, where the side attachment mechanism of the lockers will roll along the wheels to guide movement.

Testing should be done to ensure that movement of multiple payload lockers at the same time does not cause any interference with the sides of the payload lockers rolling over wheels, but otherwise the components have been properly measured and tested in movement. While the exact distance between the payload lockers does not need to be recorded or varied, verifying that the lockers stay flush to the roller rails and do not interfere validates the functionality of the roller rails.

10.1.8 Latch

Testing shows promising results, and that the chosen toggle latches are capable of securing the payloads and enduring disturbances. They also show that the users find no difficulty in the operation of the latches, and the latches do not interfere with the lockers as desired. The design works. However, usability results point that the latch mechanism should be improved in the idealized design, so that the initial "wants" can be completely fulfilled, namely, ease of use. In the idealized design, the latches are the ideal length, and do not need to be attached at an angle on the rack. However, since the tests were mainly about the concept of a toggle latch, and the concept of the general direction of securing, the tests are applicable to validating our ideal design.

First, changes in the design of the toggle latch so that the latch can be a swift singular movement to unlatch and secure are necessary. Improvements to the design so that the latches can prevent the payload locker from moving completely would also be ideal. A possible direction of further improvement would be the securing direction to be directly against the payload's traversal direction. Further considerations of what the necessary actions to unlatch/latch should also be considered, and placement on the rack itself should also be considered. Moreover, there should be different latches for payload lockers that are either on the very top of the rack or the very bottom, to minimize discomfort for the user in latch operation.

10.1.9 Payload Locker

Our design did work as expected when used in the necessary subsystem tests that required a model payload locker. It was sturdy, easy to attach to the rack, and able to support more weight than what would be needed in an idealized rack. Given more time and resources, it

would be optimal to create a fully integrated prototype locker with acrylic. This would allow us to test different weight distributions and see how effectively the locker functions for storage purposes. In conclusion, our design is practical and simple, and it would be effectively implemented into an idealized rack as well.

If we had unlimited time and resources, we would build a full-scale 1:1 model of the payload locker. This would allow us to conduct more thorough testing on the locker itself and obtain an accurate weight for integration into other subsystem tests. The idealized payload locker would also require a custom gasket to ensure a fully gas-tight seal, and the back plate would need additional holes for the habitation tubes. The current slider rails feature a spacer on top to ensure proper alignment and a snug fit with the frame; however, further improvements to this area would be beneficial. Additionally, handle placement can be adjusted during testing to evaluate whether the acrylic or aluminum plates can withstand the applied forces, enabling refinement of handle positioning.

We would also expand our build to full prototypes of all payload locker shapes and sizes to conduct further testing.

10.2 Human Factors

There is an opportunity to improve the ergonomic design of the rack for the final idealized design. Usability of loading and securing payloads may be improved through an improved payload insert and removal mechanism, as in-house pilot testing identified emerging difficulties with lining up the payload into the loading mechanism. Additionally, different payload handle placements could be investigated and assessed which may increase the usability of loading and securing payloads by enabling alternate loading techniques. A step stool and knee-pad should also be provided to crew to assist extreme anthropometries with loading and unloading payloads at the top-most and bottom-most rows of the rack respectively. As we get closer to flight, there is also an opportunity to improve the user interface design for the rack by standardizing the art style with other software programs crew will interface with in the lunar habitat. Standardization of art styles across software will likely increase usability and helps address NASA's human spaceflight risk of Earth independent human-system operations.

Future ergonomic assessment can also be conducted to improve the usability and reduce injury-risk for the final idealized design. Usability testing can be conducted on the indication light system used to verify if a payload is powered and secured to inform future design iterations, as the study team did not have time to evaluate the proposed display design. Critically, longitudinal usability studies of the payload experiment rack should be conducted in NASA analog mission environments such as the Human Exploration Research Analog (HERA) or the Crew Health and Performance Exploration Analog (CHAPEA). Integrating the system within an analog environment to the envisioned lunar habitat can be leveraged to evaluate crew's situational awareness of rack parameters made by Earth-based support teams or other crew members and identify ways in which to improve rack anomaly response when exposed to ecologically valid attentional demands. Injury-risk can be reduced by conducting noise assessment on the final idealized rack design and introducing engineering controls as a hazard mitigation if sound levels are above safety standards. The simulation study conducted by the design team can also be extended to inform potential lifting strategies crew can adopt while loading payloads to reduce injury-risk. Using the same methodology, different lifting techniques

(e.g., squat, semi-squat, stoop) can be evaluated and compared across anthropometries at different payload loading heights to identify optimal lifting strategies.

10.3 Habitation

Before this system flies, there are a number of things that need to be done from the habitation perspective. To start, there needs to be a secondary subsystem testing campaign in order to prove the capabilities of the heating and cooling system with properly-sized pumps. Additionally, the tests should be replicated using more reliable parts and parts that can eventually be spaceflight qualified and integrated into the system.

With more time and resources, further analysis can be done. More analysis must be conducted into the air circulation and mixing via CFD. There must also be a higher-fidelity investigation into thermal and air leakage.

In order for the system to be ready for spaceflight, all components will need to be spaceflight qualified via vibrational, thermal, shock, and use cycling testing. The components will then need to be implemented within the volume of the rack structure. Finally, design tweaks must be made in order to take fault tolerance and activation following a quiescence period into consideration.

10.4 Electrical

Upon reviewing the electrical-related achievements to date, it is fair to claim that the effort to create a system that allows payload locker configuration, monitoring, and autonomous control was successful. However, this does not imply that the electrical system is, by any means, prepared for deployment.

With regards to software - that being the programming of microcontrollers and user interface - an acceptable level of confidence in its resiliency and endurance has yet to be attained. To date, the system has only been operated in sessions lasting up to three hours. Therefore, to achieve the reliability required for long-term operation, endurance and resilience testing must take place.

Due to the goals of our prototype being to prioritize functionality, certain components were intentionally excluded but will need to be implemented in future iterations. In terms of the electrical system, these components are those that enable redundancy for the subsystems most critical to the safety and functionality of the overall system. The said subsystems include, but are not limited to, power, fire detection / suppression, temperature control, and ventilation.

Lastly, it should come as no surprise that the items and materials used in the assembly of the prototype's electrical system are not suitable for spaceflight. Thus, all components, prior to deployment, must be replaced with their corresponding spaceflight qualified parts.

10.5 Experimental Payload

Given more funding and an adequate space in which to conduct such experiments, it would be ideal to repeat these studies using a high-fidelity lunar regolith simulant to determine

whether our results can be reproduced in a lunar habitat scenario. The ability to grow plants in a soil-regolith mixture is less likely to succeed at such a high ratio as we saw with volcanic ash—due to the complete lack of organic material in lunar regolith—but it is possible that a ratio can be found that would reduce the amount of soil necessary to transport to a lunar habitat in order to grow plants. It would also be pertinent to repeat these experiments using a more sensitive method of metal measurement, such as inductively-coupled plasma mass spectrometry (ICP-MS), if the budget were to allow this. While the radishes were supported in the bench top system overnight, longer-term growth of plant life within the system will be necessary to demonstrate the capability of the rack to support botanical or other biological experiments. We also aim to expand the temperature range maintained by the rack, as well as add capability to control the atmospheric conditions within a payload in order to support customers that require these additional functions. For example, allowing freezing temperatures and high-nitrogen environments within the rack will permit additional experimentation necessitating these conditions.

11 Acknowledgments

This project would not have been possible without the hard work of the members of the Rack and Stack team listed here:

- Project Lead: Lowen Walter
  - Graduated Project Co-Leads: Megan Foulk and JD Dell
- Structures
  - Subteam Lead: Isha Venkatesh
  - Albert Chen
  - Colin Stenger
  - Huan Shuo Chang
  - Jacob Lee
  - Joshua Walker
  - Lizzie Kooistra
  - Lukas Zahuranic
  - Vanessa Cano
  - Yeon Woo Kim
- Human Factors
  - Subteam Lead: Jakob Swilley
  - Preston Withun
  - Vanya Krishna
  - Zion Walker
- Habitation

  - Subteam Lead: Tobi Farbstein
  - Ava Cardenas
  - Daniela Bardi Silva
  - Hana Hasanovic
  - Hannah Yohannes
  - Jennifer Morales
  - Megan Piper
  - Noah Negron
  - Suhani Thakur
- Electrical
  - Subteam Lead: Thomas Callen
  - Andrew Chen
  - Anthony Brunswick
  - Austin Gorlitz
  - Darin Noronha
  - Joban Guron
  - Joshua Noonan
  - Kate Snowdon
  - Kevin Chen
  - Kwang Sun
  - Max Swartz
  - Michael Fabian
  - Peyton Jensen
  - Prajwal Kurapati
  - Zoe Hekneby
- Experimental Payload
  - Subteam Lead: Esme Lowry
  - Hamza Qureshi
  - Ritish Natesan
  - Vamsi Gollapalli

We would like to thank our industry sponsor at NASA Marshall Space Center for her encouragement and invaluable feedback throughout this project. Our sponsor, Dr. Tracie Prater, has played a pivotal role in empowering and supporting our project. We would also like to thank the X-Hab Program Office and the National Space Grant Foundation for providing the opportunity for the team to carry out this project.

We would also like to acknowledge our subject-matter experts from the University of Michigan, Drs. Leia Stirling, Jon Van Noord, and Pete Washabaugh, for connecting us with resources

across the university to further advance our project. We would also like to thank Dr. Emily Matula at the Johnson Space Center for sharing her knowledge of EVAs and ISS operations and BLiSS alum Chad Cerruti and current BLiSS member Christopher May for their guidance and mentorship throughout the project for both general members and project leadership. As our advisors, their help was instrumental in developing the design as it has been presented in this report.

We would also like to thank Professor Nilton Rennó, Professor Steve Battel, Sandy Pytlinski, Yvonna Olds, Ilyana Smith, and the custodial staff at the Climate and Space Research Building for their help in managing the logistics of the project.

References

[1] *Moon to Mars eXploration Systems and Habitation (M2M X-Hab) Academic Innovation Challenge – FY25 Solicitation*. 2024. URL: https://spacegrant.org/wp-content/uploads/2025/03/M2M-X-Hab-Challenge-Solicitation-2026.pdf.

[2] Ted B. Davis et al. "EXPRESS Rack Technology for Space Station". In: National Aeronautics and Space Administration, 1999. URL: https://ntrs.nasa.gov/api/citations/19990008536/downloads/19990008536.pdf.

[3] A. Sledd, M. Danford, and B. Key. "EXPRESS Rack: The Extension of International Space Station Resources for Multi-Discipline Subrack Payloads". In: National Aeronautics and Space Administration, 2002. URL: https://ntrs.nasa.gov/api/citations/20030062135/downloads/20030062135.pdf.

[4] "Human integration design handbook (2025)". In: National Aeronautics and Space Administration, 2025. URL: https://www.nasa.gov/organizations/ochmo/human-integration-design-handbook/.

[5] ARMY NATICK SOLDIER RESEARCH DEVELOPMENT and ENGINEERING CENTER MA. "2012 anthropometric survey of U.S. Army Personnel: Methods and summary statistics." In: National Aeronautics and Space Administration, 2014. URL: https://www.nasa.gov/organizations/ochmo/human-integration-design-handbook/.

[6] H. Witte, H. Preuschoft, and S. Recknagel. "Human body proportions explained on the basis of biomechanical principles". In: Zeitschrift für Morphologie und Anthropologie, 1991.

APPENDICES

A Additional Testing

B UI Testing

B.1 IRB Consent Form

INFORMATION SHEET
TITLE OF THE RESEARCH PROJECT
HUM00267863

Principal Investigator: Jakob Swilley, PhD Student, University of Michigan
Faculty Advisor: Leia Stirling, PhD, University of Michigan

You are invited to participate in a research study about **:** Evaluating the usability of a new graphical user interface (GUI) design for an experimental lunar payload rack, in order to inform emerging design decisions. Results from this study aim to inform best practices for designing intuitive and effective user interfaces in high-stakes, space exploration environments, where ease of use is critical for mission success.

If you agree to be part of the research study, you will be asked to complete a series of scenarios on a virtual mockup of the UI on an experimental laptop.

Benefits of the research: You will receive no direct benefits from participating in this study. However, results from this study will be used to inform the future development of GUIs for human spaceflight applications.

Risks and discomforts**:** There are no added risks beyond the typical risks of working at a computer.

Compensation: There will be no compensation for participating in this study.

Participating in this study is completely voluntary. Even if you decide to participate now, you may change your mind and stop at any time. You may choose not to continue for any reason.

We will protect the confidentiality of your research records by not disclosing your name or age on the Google Forms you fill out, you will be assigned a number (e.g., Study Participant #2). We will screen record the usability testing, but these recordings will exclusively be used by the research team for data analysis and will not capture audio or video feed. We will audio record the post usability testing interview, but these recordings will exclusively be used by the research team for data analysis. We will protect the confidentiality of your research records by deidentifying all abstracted information and feedback.

Your research information will be stored electronically on the cloud; the term “cloud” refers to large computers located in different parts of the world where individuals may keep and remotely access their personal and professional files. Each cloud service has its own policies and methods for preventing unauthorized individuals from accessing files stored on their cloud servers. The cloud service used to store files associated with this study meets University of Michigan protection standards.

If you have questions about this research study, please contact Leia Stirling, leias@umich.edu.

As part of their review, the University of Michigan Institutional Review Board Health Sciences and Behavioral Sciences has determined that this study is no more than minimal risk and exempt from on-going IRB oversight.

Figure 97: IRB Exempt Consent Form

B.2 NASA Modified System Usability Scale (NMSUS)

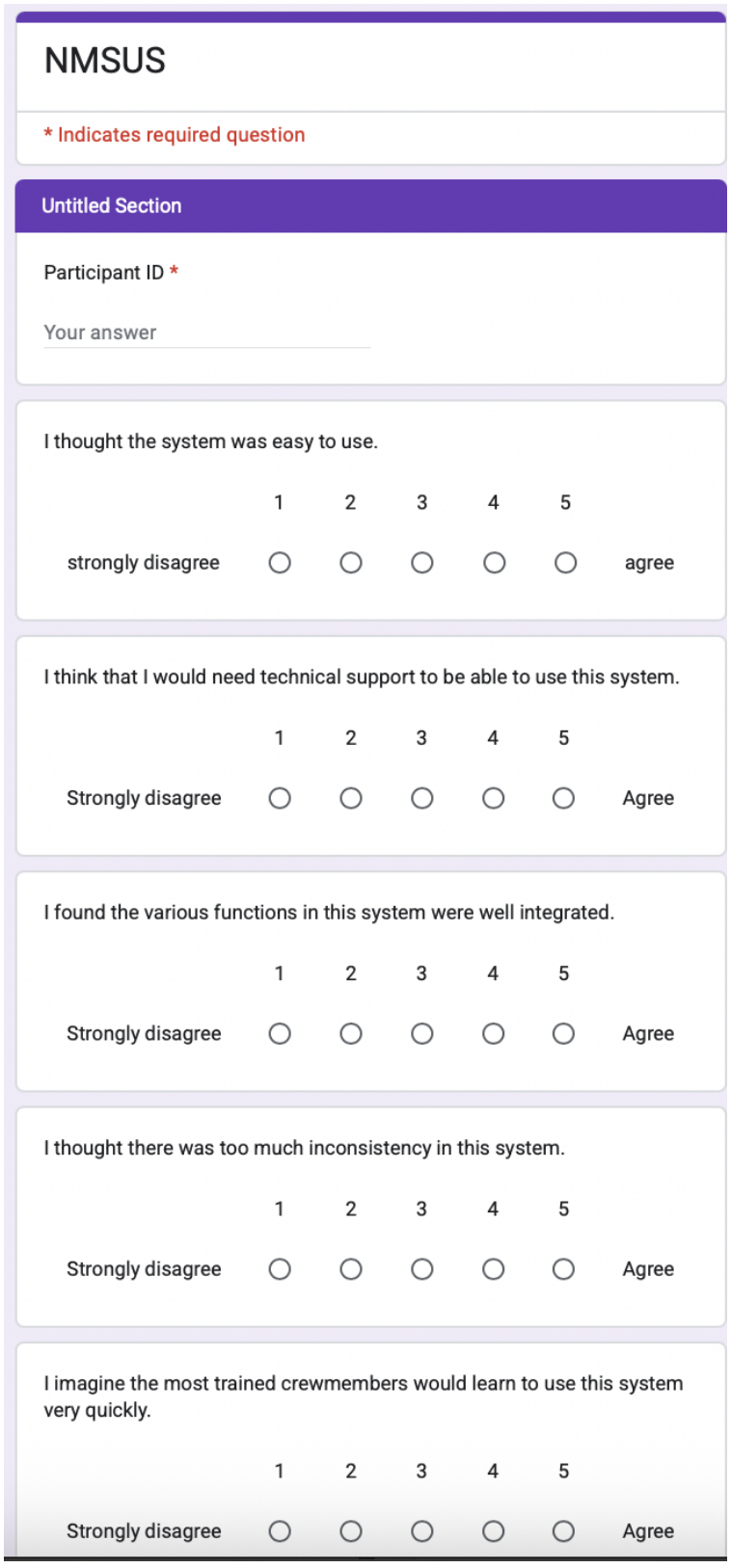

NMSUS

* Indicates required question

Untitled Section

Participant ID *

Your answer

I thought the system was easy to use.

	1	2	3	4	5	
strongly disagree	○	○	○	○	○	agree

I think that I would need technical support to be able to use this system.

	1	2	3	4	5	
Strongly disagree	○	○	○	○	○	Agree

I found the various functions in this system were well integrated.

	1	2	3	4	5	
Strongly disagree	○	○	○	○	○	Agree

I thought there was too much inconsistency in this system.

	1	2	3	4	5	
Strongly disagree	○	○	○	○	○	Agree

I imagine the most trained crewmembers would learn to use this system very quickly.

	1	2	3	4	5	
Strongly disagree	○	○	○	○	○	Agree

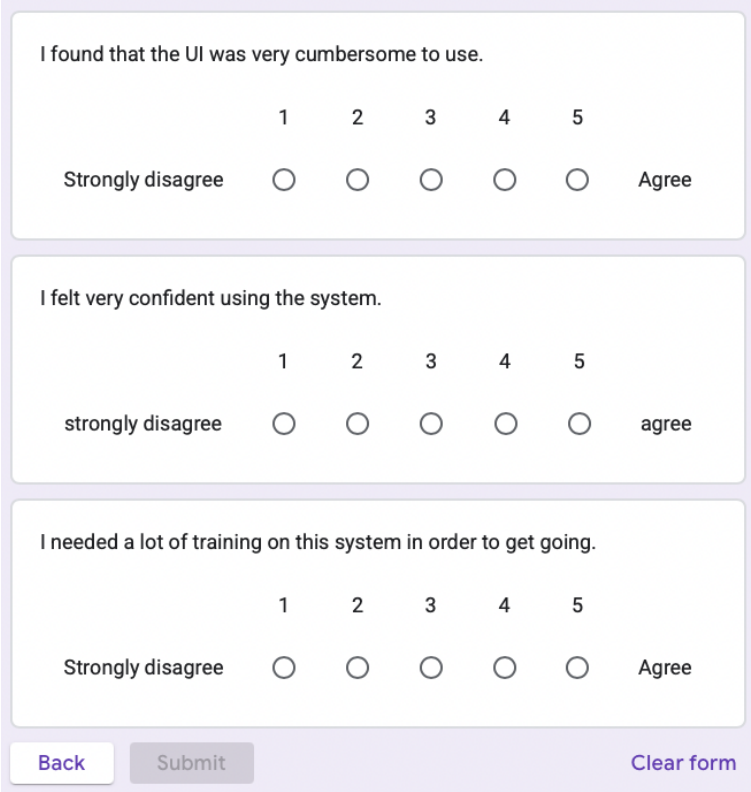

Figure 98: NMSUS

C Requirements

C.1 Level 1 Requirements

System Requirements - Level 1		
Requirement ID	**Description**	**Derived From**
Payload Capability		
PC-1.01	Each payload shall have air, water, electric, and sensor/auxillary digital signal inlets.	R12
PC-1.02	Each payload shall have air, water, electric, and sensor/auxillary digital signal outlets.	R12
PC-1.03	The payload shall have a locking mechanism securing its position in place to the rack when not in use.	R5
PC-1.04	The payload shall be able to support environments capable of sustaining botanical life.	R9
PC-1.05	The system shall record and store sensor inputs on a common storage device.	R10
User Interfacing		

UI-1.01	The system shall provide feedback upon user actions and system changes.	R3
UI-1.02	The rack interface design shall follow occupational exposure standards and recommendations to minimize the probability of crew injury.	R3
UI-1.03	All rack user interface controls shall be consistent across the entirety of the rack and payload lockers.	R7
UI-1.04	The force necessary from the crew while interacting with the system shall be less than the values specified in Table E.7.1 under the "Crit 2 Ops" column of STD-3001.	R3
UI-1.05	Each payload box shall be distinguishable and easily identifiable through two or more dimensions.	R3
UI-1.06	The system shall be designed in a manner so as to be movable by no more than two people.	R8
UI-1.07	The rack shall permit access to all components.	R8
UI-1.08	The rack and payload's frequently used components (buttons, handles, covers) shall be operable using one hand.	R8
UI-1.09	All of the rack's exposed surfaces shall be able to be both cleaned and disinfected.	R5
UI-1.10	User interfaces shall be interpretable to users with corrected 20/20 vision under nominal illuminations levels.	R3
UI-1.11	Lighting shall be adjustable according to user input.	R9
UI-1.12	The system shall be capable of recording and storing visual data.	R10
UI-1.13	The system shall be able to track and store data amounting up to 30 days.	R10
UI-1.14	The system shall use similar UI labeling standards as the heritage payload lockers and racks.	R7
UI-1.15	The system shall include handles which the user can use to counter balance oneself while accessing or putting away a payload.	R3
UI-1.16	Manual controls that interface with mission critical operations shall be guarded or shielded to prevent inadvertent activation.	R3
UI-1.17	The rack shall include interfaces to monitor and control payload support systems.	R9
UI-1.18	The rack shall not exceed a maximum background sound of 50 DBA for nominal operating conditions.	R5
System Structure and Interfacing		
SSI-1.01	The system shall be securable to a location to withstand at least 596 N of standing horizontal push force from unsuited crewmembers.	R3
SSI-1.02	The rack shall encompass any electronics, thermal systems, or additional supporting systems within its structure.	R1
SSI-1.03	The system shall be usable within the lunar gravitational environment.	R2
SSI-1.04	The system shall be compatible with tools listed in NASA's Tools and Stowage document for all preventative and corrective maintenance.	R9

SSI-1.05	The system shall be able to withstand the weight of payloads in lunar gravity.	R2
SSI-1.06	Any payload locker shall be compatible with any payload slot in the rack structure.	R14
SSI-1.07	The system shall support a payload of up to 60.3 kg on Earth scaled to lunar gravity.	R3
SSI-1.08	The system shall accommodate at least two payload geometries.	R14
Reliability, Maintenance, and Safety		
RMS-1.01	The system shall have a fire detection system.	R5
RMS-1.02	The system shall be free of sharp edges or surfaces with the ability to cause injury when handled.	R5
RMS-1.03	The system shall be usable within a 40% oxygenated environment.	R2
RMS-1.04	The system shall have a grounding wire attached to the payload.	R4
RMS-1.05	The system shall be able to operate after a period of dormancy up to 3 years.	R2
RMS-1.06	The system shall ensure the exterior surface of the payloads maintains a temperature at or below 42°C.	R5
RMS-1.07	The system shall be two fault tolerant for power failures.	R4
RMS-1.08	The system shall be two fault tolerant for data controller failures.	R4
RMS-1.09	The system shall be two fault tolerant for temperature control system failures.	R4
RMS-1.10	The system shall be two fault tolerant for ventilation control system failures.	R4
RMS-1.11	The system shall protect from overvoltage of +/- 30 V for I/O lines.	R13
RMS-1.12	The system shall provide no more than 40 mA of DC and 8 mA of AC through the crewmember.	R5
RMS-1.13	The system shall run on 120 V DC (+6/-4).	R2
RMS-1.14	The system shall switch to an auxiliary 120V DC input in the event of undervoltage.	R13
RMS-1.15	The payload drawers shall have a stopping mechanism to avoid payloads falling out of place when the payloads are fully pulled out.	R5
RMS-1.16	The payload shall have a locking mechanism securing its position in place to the rack when not in use.	R5
RMS-1.17	The fire detection system shall be two fault tolerant.	R4
RMS-1.18	The system shall keep logs of commands in memory.	R10

C.2 Level 2 Requirements

System Requirements - Level 2

Requirement ID	Description	Derived From
Payload Capability		
PC-2.01	The system shall convert or reformat all analog signal outputs to digital in order to interface with some storage device and the computer.	PC-1.02
PC-2.02	Each payload shall accommodate a selected temperature between a range of 17-28 °C (63-82 °F) +/- 2 degrees °C.	PC-1.04
PC-2.03	Each payload locker maintains an atmospheric pressure within 5% of ambient.	PC-1.04
PC-2.04	Feedwater entering the payload locker shall remain between 20-26 °C (68-80 °F) +/- 2 degrees °C.	PC-1.04
PC-2.05	The payload locker shall accommodate low, medium, and high lighting with wavelengths within the visible and UV spectrum.	PC-1.04
PC-2.06	The payload locker shall accommodate a humidity range between 30-90% relative humidity.	PC-1.04
PC-2.07	The system shall measure and record pressure.	PC-1.05
PC-2.08	The system shall measure and record temperature.	PC-1.05
PC-2.09	The system shall measure and record oxygen and carbon dioxide gas concentration data.	PC-1.05
PC-2.10	The system shall measure and record humidity.	PC-1.05
PC-2.11	The system shall accommodate manual liquid waste.	PC-1.04
PC-2.12	The data controller shall backup and store it's data on the computer or external storage device.	PC-1.05
User Interfacing		
UI-2.01	The payload racks shall be accessible by crew between the 5th percentile female and 95th percentile male reach zones.	UI-1.07
UI-2.02	The rack and payload indicators shall only use one form of distinct alert per function.	UI-1.03
UI-2.03	The one handed operations of the system shall allow for both left and right hand usage.	UI-1.08
UI-2.04	Control interfaces shall be separated between minimum and maximum distances that support one handed usage.	UI-1.08
UI-2.05	The system shall house a camera.	UI-1.12
UI-2.06	The system software shall be capable of saving recordings.	UI-1.12
UI-2.07	Any surface to which the bare skin of the crew is exposed shall, under nominal conditions remain within the temperature limits of the attached table: Skin Temperature Injury Limits.	UI-1.02
UI-2.08	All text present on the rack shall use Helvetica font.	UI-1.10
UI-2.09	Labels shall be horizontally orientated whenever possible.	UI-1.10
UI-2.10	The force required to pull out any payload secured to the rack shall be less than 147 Newtons.	UI-1.04
UI-2.11	Force requirement to lift guarding mechanism should not exceed 13 Newtons.	UI-1.16

UI-2.12	An open cover guard should not interfere with the operation of the protected device or adjacent controls.	UI-1.16
UI-2.13	Control interfaces shall provide an audio, visual, or haptic indication of activation.	UI-1.01
UI-2.14	User interface controls shall align with the compatibility of movement standards established by Figure 10.4-26 in the Human Integration Design Handbook.	UI-1.03
UI-2.15	Control interface dimensions shall be between minimum and maximum distances that support one handed usage.	UI-1.08
UI-2.16	Control interface activation forces shall be between the minimum and maximum values that support one handed usage.	UI-1.08
UI-2.17	Control interfaces with multiple possible states shall provide a visual indication of it's current state.	UI-1.01
UI-2.18	Auditory alerts from the rack shall be above 70 DBA.	UI-1.18
UI-2.19	Payload locker placements shall align with NIOSH recommendations for safe lift zones.	UI-1.02
UI-2.20	The cameras footage shall collect into one common storage device and be read from the computer.	UI-1.12

System Structure and Interfacing		
SSI-2.01	The system shall need no more than 10 minutes of routine maintenance per week while in use.	SSI-1.04
SSI-2.02	The system shall require no more than 60 minutes of maintenance before starting up after dormancy.	SSI-1.06
SSI-2.03	The system's structure shall be able to support a load of 805 kg under lunar gravity.	SSI-1.05
SSI-2.04	The payload slots shall accommodate payload dimensions of 20.30 in x 18.13 in x 10.50 in and 23.54 in x 16.25 in x 6.15 in.	SSI-1.06
SSI-2.05	Maintenance access points shall be designed to allow clearance for tool operation.	SSI-1.04
Reliability, Maintenance, and Safety		
RMS-2.01	System shall have no exposed electrical wiring.	RMS-1.12
RMS-2.02	The system shall be able to access a primary and redundant power source.	SSI-1.07
RMS-2.03	System shall automatically detect the event of an undervoltage.	RMS-1.15
RMS-2.04	The system shall use the oxygen meter to ensure a 40% oxygenated environment.	RMS-1.03
RMS-2.05	The system shall be able to detect fires that produce smoke as a byproduct.	RMS-1.18
RMS-2.06	The system shall have an insulating layer such that the exterior of the payloads maintain a temperature at or below 42 °C	RMS-1.06
RMS-2.07	The system shall utilize a fuse system in the case of exceeding a current limit.	RMS-1.11

RMS-2.08	The rack shall contain limit stops to prevent the drawer from being unintentionally pulled out of the rack and hold the drawer in the open position.	RMS-1.16

D Risk

D.1 Risk Matrices

		Fever Chart - Before Mitigation				
Estimated Likelihood	80%-100%					
	60%-80%					
	40%-60%		9			22
	20%-40%	6	1, 7	8, 39, 40, 43	13, 23	11, 34, 42
	0%-20%		2, 4, 5, 10, 16, 17, 18		14	3, 19, 20, 21
		Negligible	Minor	Moderate	Critical	Catastrophic
		Consequence				

Figure 99: System Risk Matrix Before Mitigation

		Fever Chart - After Mitigation				
Estimated Likelihood	80%-100%					
	60%-80%					
	40%-60%	9				
	20%-40%	1		22		
	0%-20%	2, 4, 5, 6, 15, 16, 17, 18	7, 10, 19, 20, 23, 34, 39, 40, 43	8, 11, 13, 42	3, 14, 21	
		Negligible	Minor	Moderate	Critical	Catastrophic
		Consequence				

Figure 100: System Risk Matrix After Mitigation

		Fever Chart - Before Mitigation				
Estimated Likelihood	10%-100%					
	1%-10%			26, 27, 28		
	0.1%-1%	35		29		
	0.1%-0.01%		24, 33	37	12, 32	25, 38, 41
	<0.01%		31	30		36
		Negligible	Minor	Moderate	Critical	Catastrophic
		Consequence				

Figure 101: Human Risk Matrix Before Mitigation

		Fever Chart - After Mitigation				
Estimated Likelihood	10%-100%					
	1%-10%					
	0.1%-1%					
	0.1%-0.01%	35		29		
	<0.01%	26, 27, 28	24, 31, 32, 33, 36, 38	12, 30, 37, 41		25
		Negligible	Minor	Moderate	Critical	Catastrophic
		Consequence				

Figure 102: Human Risk Matrix After Mitigation

D.2 Risks

Risk ID	Subsystem Risk ID	Risk Item Title	Risk Description	Impacted Areas	Human or System Risk?	Technical/Cost/Schedule/Safety?	Accept/Watch/Mitigate?	Consequence	Likelihood	Risk Score	Justification	Mitigation Strategy	Consequence after Mitigation	Likelihood after Mitigation	Risk Score after Mitigation
1	ELC-1	Communication failure	If the transmission of payload data to Ground fails, then experiments cannot be analyzed	Data	System	Technical	Mitigate	2	2	4	Temporary loss of data is bad, but no components are at risk of damage and no health hazards are present.	Backup critical data in storage on the SH	1	2	2
2	ELC-2	Excess Voltage or Power	If too much voltage is applied across a single component or payload, then the components run the risk of overheating the payload environment	Payload Habitat, Electronics	System	Technical	Mitigate	2	1	2	Overvoltage is possible, but unlikely. The amount of voltage being applied to components of the payload environment should be monitored to maximize the longevity of payloads.	We can implement an automatic voltage stabilizer (AVS) to regulate the voltage and power.	1	1	1
3	ELC-3	Excess Voltage or Power	If too much power is applied across a single component or payload, then the components run the risk of destroying the payload environment.	Payload Habitat, Electronics	System	Technical	Mitigate	5	1	5	Overvoltage is possible, but unlikely. The amount of voltage being applied to components of the payload environment should be monitored to maximize the longevity of payloads.	We can implement an automatic voltage stabilizer (AVS) to regulate the power.	4	1	4
4	ELC-4	Undervoltage	If not enough voltage or power is applied across a single component, then the it can overheat.	Payload Habitat, Electronics	System	Technical	Mitigate	2	1	2	While the probability of undervoltage occuring is low, to prevent overheating, it is necessary to watch for the occurence of undervoltage.	Implement an automatic voltage stabilizer (AVS)	1	1	1
5	ELC-5	Undervoltage	If not enough voltage or power is applied across a single component, then its lifespan can be reduced.	Payload Habitat, Electronics	System	Technical	Mitigate	2	1	2	While the probability of undervoltage occuring is low, to maximize the longevity of payloads sensors, it is necessary to watch for the occurence of undervoltage.	Implement an automatic voltage stabilizer (AVS)	1	1	1
6	ELC-6	Processor Failure	If the processor begins to fail, then the system may begin to overheat.	Data	System	Technical	Mitigate	1	2	2	Overheating will cause the temperature of the payload to fluctuate and slow computations	Introduce a monitor to keep track of both power and temperature through the processor	1	1	1
7	ELC-7	Processor Failure	If the processor begins to fail, then the system may begin to freeze.	Data	System	Technical	Mitigate	2	2	4	A freeze will create a momentary loss of data	Introduce a monitor to keep track of both power and temperature through the processor	2	1	2
8	ELC-8	Processor Failure	If the processor begins to fail, then the system may begin to corrupt data files.	Data	System	Technical	Mitigate	3	2	6	Corruption can cause a loss in previously collected data while momentarily preventing further data collection.	Introduce a monitor to keep track of power through the processor	3	1	3
9	ELC-9	Sensor Miscalibration	If a sensor becomes uncalibrated, then the sensor will provide data that is inaccurate.	Data	System	Technical	Mitigate	2	3	6	Given that the payloads should should provide accurate data when possible, this is something to watch out for.	Implement regular calibration and automated self-check protocols for the sensor to ensure accurate data and detect potential deviations.	1	3	3
10	ELC-10	Data Mishandling	If solar radiation enters the data system, then data may be corrupted by a flipped bit	Data	System	Technical	Mitigate	2	1	2	While the probability of solar radiation impacting the environment is unlikely, it is important to watch and make sure there is radiation shielding to protect the data bus' integrity.	Radiation shielding with teflon or otherwise	2	1	2
11	ELC-11	Electrical Short	If an electrical short occurs, then a fire can occur.	Electronics	System	Technical	Watch	5	2	10	Electrical shorts can start fires and cause arcing that can further damage components	Maintain effective grounds and keep appropriate organization or space between components.	3	1	3

Risk ID	Subsystem Risk ID	Risk Item Title	Risk Description	Impacted Areas	Human or System Risk?	Technical/Cost/Schedule/Safety?	Accept/Watch/Mitigate?	Consequence	Likelihood	Risk Score	Justification	Mitigation Strategy	Consequence after Mitigation	Likelihood after Mitigation	Risk Score after Mitigation
12	ELC-12	Operator Shock	If the electrical components are not housed as intended within the structure (poking out, not neatly packed in, sharp twists due to structure), then current may go through the crew member	Astronaut Health	Human	Safety	Mitigate	4	2	8	Because the wires are not easily accessable this is not a likley occurrence. The damage caused by an electral shock can range from small to great depending on the amps and voltage present.	Have no exposed wires. Make use of an electrical ground.	3	1	3
13	ELC-13	Liquid Exposure	If water gets into the electrical systems, then a short can ocurr.	Data collection	System	Technical	Mitigate	4	2	8	Unlikley but the short can cause greater damage to systems and personel	Isolate the electrical system from outside interference (radiation, water, etc.) with shielding	3	1	3
14	ELC-14	Power Failure	If the main power system and the auxiliary power to the payload fails, then the experiments in the habitat can not be maintained by the payload, and the sensors can no longer collect data	Habitat, Data	System	Technical	Accept	4	1	4	While the likelihood this happens is near zero, if total power failure occurs, this would be catastrophic for the experimentation	In the event of total power failure, there is likely not much to be done.	4	1	4
15	ELC-15	O2 Sensor Failure	If the O2 sensor fails, then the team will be unable to ensure a properly oxygenated environment for the payloads	Payload, Data	System	Technical	Mitigate	2	1	2	It is possible but unlikely for the O2 sensor to fail. Failure of the sensor does not itself create any problems, but allows for other failures to potentially go undetected.	Failure of the sensor will become immediately evident from a cessation in the recording of O2 data. Storing backup sensors to replace the defective one would render the consequence of sensor failure negligible.	1	1	1
16	ELC-16	Temperature/Humidity Sensor Failure	If the temperature/humidity sensor fails or gives erroneous data, then the team will be unable to ensure a proper temperature environment for the payloads	Payload, Data	System	Technical	Mitigate	2	1	2	It is possible but unlikely for the temperature/humidity sensor to fail. Failure of the sensor does not itself create any problems, but allows for other failures to potentially go undetected.	Failure of the sensor will become immediately evident from a cessation in the recording of temperature/humidity data. Storing backup sensors to replace the defective one would render the consequence of sensor failure negligible. Or an algorithm to compare multiple temperature sensors and output the more realistic reading.	1	1	1

Risk ID	Subsystem Risk ID	Risk Item Title	Risk Description	Impacted Areas	Human or System Risk?	Technical/Cost/Schedule/Safety?	Accept/Watch/Mitigate?	Consequence	Likelihood	Risk Score	Justification	Mitigation Strategy	Consequence after Mitigation	Likelihood after Mitigation	Risk Score after Mitigation
17	ELC-17	Pressure Sensor Failure	If the pressure sensor fails, then the team will be unable to ensure a properly pressured environment for the payloads	Payload, Data	System	Technical	Mitigate	2	1	2	It is possible but unlikely for the pressure sensor to fail. Failure of the sensor does not itself create any problems, but allows for other failures to potentially go undetected.	Failure of the sensor will become immediately evident from a cessation in the recording of pressure data. Storing backup sensors to replace the defective one would render the consequence of sensor failure negligible. Or an algorithm to compare multiple temperature sensors and output the more realistic reading.	1	1	1
18	ELC-18	Maxing out data storage	If the computer being used to collect data no longer has free storage, then there is a risk of losing previously collected data.	Data	System	Technical	Mitigate	2	1	2	It is possible for the laptop to run out of data and there is a risk of losing previous data.	Losing previously collected data can be mitigated by backing up data on a hard drive to ensure that data is not overwritten on the laptop. Also, setting up a system where data limits are clearly communicated will be beneficial to plan out when or how frequently to backup data.	1	1	1
19	HAB-1	Valve Failure	Valve failure can lead to excessive pressure build up and inability to regulate payload environment	Payload and Plumbing	System	Technical Safety	Mitigate	5	1	5	All plumbing is made of plastic tubing which would break prior to any pressure breaches	Design mitigation, plastic tubing and safety glasses	2	1	2
20	HAB-2	Fan Failure	If the fan fails, then this can lead to inability to regulate pressure and payload environment	Payload and Plumbing	System	Technical Safety	Mitigate	5	1	5	All plumbing is made of plastic tubing which would break prior to any pressure breaches	Design mitigation, plastic tubing and safety glasses	2	1	2
21	HAB-3	Electrical Shortage	If mist or droplets from the feedwater system wet electronics system, then an electrical short could occur	Electronics Payload	System	Technical Safety	Mitigate	5	1	5	Feedwater spraying lighting for example	Design mitigatation covering all open electrical wiring or components with waterproof coverings	4	1	4
22	HAB-4	Payload control failure	If payload controls fail, then this could lead to loss of payload.	Payload	System	Technical	Mitigate	5	3	15	If the controls are not working, then the experiments could fail, leading to mission set backs.	Add redundant controls and warning systems to detect failure.	3	2	6
23	HAB-5	Payload monitoring failure	If the monitoring systems for the payload fail, then this could lead to a loss of critical experimental data.	Data collection	System	Technical	Mitigate	4	2	8	If telemetry recorded is wrong, this could lead to systme failure or false scientific conclusions	Add redundant sensors and cameras, as well as warning systems.	2	1	2

Risk ID	Subsystem Risk ID	Risk Item Title	Risk Description	Impacted Areas	Human or System Risk?	Technical/Cost/Schedule/Safety?	Accept/Watch/Mitigate?	Consequence	Likelihood	Risk Score	Justification	Mitigation Strategy	Consequence after Mitigation	Likelihood after Mitigation	Risk Score after Mitigation
24	HF-1	Payload handling failure	If the payload is too heavy for the astronaut to handle, then it could fall on the astronaut and injure them.	Astronaut health	Human	Safety	Mitigate	2	2	4	Users will be loading payloads from a safe condition so any harm from improper lifting techniques from the ground are unlikely and minimal. The worst case scenario is unloading a payload which was already secured inside the rack and dropping it onto their foot. This potentially could break a metatarsal requiring medical attention.	Apply a placard near lifting handles stating caution should be used when ligfting the payload as weight and center of mass may catch the user off guard	2	1	2
25	HF-2	Ground Fault Accident	If there is a component failure leading to a contact surface to become electrically energized, and if the astronaut were to come in contact with the energized surface, then this would lead to a ground fault accident.	Astronaut health	Human	Safety	Mitigate	5	2	10	If a astronaut were to come in contact with an energized system there is the potential for the electric shock to send them into cardiac arrest, potentially killing them. This event however is very unlikely to happen.	Installing a ground fault circuit interupter in the habitat and ensuring each conductive contact surface on the rack (which has the potential to be energized) has a conductive path back to the ground through a three pronged plug.	5	1	5
26	HF-3	Excessive Noise Exposure	If there is an excessive level of noise produced by the rack, then this could reduce the astronauts' ability to communicate.	Astronaut health	Human	Safety	Mitigate	3	4	12	Noise is a well known phyiscal hazard that can effect the crews situational awareness and ability to communicate. This is a well known issue on the ISS, and if left unaddressed it may continue to be an issue.	Noise dampening where necessary	1	1	1
27	HF-3	Excessive Noise Exposure	If there is an excessive level of noise produced by the rack, then this could lead to noise induced hearing loss.	Astronaut health	Human	Safety	Mitigate	3	4	12	Noise is a well known phyiscal hazard that can effect the crews situational awareness and ability to communicate. This is a well known issue on the ISS, and if left unaddressed it may continue to be an issue.	Noise dampening where necessary	1	1	1
28	HF-4	Excessive Noise Exposure	If there is an excessive level of noise produced by the rack, then this could disrupt the astronauts' sleep cycle.	Astronaut health	Human	Safety	Mitigate	3	4	12	Noise is a well known phyiscal hazard that can effect the crews situational awareness and ability to communicate. This is a well known issue on the ISS, and if left unaddressed it may continue to be an issue.	Noise dampening where necessary	1	1	1
29	HF-5	Rack Striking Crew Member	The act of moving the rack, or the act of opening and closing the experimental payload has the potential to punch or crush the user's limbs.	Astronaut health	Human	Safety	Mitigate	3	3	9	Normal operation of the rack will involve pulling out and pushing in experimental payloads, and moving the rack to different locations. Each of these actions has the potential to use any built up momentum to forcefully pinch or crush the user.	Label pinch points with warning signs/colors. And place a warning to advis caution when moving the rack.	3	2	6
30	HF-6	Sharp Edges Harming Crew Member	If the rack contains sharp or hard corners or contact surfaces, then they could cut the user during normal operations.	Astronaut health	Human	Safety	Watch	3	1	3	Any sharp edge on the rack would only leave a superficial cut. The astronaut is not at any great risk of cutting themselves. Especially becuase the rack is already designed to remove most sharp corners. Likelyhood of a cut occuring is very small.	Ensure there are no sharp edges on contact surfaces and watch to ensure no additional measures are needed.	3	1	3
31	HF-7	Trip Hazard Harming Crew Member	If the rack has loose wiring coming out from it, then the astronaut could trip over it and hurt themselves	Astronaut health	Human	Safety	Mitigate	2	1	2	In low gravity, the consequence of tripping over a rack would at worst lead to minor injuries. The chances of this happening is also extremely low due to there being no known reason for a crew member to go behind the rack after it is set up to opperate in position.	Place a label on the side and back of rack to warn against tripping hazards.	2	1	2

Risk ID	Subsystem Risk ID	Risk Item Title	Risk Description	Impacted Areas	Human or System Risk?	Technical/Cost/Schedule/Safety?	Accept/Watch/Mitigate?	Consequence	Likelihood	Risk Score	Justification	Mitigation Strategy	Consequence after Mitigation	Likelihood after Mitigation	Risk Score after Mitigation
32	HF-8	Stressfull Posture Harming Crew Member	If the astronaut loads the payload with the incorrect form, then they may injure their back due to improper lifting form.	Astronaut health	Human	Safety	Mitigate	4	2	8	In low gravity, the consequence of poor posture at worst will lead to back pain. The chance of this happening is reasonable considering the potential for a crew member to load and unload a scientific payload.	Place a label on the side of the payloads near the lifting handle, showing how to use proper lifting techniques to avoid injury. Include rigourous training pre-flight.	2	1	2
33	HF-9	Contact with thermal hazard inside the experimental payload locker harming astronaut	If that payloads get hot from their inside temperatures, then the astronaut could be injured when they touch them.	Astronaut health	Human	Safety	Mitigate	2	2	4	A thermal injury is likely to only harm a hand or arm. Burns to this area are considered minor due to the lack of surface area which is harmed. The chances of this happening are very low.	If a payload contains a greater potential for a thermal hazard, the front of the payload shall have a label warning the astronaut. Include insulation within the payload to mitigate conduction.	2	1	2
34	SI-1	Jammed payload	If the payload locker gets stuck and cannot be pulled out or pushed back in, then it could be detrimental to the payload inside.	Payload	System	Technical	Mitigate	5	2	10	It could cause the mission to fail if some component inside the payload needs to be fixed or replaced, but it won't get stuck normally.	Implement methods to facilitate payload removal/insertion.	2	1	2
35	SI-2	Frame pinch points	If the rack has pinch points, then the astronauts could injure themselves on them.	Astronaut health	Human	Safety	Mitigate	1	3	3	Any point at which an open torque is applied could be a risk when interacting with the rack. It could happen often but it would not cause major injuries.	Label pinch points with warning signs/colors	1	2	2
36	SI-3	Particulates	If repeated abrasion occurs from metal-on-metal contact between the payload slot and slider, particulates could be created which pose health risks.	Payload, Astronaut Health	Human	Safety	Mitigate	5	1	5	A fire would be devastating though very unlikely to occur due to the metal abrasion, both the health risks and fire risks can be mitigated through safety training	Regularly check and clean rack, including sliding areas	2	1	2
37	SI-4	Securing failure	If the rack securing mechanism is not designed with multiple step to unlock, then it may accidentally detach without intent.	Payload, Astronaut Health	Human	Safety	Mitigate	3	2	6	With only one point of security, if that one point fails then it is insecure. If rack is not secure, then it is potentially not safe, combined with unareness. This can be designed against.	Train users to double check securing, as well as always be cautious. Integrate a double latch securement system	3	1	3
38	SI-5	Mobility failure	If the rack wheels get stuck, then the rack may be knocked over and injure a crew member.	Payload, Data, Astronaut health	Human	Safety	Mitigate	5	2	10	Even though the rack may not be able to move, rack being knocked over is unlikely. Rack securing mechanism will protect the system	Regularly check wheels for proper function. Use lubricant or spare wheels (if applicable) if the wheels do not move.	2	1	2
39	SI-6	Structural failure	If insertion mechanism is damaged, then any new payload may not properly insert	Payload, Rack Functionality	System	Technical	Mitigate	3	2	6	Not very likely to get hit hard enough that the payload can not be inserted properly, but would have a high impact to the payload meant to go into the space. May not affect all shelves.	Allow for rack to sustain sudden high impacts; include a margin for excessive force in design	2	1	2

Risk ID	Subsystem Risk ID	Risk Item Title	Risk Description	Impacted Areas	Human or System Risk?	Technical/Cost/Schedule/Safety?	Accept/Watch/Mitigate?	Consequence	Likelihood	Risk Score	Justification	Mitigation Strategy	Consequence after Mitigation	Likelihood after Mitigation	Risk Score after Mitigation
40	SI-7	Vibrational damage	If the outer shell gets knocked into, then the internal structure could experience vibrations that may damaged the system	Payload	System	Technical	Mitigate	3	2	6	It is unlikely that the rack would experience a force great enough to cause this	Allow for rack to sustain sudden high impacts; include a margin for excessive force in design. Check for harmonic frequencies.	2	1	2
41	SI-8	Rack collapse	If the rack collapses due to excessive load, then the payloads and nearby people may be harmed	Astronaut health	Human	Safety	Mitigate	5	2	10	The rack collapse could large human damage on the scale of broken bones if a human is close enough	Inspect the state of rack regularly to ensure any material defects or spots of failure are caught early on; reinforce rack such that it has a safety factor above 1.5.	3	1	3
42	SI-9	Rack collapse	If the rack collapses due to excessive load, then the payloads may be harmed	Payload, rack structure	System	Technical	Mitigate	5	2	10	The rack collapse could large human damage on the scale of broken bones if a human is close enough	Inspect the state of rack regularly to ensure any material defects or spots of failure are caught early on; reinforce rack such that it has a safety factor above 1.5.	3	1	3
43	SI-10	Liquid exposure	If liquid drips constantly from the habitat, then the rack material may rust or brittle	Rack structure	System	Technical	Mitigate	3	2	6	Not very likely to occur as any leaks or liquids should be caught and cleaned so that there is no long term exposure.	Make rack out of materials that are resistant to corrosion and embrittlement as a result of exposure to liquids	2	1	2